Towards the Generation of
Catalytic Antibodies for Glycoside Hydrolysis

by

Pamela Michael Jeffrey England

B.S. 1989
University of California, Los Angeles

Submitted to the Department of Chemistry
in Partial Fulfillment of the Requirements
for the Degree of

Doctor of Philosophy
in Chemistry
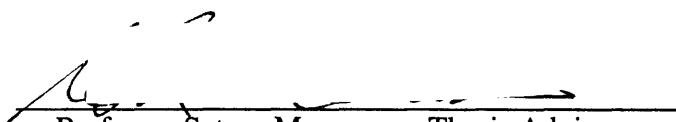
at the

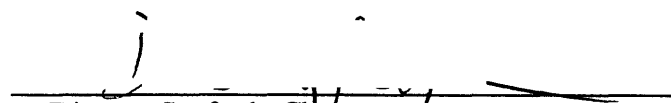Massachusetts Institute of Technology

June, 1995

Signature of Author _____
Department of Chemistry, May 22, 1995

Certified by _____
Professor Satoru Masamune, Thesis Advisor

Accepted by _____
Dietmar Seyferth, Chairman
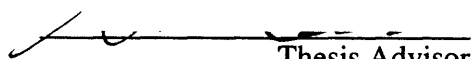Departmental Committee on Graduate Students

This doctoral thesis has been examined by a Committee of the Department of Chemistry as follows:

Professor Jun Liu

Chairman

Professor Satoru Masamune

Thesis Advisor

Professor Frederick D. Greene

"Imagination is more important than knowledge."

Albert Einstein

Acknowledgments

I would like to express my gratitude to my graduate advisor, Professor Satoru Masamune, for creating a research environment that inspired creativity, resourcefulness and independence.

I am deeply indebted to Professor JoAnne Stubbe for her support and her extraordinary example. The time I spent working in JoAnne's laboratory was among the most enjoyable of my graduate school experiences.

I would also like to express my heartfelt thanks to John Roberts, Orin Tempkin, Squire Booker, Mike Absalon, Stuart Licht, Wing Hang Tong, Wei Wu, and Andrea Cochran for their friendship, moral support, and wisdom.

Finally, I would like to thank Professor Robert W. Armstrong, my research advisor at UCLA and my friend, for all that he has taught me and his unwavering encouragement over the years.

Towards the Generation of
Catalytic Antibodies for Glycoside Hydrolysis

by

Pamela Michael Jeffrey England

Submitted to the Department of Chemistry
on May 22, 1995 in partial fulfillment of the requirements for the
Degree of Doctor of Philosophy

Abstract

Two studies, directed towards the generation of antibodies cabable of catalyzing the hydrolysis of β-glycosides, are described. Two different haptens, each designed to elicit antibodies with combining site features cabable of stabilizing the putative transition state for glycoside hydrolysis, were synthesized and used to generate mononclonal antibodies. The first hapten, a 1,4-disubstituted cyclohexene derivative, was designed to be a half-chair conformational mimic of the transition state associated with the hydrolysis of the corresponding glycopyranoside. The second hapten, a 1,4-disubstituted cyclohexane derivative carrying a quarternized amine, was designed to elicit an antibody combining site carboxylate residue that would serve to electrostatically stabilize the positively charged oxocarbonium ion transition state. The results of these studies provide insight into the hapten design features required for the generation of antibodies for glycoside hydrolysis.

Thesis Supervisor: Professor Satoru Masamune

Title: Professor of Chemistry

5

Table of Contents

7

8

Chapter 1

Introduction

Chemists and biologists alike have long been fascinated by nature's ability to generate the complex molecular structures that carry out the remarkable processes of life such as molecular recognition, signal transduction, and catalysis. The area of host-guest chemistry represents one of chemistry's efforts to mimic and understand these ligand/receptor interactions found in nature. That this area warrants such attention is attested to by the award of the 1987 Nobel Prize to three pioneers in this area, namely, Cram, Lehn, and Pederson. This award served as a statement of the importance of continued research in this field and as an inspiration for new ideas.

The chemist's ability to synthesize both small molecule guests as well as slightly larger hosts, has allowed for the design of numerous host-guest systems capable of a variety of functions. In recent years, these host-guest systems have focused on emulating naturally occurring biological systems. Rebek has designed and synthesized self-replicating polymers in effort to model evolution at the molecular level.[1,2] Dougherty has designed a synthetic receptor for the neurotransmitter acetylcholine, demonstrating the importance of the cation-π effect in receptor/neurotransmitter interactions.[3] Breslow has functionalized cyclodextrins in attempt to provide enzyme mimics.[4] These systems, while elegant in both their conception and design, require an intense synthetic effort. Regardless of their function, host-guest systems are necessarily characterized by tight binding interactions between the host and the guest. Even with the aid of molecular modeling, such strong interactions are difficult to achieve through *de novo* design. The result is often synthetic trial and error in order to attain high affinities for the guest by the host. Catalytic antibody research is another area of host-guest chemistry, intent on probing and mimicking enzyme function, which has found an ingenious way to circumvent the synthetic difficulties associated with generating tight binding, specific hosts. Specifically, the immune system is

9

used to generate antibodies (hosts) capable of binding to and catalyzing the chemical transformation of substrates (guests).

The immune system has the remarkable ability to synthesize antibodies that will bind virtually any natural or synthetic molecule with high affinity and exquisite specificity. In terms of the normal functioning of the immune system, antibodies serve to protect organisms from foreign invaders, such as pathogenic bacteria and viruses, parasites, and cancer cells. The primary immune response consists of approximately 10^8 unique antibody molecules, each individually stored on the surface of cells called lymphocytes. A complex screening mechanism allows the immune system to select from this vast array of molecules, antibodies with desired properties. Specifically, when a lymphocyte encounters an antigen (hapten), it undergoes division and differentiation and, subsequently, begins to produce soluble antibody molecules. At the same time, the genes encoding the antibody binding site undergo somatic mutation and affinity maturation to produce structural variants of the antibody. The resulting antibodies have an increased specificity and affinity for the hapten. With the advent of hybridoma technology, it has become possible to exploit the highly evolved machinery of the immune system to generate, *in vitro*, large amounts of homogeneous, high-affinity antibody binding sites with tailor-made specificities.[5] Chemists have combined the diversity and specificity of the immune system with their understanding of chemical reactivity to generate a new class of antibody molecules-- catalytic antibodies.

The concept of inducing antibodies that would possess catalytic potential, in addition to exquisite ligand specificity, has its roots in the seminal contributions of Pauling.[6,7] Pauling proposed that the ability of an enzyme to speed up a chemical reaction stemmed from the complementarity of the enzyme's active site structure to the transition states of the reactions being catalyzed. At the time, thinking about enzymes generally centered on how they fit the substrate and not the transition state. Pauling's views received strong support, however, when transition state analogs were found, as predicted, to bind

enzymes orders of magnitude more strongly than the natural enzyme substrates. Based on this idea of transition state stabilization, W. P. Jencks suggested in 1969 that an antibody made to a synthetic mimic of the transition state for a given reaction should serve to catalyze that reaction.[8] A comparison of enzymes and antibodies provides support for such progressive thinking. Both antibodies and enzymes are high molecular weight proteins characterized by high affinities for their ligands. It has been proposed that, in both cases, most of the protein simply functions as a scaffold for the binding site. Indeed, both enzymes and antibodies have association constants that range as high as 10^{14} M^{-1} for their respective ligands. The fundamental difference between enzymes and antibodies is that the former selectively bind transition states and the latter bind ground states. The other major distinction is that antibody specificity evolves on a time scale of weeks, whereas enzyme specificity evolves over millions of years. Since highly specific, tightly binding antibodies can be obtained for virtually any ligand, Jenck's proposal could be readily tested. By introducing a transition state analog for a particular reaction as a foreign antigen, antibodies that would specifically recognize and bind to the transition state of the chosen reaction could be elicited. These antibodies could then be tested for their ability to catalyze the reaction of interest. The successful generation of catalytic antibodies would lend further support to the notion of transition state stabilization in enzyme catalysis.

The first detailed and well-planned attempt to design a hapten and raise antibodies having catalytic properties was reported by Raso and Stollar in 1975.[9,10] These investigators attempted to prepare *polyclonal* antibodies capable of catalyzing the condensation of pyridoxal phosphate and tyrosine by raising antibodies against a hapten resembling the Schiff base intermediate. This intermediate is formed by condensation of L-tyrosine and pyridoxal phosphate as the first step in pyridoxal phosphate-dependent enzymatic reactions such as transamination, decarboxylation, racemization, etc. (Figure 1.1). While the authors did observe a rate enhancement in the antibody catalyzed transamination, they considered their findings to be of only theoretical interest because the

11

Figure 1.1   Antibody Catalyzed Schiff Base Formation

Hapten
(reduced Schiff base)

Pryridoxal-P   Tyrosine   Schiff base
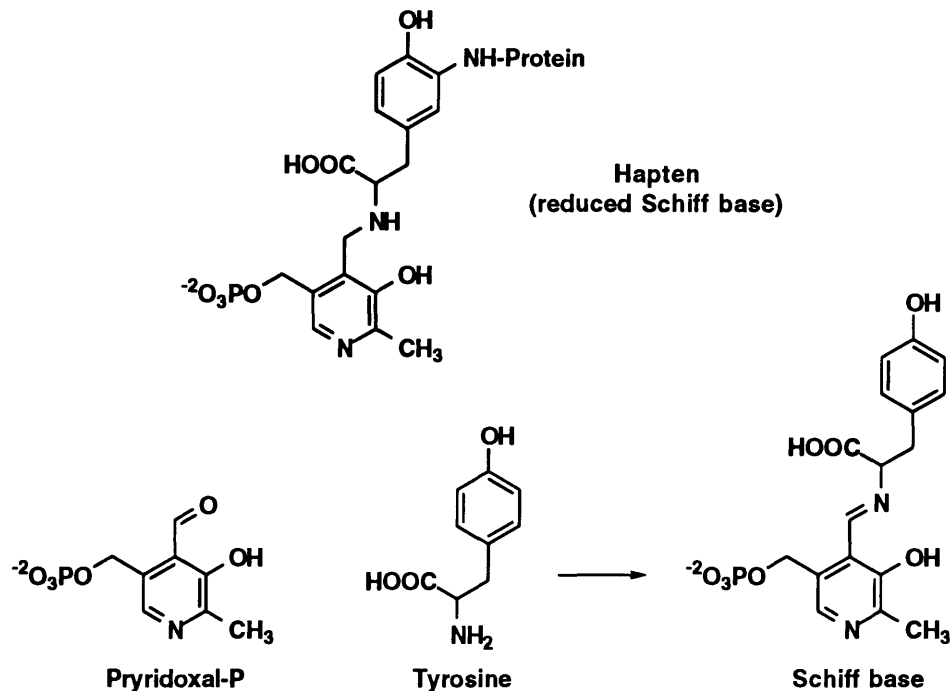
rate enhancement was much less than that provided by enzymes. These authors were, of course, unable to characterize any individual catalyst(s) because they had used polyclonal antibodies (the methods for producing monoclonal antibodies had not yet been reported). Because polyclonal antibodies are most certainly an inseparable mixture of predominantly non-catalytic antibodies and catalytic antibodies (assuming an appropriately designed hapten/transition state analog), detection and characterization of catalytic activity becomes prohibitive.

The first successful generation of catalytic antibodies was reported independently by Lerner and Schultz in 1986.[11,12] Both groups demonstrated that monoclonal antibodies raised to a tetrahedral, negatively charged phosphate and phosphonate transition state analogs could selectively catalyze the hydrolysis of the corresponding carbonates and esters, respectively (Figure 1.2).

12

Figure 1.2 Antibody Catalyzed Carbonate/Ester Hydrolysis

<u>Schultz</u>

O_2N —⟨benzene⟩— ... O⁻ ... P ... O ... $\overset{+}{N}Me_3$

Hapten

O_2N —⟨benzene⟩— O ... $\overset{O}{\underset{}{C}}$ ... O ... $\overset{+}{N}Me_3$

Substrate

<u>Lerner</u>

O_2N —⟨benzene⟩— ... O⁻ ... P ... NH-Protein

Hapten

O_2N —⟨benzene⟩— O ... $\overset{O}{\underset{}{C}}$ ... O

Substrate
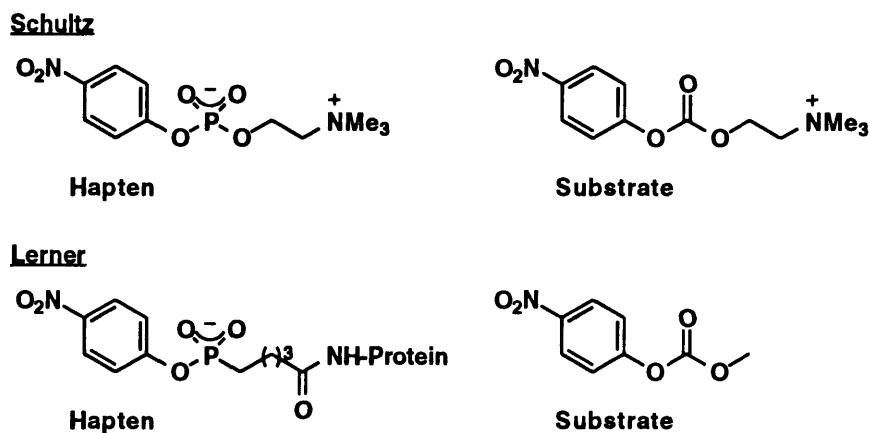
Since that time there have been over 60 examples of catalytic antibodies reported in the literature.[13,14] Catalytic antibodies have been effectively used to test predictions of how binding energy and active site architecture contribute to enzyme catalysis. In addition to transition state stabilization, investigators have demonstrated that antibodies, like enzymes, can achieve catalysis through orientation/proximity effects, participation of combining site residues as acids, bases, and nucleophiles, medium effects, and strain effects.

The role of proximity/orientation effects in catalysis is evidenced by the generation of antibodies that catalyze a Claisen rearrangement, a Diels-Alder reaction, and an oxy-Cope rearrangement, for example. In these reactions, the antibody binding energy serves to reduce the translational and rotational motion of the reactants and, thereby, lowers the entropic barrier to reaction. The antibody catalyzed Claisen rearrangement is an interesting example of antibody catalysis because two different research groups generated antibodies for the identical reaction, yet the nature of the antibodies produced was substantially different. Both Schultz and Hilvert generated antibodies that catalyze the Claisen rearrangement of chorismic acid to prephenic acid (Figure 1.3).[15-18] In microorganisms and plants this reaction is the first committed step in the biosynthesis of tyrosine and phenylalanine, and the enzyme chorismate mutase accelerates this reaction by more than a

13

million. The chorismate catalyzed reaction is characterized by a favorable entropy of activation compared to thermal rearrangement. The bicyclic transition state analog inhibitor of chorismate mutase was used by both groups to raise antibodies. The Schultz group isolated an antibody that increased the rate of rearrangement 10,000-fold while the Hilvert group isolated an antibody that provided only a 200-fold rate enhancement. The mechanism of catalysis by these two antibodies was also apparently quite different. The activation parameters for the Schultz catalyst indicated that their antibody functioned as an entropy trap. Hilvert's catalyst, in contrast, appeared to have a larger effect on the enthalpy of reaction (Figure 1.3). The Schultz antibody clearly supports the notion that conformational restriction plays an important role in this antibody catalyzed reaction, just as it does in the analogous enzyme catalyzed reaction. On the one hand, these two studies serve to highlight the inherent diversity associated with the immune system's response to a single immunogen. On the other hand, these results may also be interpreted to mean that the technology associated with production and/or screening of catalytic antibodies could be improved.

Figure 1.3   Antibody Catalyzed Claisen Rearrangement

Schultz
$k_{cat}/k_{un} = 10^4$
$\Delta S^\ddagger = -1.2$ cal K^{-1} mol^{-1}
$\Delta H^\ddagger = 18.3$ kcal mol^{-1}
$\Delta G^\ddagger = 18.7$ kcal mol^{-1}

Hilvert
$k_{cat}/k_{un} = 10^2$
$\Delta S^\ddagger = -22$ cal K^{-1} mol^{-1}
$\Delta H^\ddagger = 15.0$ kcal mol^{-1}
$\Delta G^\ddagger = 21.3$ kcal mol^{-1}

Transition state analog

R = attachement site
to carrier protein

Chorismate mutase
$k_{cat}/k_{un} = 10^6$
$\Delta S^\ddagger = 0$ cal K^{-1} mol^{-1}
$\Delta H^\ddagger = 15.9$ kcal mol^{-1}
$\Delta G^\ddagger = 15.9$ kcal mol^{-1}

Uncatalyzed
$\Delta S^\ddagger = -12.9$ cal K^{-1} mol^{-1}
$\Delta H^\ddagger = 20.5$ kcal mol^{-1}
$\Delta G^\ddagger = 24.2$ kcal mol^{-1}

14
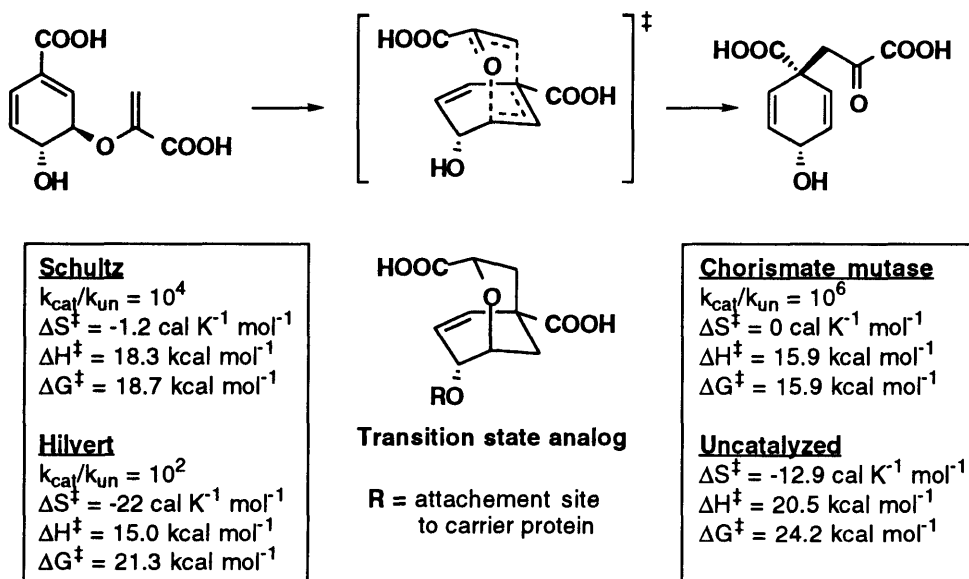
One of the first examples of the participation of an antibody combining site residue in catalysis was reported by Schultz. In the 1950's several investigators showed that electrostatic interactions play an important role in the recognition of charged haptens by antibodies. They found that negatively charged aspartate or glutamate residues were present in the combining sites of antibodies raised toward p-azobenzenetrimethyl-ammonium cation, and conversely, positively charged arginine and lysine residues were present in the combining sites of antibodies elicited against negatively charged p-azobenzoate. Using this idea of electrostatic complementarity, Schultz raised antibodies to an alkylammonium ion in an effort to produce an antibody with a negatively charged carboxylate in its combining site (Figure 1.4).[19] The antibody would serve to bind the corresponding β-fluoroketone substrate, and a combining site carboxylate, correctly aligned to abstract an α-carbon proton, would serve to catalyze the elimination of HF from the substrate. That the carboxylate functioned as a base (pK$_a$ 6.2) was made evident by isotope effect studies which demonstrated that the rate-determining step in the elimination reaction was deprotonation of the β-fluoroketone.[20] This antibody study served as the genesis for subsequent efforts to achieve catalysis through the formation of various catalytic combining site residues.

Figure 1.4 Antibody Catalyzed Hydrogen Fluoride Elimination
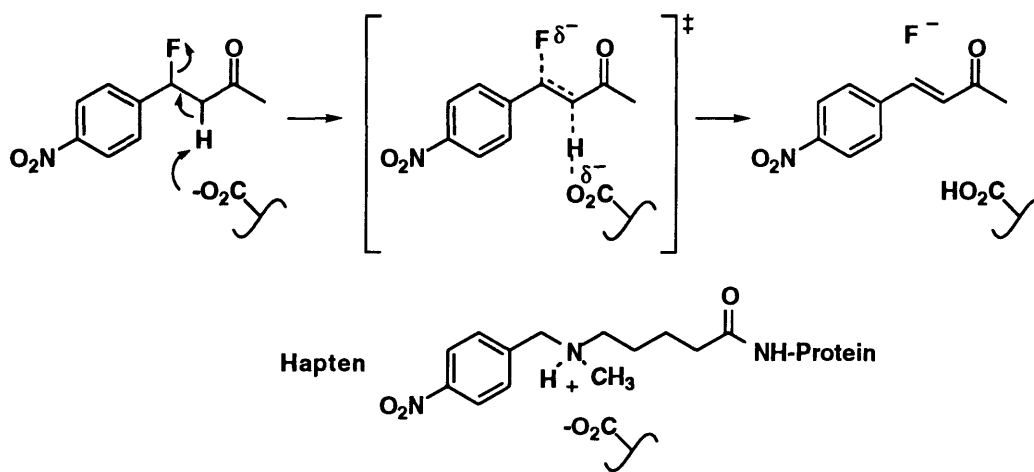
The high catalytic efficiency of enzymes has also been ascribed in part to the rate accelerations caused by extraction of reactants from aqueous solution into the low-dielectric environment of a protein binding site. It is, however, experimentally difficult to measure the extent to which medium effects contribute to the overall rate enhancement of an enzyme catalyzed reaction because enzymes typically display complex catalytic mechanisms. Catalytic antibodies have provided a means of exploring the contribution that medium effects may make in enzyme catalysis. Hilvert, for example, generated an antibody that catalyzes the decarboxylation of a substituted 3-carboxybenzisoxazole with a 19,000-fold acceleration over the rate in aqueous buffer (Figure 1.5).[21,22] The nature of the catalyst's

Figure 1.5 Antibody Catalyzed Decarboxylation
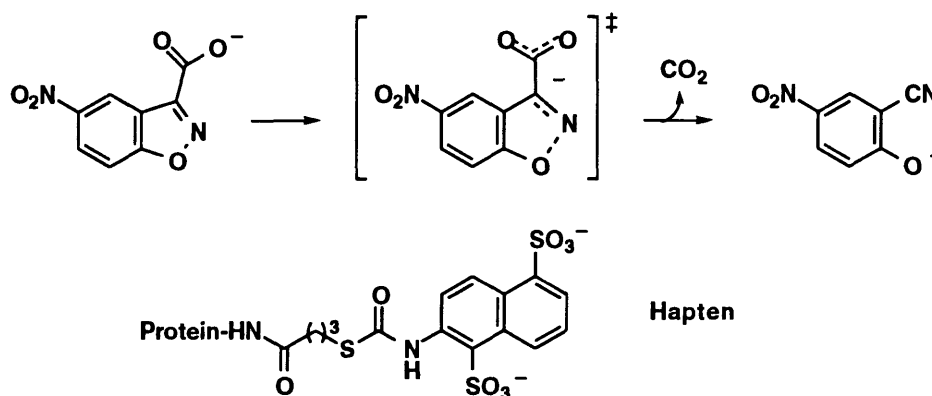
combining site was thoroughly characterized and was found to be apolar and nearly completely inaccessible to water molecules when occupied. Hilvert proposed that the antibody effected catalysis by performing two tasks: first, destabilization of the substrate by stripping the carboxylate of its hydration shell and, thereby, protecting it from hydrogen-bonding interactions with the solvent; and second, stabilization of the charge-delocalized transition state by promoting dispersion interactions within the hydrophobic microenvironment. Indeed, the decarboxylation of 3-carboxybenzoisoxazoles is known to be remarkably sensitive to solvent effects. Hilvert's investigation both elucidates the role of medium effects in catalysis and highlights the fact that antibody combining sites are, in

1 6

general, very hydrophobic environments from which water molecules often are excluded. It is likely that many antibody catalysts achieve rate accelerations as a result of, in part, medium effects.

Strain, or ground state distortion, is another mechanism by which enzymes are believed to achieve catalysis. Interestingly, there is only one report of a catalytic antibody which purports to demonstrate the role of strain in catalysis. Schultz generated antibodies specific for a hapten resembling a distorted conformation of a substrate to catalyze the metallation of porphyrin (Figure 1.6).[23] Ferrochelatase, the terminal enzyme in the heme biosynthetic pathway, catalyzes the biological insertion of iron (II) into protoporphyrin. A potent inhibitor of this enzyme is the bent porphyrin, N-methylprotoporphyrin. The distorted structure of the methylated porphyrin macrocycle results from steric crowding due

Figure 1.6   Antibody Catalyzed Porphyrin Metallation

$$M^{2+}$$

M = Zn, Cu, Co, Mn

Hapten

17
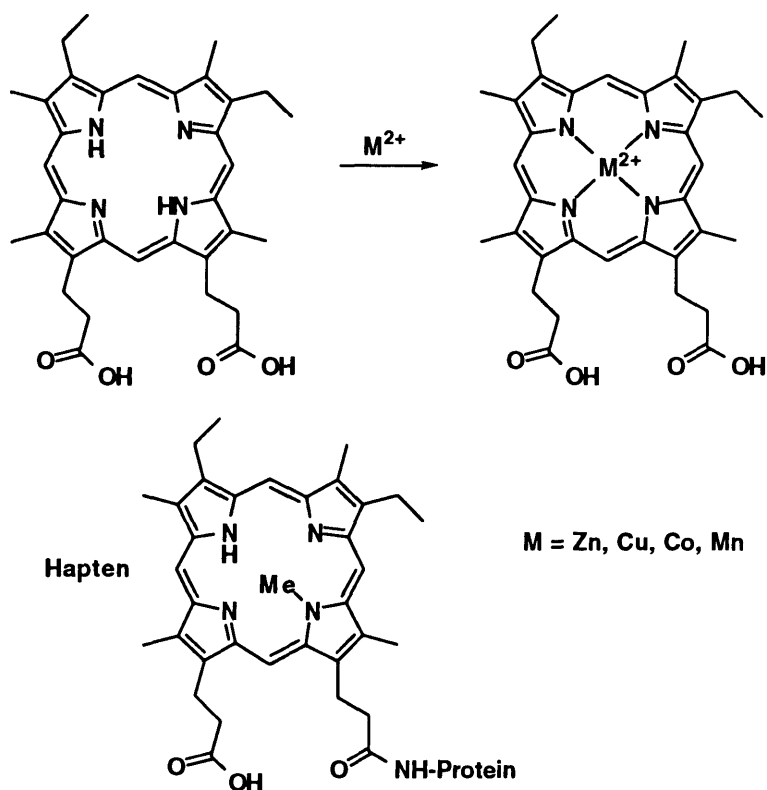
to the internal methyl substituent and is thought to resemble the transition state of porphyrin metallation catalyzed by ferrochelatase. This distortion of the macrocyclic ring system forces the chelating nitrogen lone pairs into a position that is more accessible for binding to the incoming metal ion. Schultz demonstrated that antibodies raised to N-methylmeso-porphyrin catalyzed the metallation of the planar, non-methylated porphyrin substrate and attributed the catalysis to ground state distortion of the substrate in the antibody combining site. It is unfortunate that the authors provided no direct evidence of a porphyrin conformational change upon binding to the antibody. The distinction between transition state stabilization and ground state destabilization, although subtle, is significant. Catalytic antibodies may be especially qualified to elucidate the difference between these two mechanistic alternatives as they can be raised to bind to virtually any ligand.

This first decade of antibody research has been characterized by the production of catalysts for a wide variety of transformations, exemplifying catalytic strategies similar to those of enzymes. Further, the specificity of these antibody catalyzed reactions has often rivaled or exceeded that of enzymatic reactions. Finally, antibody catalyzed reactions typically proceed with rates 10^3- to 10^6- fold faster than the corresponding uncatalyzed reactions and, in some cases, with rates approaching those of enzymes. Despite these remarkable advances, the potential of catalytic antibodies remains, perhaps, largely untapped. The next generation of catalytic antibodies may fulfill their promise to become practical, highly efficient catalysts following several technological developments which appear to be in the offing.

To widen the scope and better the efficiency of catalytic antibodies, investigators are turning their attention to improving each of the stages involved with the production of antibody catalysts. The first stage involved with the production of catalytic antibodies involves eliciting an immune response to a synthetic hapten, typically a stable analog of a transition state for a reaction of interest. Transition state analogs have clearly served well to elicit catalytic antibodies for numerous reactions. However, a few important reactions,

such as peptide and glycoside bond hydrolysis, have eluded the scope of efficient antibody catalysis, suggesting that the hapten designs may be improved. The efforts to hydrolyze peptide bonds, for example, have thus far focused entirely on stabilizing the tetrahedral transition state. Most commonly, phosphate/phosphonate haptens have been utilized as mimics of the charged tetrahedral transition state. The antibodies raised to these haptens, for which there are over 20 examples, have proven to be efficient at hydrolyzing ester bonds, and with few exceptions,[24-26] to be completely incapable of hydrolyzing peptide bonds. Haptens might be better designed to take advantage of the binding energy provided by antibody binding sites (estimated to range as high as 20 kcal/mol). Antibodies might be used to twist a peptide bond out of planarity and, thereby, render it more susceptible to hydrolysis, for example. Indeed, it has been postulated that enzyme catalyzed peptide bond hydrolysis may involve such ground state destabilization. Haptens designed to mimic a distorted peptide substrate represent an as yet untested approach to eliciting peptidase antibodies.

The mechanistic complexity of some reactions, including peptide bond hydrolysis, may, however, preclude the design of suitable transition state analogs. Enzyme catalyzed peptide bond hydrolysis is known to involve the concerted effort of multiple active site residues. In the case of the aspartate proteases there is both an active site acid and a base. While it has proven to be possible to elicit a single acid or base in an antibody combining site, it is substantially more difficult to elicit two catalytic combining site residues. The Masamune group has developed a method that may allow for the generation of antibodies with multiple combining site residues. Termed heterologous immunization, this technique involves manipulating the immune response with two different haptens, each designed to induce the formation of a unique combining site residue.[27] The first hapten is used to generate the initial immune response, and the second hapten is used in the final immunization to select for cross reactive antibodies. The initial effort in this area proved encouraging; cross reactive antibodies capable of hydrolyzing an aryl ester were

1 9

prepared.[27] Further, characterization of the hydrolytic antibody led the authors to conclude that the combining site, indeed, contained both an acid and a base. The structures of the two haptens used are shown in Figure 1.7. Structurally the two haptens are very similar, both contain the tetrahedral geometry associated with the transition state and the two aromatic moieties. The two haptens are dissimilar in that the first hapten contains the positively charged ammonium residue and the second hapten contains the negatively charged phophonamidate, designed to induce the formation of a base and an acid, respectively. Although the antibodies produced did not catalyze the hydrolysis of the amide substrate, heterologous immunization may prove to be a powerful technique in the future.

Figure 1.7   Heterologous Immunization

Hapten One:
primary immunizations

Hapten Two:
final immunization

Ester Substrate: X = O
Amide Substrate: X = N
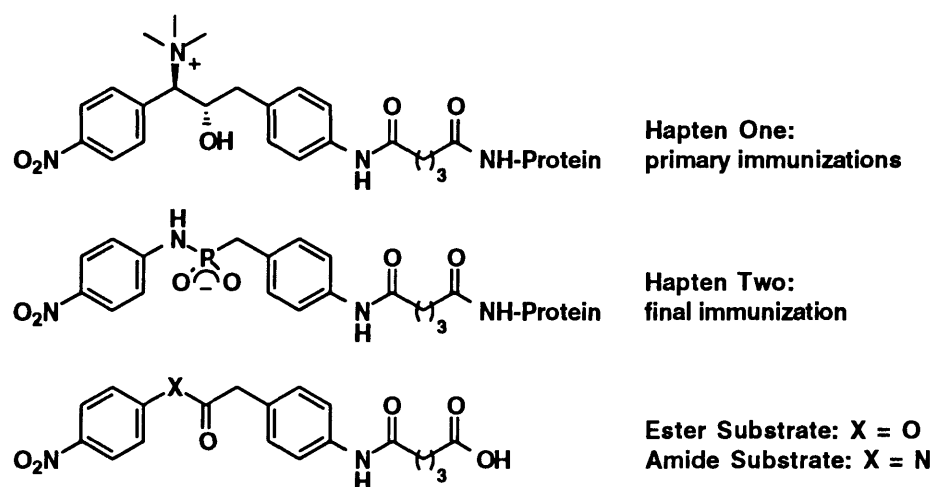
Another strategy for creating more enzyme-like antibodies is being pursued by Lerner. Specifically, a general approach to installing metal binding sites into antibodies has been developed.[28] Many enzymes use cofactors to catalyze reactions, with the protein serving to bring the reaction partners together. A versatile class of enzyme cofactors are transition metal ions, which are involved in a variety of transformations including DNA and protein hydrolysis, redox reactions and acyl group transfers. Unique to metal ions are their small size and readily tunable properties, where ligand or metal substitution can alter the specificity or the course of the catalyzed reaction. In addition, because ligand geometry can

be readily distorted, metal ion catalysis may permit a wider range of catalytic geometries. Taking advantage of the fact that antibody binding sites are composed of two separate peptide chains, Lerner first built a metal binding site into one of the two chains.[29,30] The zinc binding domain of carbonic anhydrase was used as a structural guide to design a series of mutant light chains containing a metal binding domain. These light chains were then recombined with the heavy chain from an antibody specific for fluorescein. The resulting antibody binding sites were found to simultaneously bind both fluorescein and a variety of metals with micromolar dissociation constants. One of these metallo-light chains was then introduced into a murine genome to produce transgenic mice containing the metallo-light chain in their naive antibody light chain repertoire.[28] The transgenic mice were subsequently immunized with fluorescien and anti-fluorescein antibodies were isolated. Sequence analysis of the anti-fluorescein antibodies indicated that several of the antibody combining sites contained the metallo-light chain. In theory, these metallo-light chains will be similarly recruited in an immune response to any hapten. The resulting antibodies may then productively bind a substrate and a metal and, thereby, provide for metal assisted catalysis (Figure 1.8). Further efforts with this newly developed approach will reveal its merits as a means of generating metalloantibody catalysts.

Figure 1.8   Metallo-Antibodies
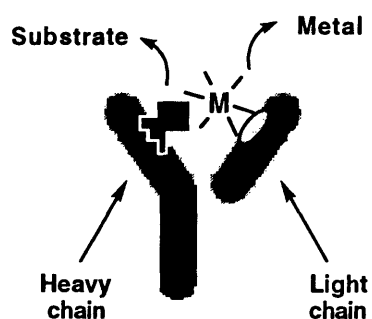
The second stage in the generation of catalytic antibodies involves the production and screening of stable antibody producing cell lines. The repertoire of antibody producing B-cells, resulting from immunization, is first immortilized as hybridomas. The hybridomas
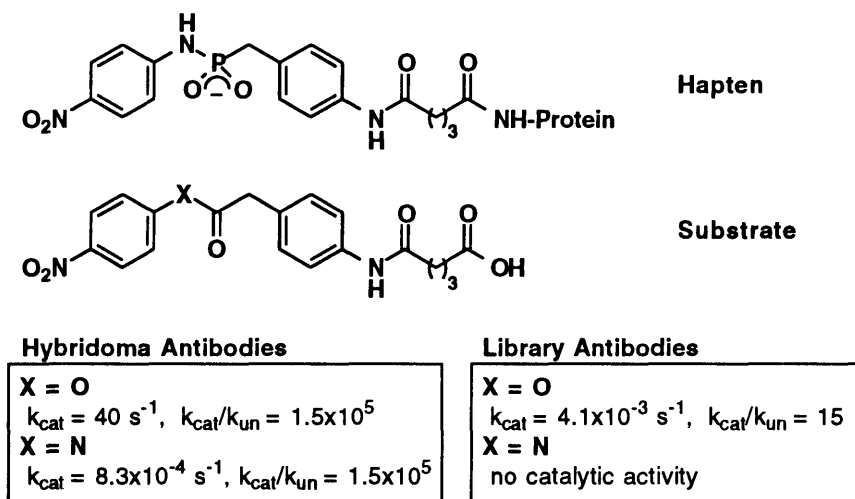
are then screened to select those clones producing monoclonal antibodies that bind the immunizing hapten. Desirable clones, typically 10-50, are pursued for the production of large quantities of monoclonal antibodies. These antibodies are then purified and screened for catalytic activity. There are two limitations associated with this approach to locating a catalytic antibody. First, the number of B-cells that are successfully immortalized as hybridomas and subsequently selected from binding studies with the hapten is often too few in number to constitute a representative sample of the repertoire of antibody producing B-cells. Second, potential catalytic antibodies are initially selected on the basis of binding to hapten, rather than on the basis of catalytic activity. In the end, the result may be that potential catalytic antibodies are simply being missed. That this is a concern is made evident by the aforementioned Claisen rearrangement studies by Schultz and Hilvert. Both investigators used the same immunizing hapten, yet two significantly different catalysts were isolated. Solutions to these problems are being pursued by several investigators.

Lerner, for example, has developed a method for generating combinatorial libraries of antibody binding sites (Fab's) and expressing the Fab's in *Escherichia coli*.[31] These libraries provide a source of novel antibody binding sites, numbering in the millions. Fab's, which function just as efficiently as whole antibodies in terms of binding and catalysis, consist of a truncated heavy and light chain. The construction of these libraries involves the random combination of the heavy and light chains to yield novel Fab's. The creation of the library involves the following: first, a plasmid library is constructed from mRNA isolated from the spleen of a mouse that has been immunized with a hapten; and second, the library clones are then expressed in bacteria using the λ phage expression system. Lerner has demonstrated that this system is capable of expressing on the order of 10^7 unique Fab's. In an initial effort to isolate a catalyst from a library, an Fab combinatorial library was generated from the spleen of a mouse immunized with a phosphonamidate hapten (Figure 1.9).[32] This hapten, a transition state analog for amide/ester hydrolysis, was previously used to generate catalytic antibodies with

22

amidase/esterase activity using standard hybridoma technology. Upon screening the expressed library for Fab's that would bind the hapten, 22 clones were isolated. Purified Fab's from six of these clones were assayed for catalytic activity, and three were found to be active for hydrolysis of the ester substrate. None of these antibodies were, however, nearly as efficient as the original catalyst identified in the hybridoma experiments. In theory, this method should provide a means of identifying greater numbers of catalysts and, therefore, more efficient catalysts. Further efforts with this approach are required to confirm its true efficacy.

Figure 1.9 Catalytic Antibodies from a Combinatorial Library

Hybridoma Antibodies

X = O
k_{cat} = 40 s^{-1}, k_{cat}/k_{un} = 1.5x10^5
X = N
k_{cat} = 8.3x10^{-4} s^{-1}, k_{cat}/k_{un} = 1.5x10^5

Library Antibodies

X = O
k_{cat} = 4.1x10^{-3} s^{-1}, k_{cat}/k_{un} = 15
X = N
no catalytic activity

Hilvert and Schultz are independently pursuing another strategy specifically aimed at improving the efficiency of existing catalytic antibodies.[33,34] Their approach relies on a combination of random mutagenesis and genetic selections. The methodology involves the following steps. First, the gene encoding a particular catalytic antibody is isolated from the hybridoma cell line expressing the catalyst and is inserted into a plasmid expression vector. Next, random mutagenesis is used to create point mutations in the antibody sequence. The new antibody sequences are then excised, amplified, and reinserted into plasmids. Finally, the plasmids are expressed in cells that require the catalytic activity of the antibody for their survival. Schultz, for example, is using a strain of *E. coli* deficient in the biotin

biosynthetic genes to select for an antibody with enhanced hydrolytic activity (Figure 1.10).[33] This antibody, originally generated and characterized using standard hybridoma technology, was shown to have significant esterase activity. By attaching an ester moiety to biotin, the release of biotin is contingent on the esterase activity of the antibody. Biotin is essential for growth of *E. coli*. Deletion of the biotin biosynthetic locus provides a convenient mutation that can be complemented by free biotin supplied by the activity of the catalytic antibody. Hilvert is using a strain of yeast *Saccharomyces cerevisiae* containing a mutation in the gene for the enzyme chorismate mutase to select for an antibody that will catalyze the Claisen rearrangement of chorismate into prephenate with enhanced efficiency.[34] As was discussed above, Hilvert had previously generated a relatively slow catalytic antibody for this reaction using standard hybridoma technology. By expressing mutated versions of this antibody in yeast lacking the corresponding enzyme, Hilvert can select for catalysts with enhanced activity on the basis of the survival of the resulting yeast colonies. Neither Schultz or Hilvert have, thus far, generated antibodies with enhanced activity. Nonetheless, as these systems are newly developed, they remain a potentially powerful means of generating and selecting for highly efficient catalytic antibodies.

Figure 1.10 Catalytic Antibodies *In Vivo*
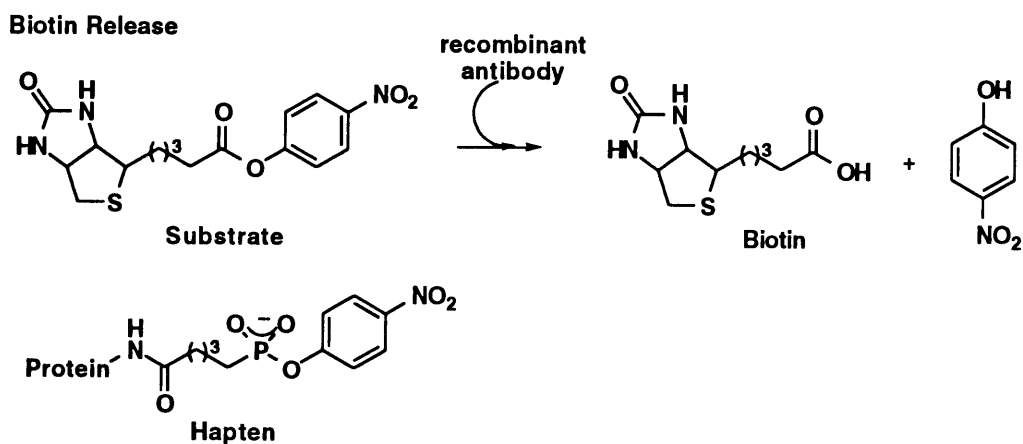
Hilvert and Green have independently developed a new screening methodology.[35,36] Termed catELISA, this technique provides a means of simultaneously

assaying large numbers of antibodies for catalytic activity at a much earlier stage in antibody production protocol than is provided by the standard assay methods. According to the standard screening protocol, antibody producing hybridoma cell lines, typically 5000, are initially screened for binding to the immunizing hapten (as opposed to being screened for catalytic activity). This screen narrows the number of hybridoma cell lines that are further pursued for the production of monoclonal antibodies to, typically, 100 cell lines. It is only after large quantities of monoclonal antibodies, typically 50 unique antibodies, have been generated and purified from these cell lines that they are screened for catalytic activity. Thus, screening for catalytic activity occurs in the final stage of the protocol, when the number of possible catalysts has been considerably lowered relative to the original number of potential catalysts.

The catELISA provides a powerful alternative to the existing screening methodology. Specifically, instead of screening the original (5000) hybridoma cell lines for binding, they may now be screened directly for catalytic activity. Shown schematically in Figure 1.11, catELISA is a colorimetric assay for product production. The antibody

Figure 1.11   The catELISA Screening Assay
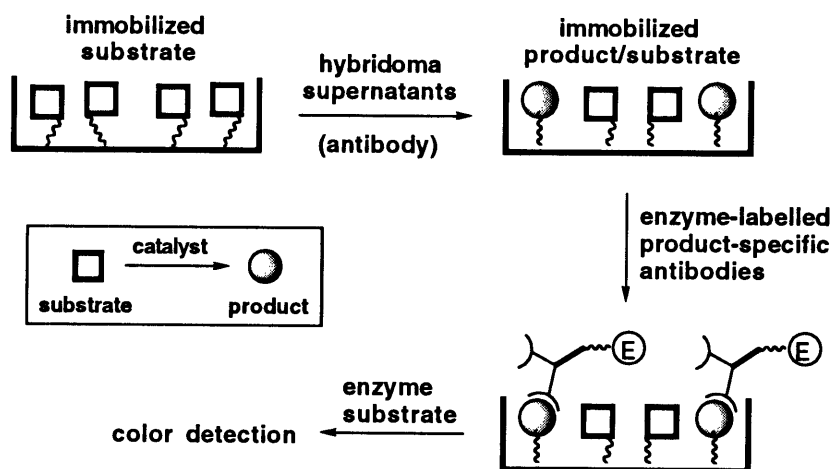
substrate is immobilized on microtiter plates and is then bathed in hybridoma cell culture supernatants. These cell culture supernatants contain secreted antibody. If the antibodies are catalytically active, they will transform the immobilized substrate into an immobilized

2 5

product. Product-specific antibodies that are linked to the enzyme peroxidase, are then applied to the microtiter plate. Finally, the peroxidase substrate is applied to the microtiter plate and the peroxidase enzyme converts this substrate to a colorimetrically active product. The peroxidase enzyme is only present in the microtiter plate wells containing the antibody product and, therefore, serves to identify antibody catalysts.

In an initial effort to demonstrate the efficacy of this methodology, Green raised antibodies to a phosphonate transition state analog for amide/ester hydrolysis.[35] Phosphonate transition state analogs have been previously shown to provide antibodies with esterase activity and, less commonly, with amidase/peptidase activity. A total of 1570 antibodies were screened for catalytic activity against ester and amide substrates using the catELISA screen. Nine of these antibodies were found to catalyze the hydrolysis of an ester substrate, while none hydrolyzed an amide substrate. Following further kinetic characterization, one of the esterase antibodies proved to be a highly efficient catalyst. Notably, of the 1570 hybridoma clones screened, 970 were found to produce antibodies that bound the hapten. According to the standard protocol for identifying catalytic antibodies, an average of only 50 of the 970 hapten binding antibodies would have been pursued for catalytic screening, and the esterase antibody may, therefore, have been overlooked.

This point is made salient in Hilvert's initial use of the catELISA methodology.[36] Prior to the development of catELISA, Hilvert identified a catalyst for a Diels-Alder reaction using the standard protocol for identifying catalytic antibodies.[37] Specifically, following the standard protocol, hybridomas were initially screened for binding to the hapten. From this initial screen, only five "high-affinity" antibodies were further pursued for the generation of large quantities of pure monoclonal antibodies. The five antibodies were then assayed for catalytic activity, and one was found to catalyze a Diels-Alder reaction. With the development of catELISA, Hilvert has recently gone back and screened all of the original hybridomas for catalytic activity. From this screen, four new Diels-Alder

2 6

catalysts were identified and one was judged to be substantially more active than the originally identified catalyst (kinetic data was not provided).[36] These four catalysts were apparently not pursued in the initial study because they demonstrated a relatively poor affinity for the hapten. In addition to demonstrating the efficacy of the catELISA, this study serves to illustrate an important concept in catalysis. Namely, stabilization of the transition state alone is necessary but not sufficient to provide catalysis, which requires differential binding of the substrate and the transition state. An initial screen for potential catalysts that is based solely on high antibody affinity for the hapten may, indeed, serve to eliminate catalytic antibodies from the pool of antibodies that is subsequently tested for catalytic activity. The catELISA, which provides an effective alternative to existing strategies for identifying catalysts, will become increasingly more important as the methods for producing large combinatorial libraries of antibodies are further developed.

The use of improved transition state analogs and novel antibody production technologies combined with direct screening methodologies may afford efficient antibody catalysts for more demanding chemical reactions and challenging biomedical applications. Glycosidase type antibodies, for example, might find use as therapeutic agents to selectively hydrolyze carbohydrate coats of viruses, cancer cells, or other physiological targets. Described in the following chapters are our efforts towards the production of glycosidase antibodies. Chapter two provides a summary of the literature concerning the chemical, enzymatic, and antibody catalyzed hydrolysis of glycosides that served to influence our hapten designs. Chapter three describes the design and synthesis of the haptens. Chapter four details the production and characterization of antibodies generated to the haptens. Chapter five provides the experimental details surrounding these studies.

Chapter 2

Background

The generation of catalytic antibodies necessarily begins with a thorough analysis of the putative transition state for the reaction of interest. In the case of glycoside hydrolysis, consideration of both the enzyme catalyzed and the uncatalyzed reaction provided insight into the specific requirements for glycoside hydrolysis. Our examination of the enzyme catalyzed process included a review of structural and mechanistic data combined with a survey of inhibitors of the reaction. Our study of the uncatalyzed process involved a survey of chemical model systems. The insights provided by each of these investigations are presented in this chapter. Reported progress towards the generation of catalytic antibodies for glycoside hydrolysis is also presented.

2.1. Enzymatic Glycoside Hydrolysis

Lysozyme, the most thoroughly studied glycoside hydrolyzing enzyme (glycosidase), was selected as the representative for the enzyme catalyzed hydrolysis of glycosides.[38] Lysozyme, a 1,4-β-N-acetylmuramidase, selectively cleaves the glycosidic bond between the C-1 atom of N-acetylmuramic acid (NAM) and the O-4 of N-acetylglucosamine (NAG) found in the natural cell wall peptidoglycan of gram negative bacteria. The enzyme binding site for the NAM-NAG copolymer substrate consists of six subsites labeled A-F (Figure 2.1).

Figure 2.1   Lysozyme Substrate and Binding Site
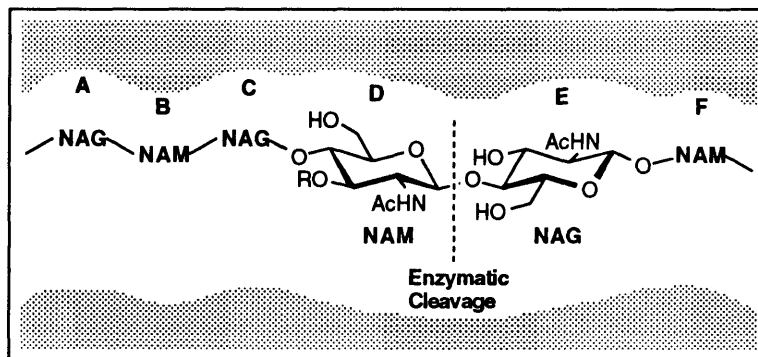
Each subsite is filled by alternating NAM and NAG residues. Enzymatic cleavage occurs between a NAM residue in the D subsite and a NAG residue in the E subsite.

The currently accepted catalytic mechanism of action of lysozyme includes the following three mechanistic features (Scheme 2.1).[39,40] First, the pyranoside is distorted from the chair conformation to a half-chair conformation upon binding to the D subsite. Second, a glutamate residue (Glu-35), acting as a general acid catalyst, facilitates bond rupture by donating a proton to the C(4)-O of the leaving group. Third, the developing oxocarbonium ion is electrostatically stabilized by an aspartate residue (Asp-52). Following departure of the leaving group, the carbonium ion is stereochemically quenched by solvent or a saccharide acceptor which enters the subsites vacated by the leaving group.

Scheme 2.1   Lysozyme Mechanistic Features
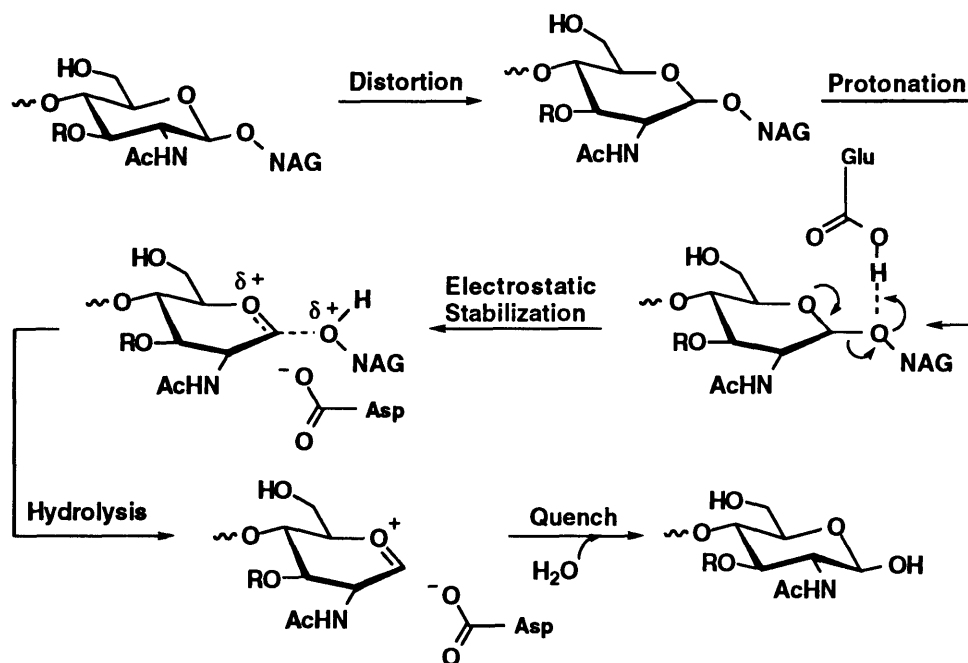
These three proposed mechanistic features (distortion, protonation, and electrostatic stabilization) act in concert to facilitate hydrolysis. Lysozyme's mechanism of action has been extensively probed by several investigators. A brief summary of the data concerning the importance of each of these three mechanistic features is presented.

2.1.a. Distortion

Distortion of the pyranose ring has been the most contentious feature of the mechanism. Efforts to evaluate the importance of this mechanistic feature have focused on structural analyses, binding and hydrolysis experiments, and theoretical studies.

In 1967 Phillips proposed, on the basis of model building, that the enzyme's role in catalysis was to induce and stabilize a conformational change in the substrate.[40] Specifically, upon binding to the D subsite, the pyranose ring is distorted from the normal chair conformation to the half-chair conformation in which the carbon atoms 1,2, and 5 and the ring oxygen all lie in the same plane. The strain associated with this distortion of the substrate is then relieved in the transition state; the transition state resembles an oxonium ion for which the most stable conformation is the half-chair.

The first indication that this hypothesis was correct resulted from binding[41,42] and hydrolysis[43] studies with hen egg-white lysozyme (HEWL) and a series of substrates. The measured free energies of association and cleavage rates of a variety of oligosaccharides with HEWL suggested that the binding of the sugar residue in the D subsite was energetically unfavorable by approximately 6 kcal/mol. Presumably, the chair to half-chair conformational change of the D subsite saccharide is the source of this unfavorable energy term. Indeed, although probably fortuitous, it was noted in the hydrolysis studies that the chair to chair interconversion barrier for six membered rings is also approximately 6-10 kcal/mol.[44] These studies prompted several authors to conclude that the proposed role of the enzyme in inducing and stabilizing a conformational change in the substrate was correct.

The most convincing support for Phillips' hypothesis was provided by a recent crystal structure of HEWL with a truncated substrate.[45] The trisaccharide (2-acetamido-2-deoxy-D-muramic acid)-β(1-4)-(2-acetamido-2-deoxy-D-glucosyl)-β(1-4)-(2-acetamido-2-deoxy-D-muramic acid), β,β,β-MGM, was co-crystallized with HEWL and the structure determined to 1.5 Å resolution. The structure of β,β,β-MGM bound to the B, C and D

subsites indeed revealed that the β-NAM residue bound in the D subsite is distorted from the expected chair conformation **1** towards a half chair conformation **2** (Figure 2.2). When modeled in the chair conformation, the D subsite saccharide makes several unfavorable contacts with the enzyme. Specifically, the substrate's C-5 hydroxymethyl group and the O-3 lactyl group are not accommodated in the binding site. When modeled in the half-chair conformation, on the other hand, these unfavorable contacts are eliminated.

Figure 2.2. The Lysozyme Unbound and Bound Substrate Conformations

Unbound Conformation   Enzyme bound Conformation

Chair Conformation   Half Chair Conformation
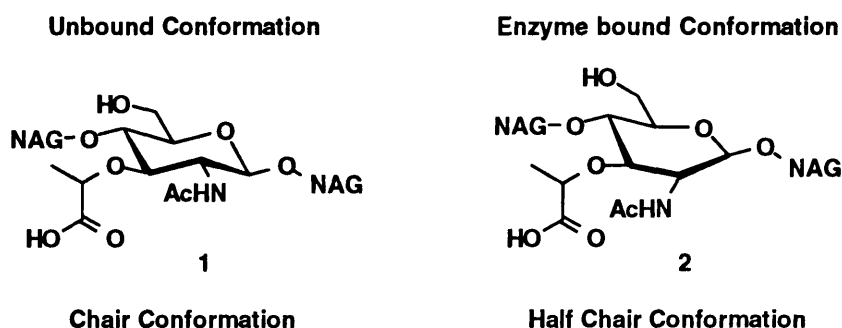
A number of other studies do not, however, support the notion of ground state distortion. An ^{1}HNMR study of the binding of β,β,α-MGM to HEWL by Patt, for example, suggested there was no difference in the conformation of the free and bound D subsite saccharides.[46] The coupling constant (J) between C(1)-H and C(2)-H, diagnostic of the dihedral angle between these two protons, was used to delineate the conformations of the complexed and the uncomplexed D subsite saccharides. Both the bound and the unbound D subsite saccharides had a $J_{1,2}$ equal to 2.6 Hz, indicative of a dihedral angle of 60°. As the C1(H)-C2(H) dihedral angle of the α-anomer of a saccharide in the chair conformation is 60°, the authors concluded that both the complexed and the uncomplexed D subsite α-anomer saccharides sugars existed in the chair conformation. The relevance of this particular result becomes questionable, however, in light of the fact that the natural lysozyme substrate is composed of all 1,4-β-linked saccharides. In addition, there is no

31

crystallographic evidence for the binding of the α-anomer of a NAM residue in the D subsite.

Several theoretical studies have also attempted to devalue the importance of strain in the catalytic hydrolysis of oligosaccharides by HEWL. Conformational energy calculations performed on oligosaccharide substrate models "binding" in the B, C, and D subsites suggested that they could do so without distortion of the ring in the D subsite.[47] A similar conclusion was reached from energy minimization calculations done on a model of a hexasaccharide "binding" in all six subsites (A-F) of HEWL.[48] While these two studies stressed that it was unnecessary to invoke distortion of the substrate in order to accommodate saccharide binding in the D subsite, the calculations also produced, with comparable computed energies, saccharides that were distorted from the full chair conformation.

The role of substrate distortion in the enzyme catalyzed hydrolysis of glycosides remains controversial. While there is crystallographic and energetics data to support a role for distortion in catalysis, the solution structural data and the theoretical studies suggest that ground state distortion does not play a role in the lysozyme catalyzed hydrolysis of glycosides.

2.1.b. Protonation

The role of the active site carboxylic acid (Glu-35) in catalysis is a generally accepted feature of the lysozyme mechanism. The evidence that Glu-35 acts as a general acid catalyst comes from X-ray crystallographic studies, pK_a determinations, and site directed mutagenesis experiments.

The role of Glu-35 as a proton donor is supported by several crystallographic studies. In the 1.5 Å crystal structure of the MGM-HEWL complex, Glu-35 is hydrogen bonded to the glycosidic oxygen atom of the scissile bond.[45] Such a preformed hydrogen bond between these two atoms certainly could serve to facilitate the proton transfer event during catalysis.

The pKa of Glu-35 supports its role as a general acid catalyst in the lysozyme mechanism. The pH difference spectra of native HEWL compared with derivatized HEWL (Glu-35 was esterified) indicated a pKa value of 6.1-6.5 for the acid.[49,50] The crystallographic data substantiates this perturbed pKa value; the carboxyl group of Glu-35 is situated in a relatively hydrophobic pocket.[45]

Site-directed mutagenesis experiments provide further support for the importance of Glu-35. When Malcolm replaced glutamic acid 35 with glutamine the resulting mutant enzyme was completely inactive against several lysozyme substrates.[51]

2.1.c. Electrostatic Stabilization

The role of the active site carboxylate (Asp-52) in lysozyme catalysis has been a matter of some debate over the years. The original proposal, that Asp-52 in HEWL functions to electrostatically stabilize the transition state oxocarbonium ion through ion-pairing, has been challenged. Others have proposed that the ion pair 3 collapses to form the covalent enzyme adduct 4 (Figure 2.2). The hydrolysis of 4 by hydroxide is then facilitated by the antiperiplanar orbital overlap associated with the α-anomer. Efforts to distinguish between these two possibilities have relied primarily upon structural studies and mechanistic experiments.

Figure 2.2 Amended Role for Asp-52 in Lysozyme
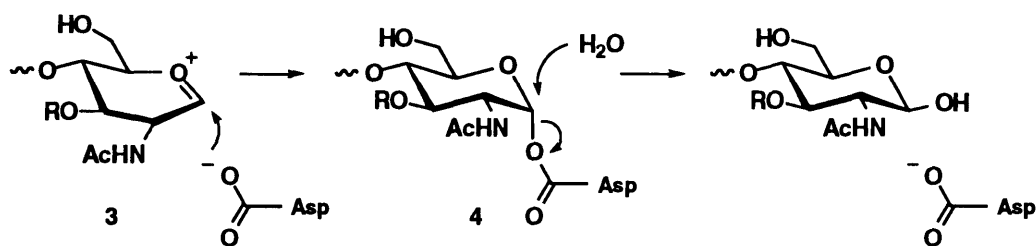
In the case of HEWL, there is no experimental evidence to support the formation of a covalent enzyme adduct. The crystal structure of the MGM-HEWL complex indicates that the formation of a covalent enzyme adduct is, in fact, precluded by both distance and stereochemical requirements.[45] The distance between the Asp-52 nucleophilic oxygen and

33

the anomeric center is 2.3 Å. The length of a covalent C-O bond (1.5 Å) requires that Asp-52 must be 0.8 Å closer to the anomeric center in order for a covalent bond to form. Stereochemical considerations also suggest the formation of a covalent enzyme adduct is unlikely in the case of HEWL. Specifically, the *syn* lone-pair oribitals on Asp-52 are not favorably oriented for the formation of a covalent acylal bond with the anomeric carbon atom. In addition to this crystallographic data, there is also no mechanistic data to support the notion of a covalent enzyme adduct in the case of HEWL. The interaction between the oxocarbonium ion and Asp-52 in lysozyme appears to be that of a long-lived ion pair.

The formation of a covalent enzyme-substrate adduct has been observed, however, in another β-glucosidase. Withers has unequivocally demonstrated the active site glutamate residue in β-glucosidase from *Agrobacterium* functions as a nucleophile.[52] In this particular glucosidase, the glutamate residue is analogous to the aspartate residue in lysozyme. Specifically, Withers used the substrate analog 2,4-dinitrophenyl- 2-deoxy-2-fluoro-β-D-glucopyranoside to trap a covalent enzyme adduct (Figure 2.3). Substitution of

Figure 2.3 Evidence for a Covalent Glycosyl-Enzyme Adduct
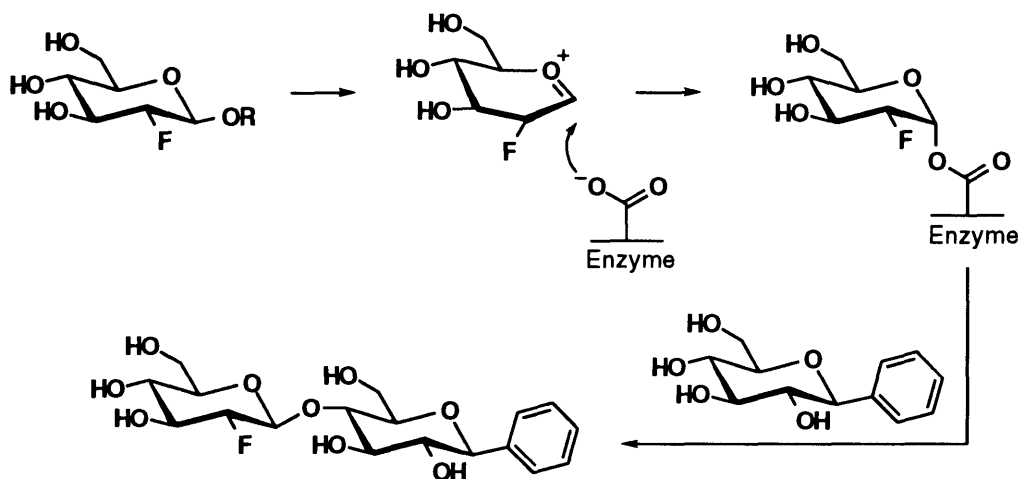
an electronegative fluorine atom for the C-2 hydroxyl group served to destabilize the oxocarbonium ion transition state in terms of both its formation and its breakdown. The highly labile 2,4-dinitrophenoxy leaving group, on the other hand, served to increase the

3 4

rate of formation of the oxocarbonium ion transition state at the same time. Together, these two design features allowed for the build up of the putative glycosyl enzyme adduct. The covalent 2-fluorodeoxyglucosyl enzyme intermediate was identified spectroscopically through ^{19}FNMR. Further, the inactivated enzyme was reactivated upon treatment with β-D-glucosylbenzene, which served as the acceptor in a transglycosylation reaction (Figure 2.3).

It is likely the case that the oxocarbonium ion-carboxylate ion-pair is stable in the case of some glucosidases and that it collapses to a covalent adduct in other glucosidases. It is important to point out that, in either case, the importance of the carboxylate in accelerating the rate of hydrolysis is evident. The transition state for both hydrolytic pathways, which includes electrostatic stabilization of the oxocarbonium ion transition state by the active site carboxylate, is identical and has already been reached at the point at which these two mechanistic alternatives diverge.

2.2. Enzyme Inhibitors

Insight into the key features associated with the transition state for glycoside hydrolysis is furthered by the results of inhibition studies with compounds designed to reversibly bind to glucosidase enzyme active sites.[53-55] Transition state theory requires that enzymes preferentially bind to and stabilize transition states over substrates or products.[8] In fact, transition state analogs often do serve well as enzyme inhibitors. In these cases, the association constant between an enzyme and its inhibitor serves as an indication of the inhibitor's structural similarity to the transition state. There are three classes of reversible glucosidase inhibitors, each designed with the three transition state features associated with glycoside hydrolysis (distortion, protonation, electrostatic stabilization) in mind. A brief discussion of the three classes of glucosidase inhibitors presented in this section serves to further elucidate the importance of each of these transition state features. This survey of glucosidase inhibitors is limited to monosaccharide inhibitors designed to mimic the glycon portion of the transition state. For the purposes of

comparison, inhibition constants with one enzyme, β-glucosidase from sweet almonds, are presented (exceptions are specifically noted in the text).

2.2.a. Half-Chair Conformational Mimics

The half-chair conformation of the pyranose ring in glycoside hydrolysis has received much attention. It has been proposed that glucosidase substrates undergo a chair to half-chair conformational change, prior to hydrolysis, upon binding at the enzyme active site (ground state distortion). Others have argued that the half-chair conformational change does not occur in the ground state, and that rather than being a precursor to hydrolysis, the conformational change occurs only as the oxocarbonium ion transition state is approached.

Figure 2.4   Half-Chair Conformation Mimic Glucosidase Inhibitors

5

6

7
$K_I = 8.8 \times 10^{-4}$ M

8
$K_I = 3.6 \times 10^{-5}$ M

9
$K_I = 3.7 \times 10^{-5}$ M

10
$K_I = 8.0 \times 10^{-6}$ M

11
$K_I = 8.4 \times 10^{-6}$ M

12
$K_I = 1.4 \times 10^{-5}$ M

36
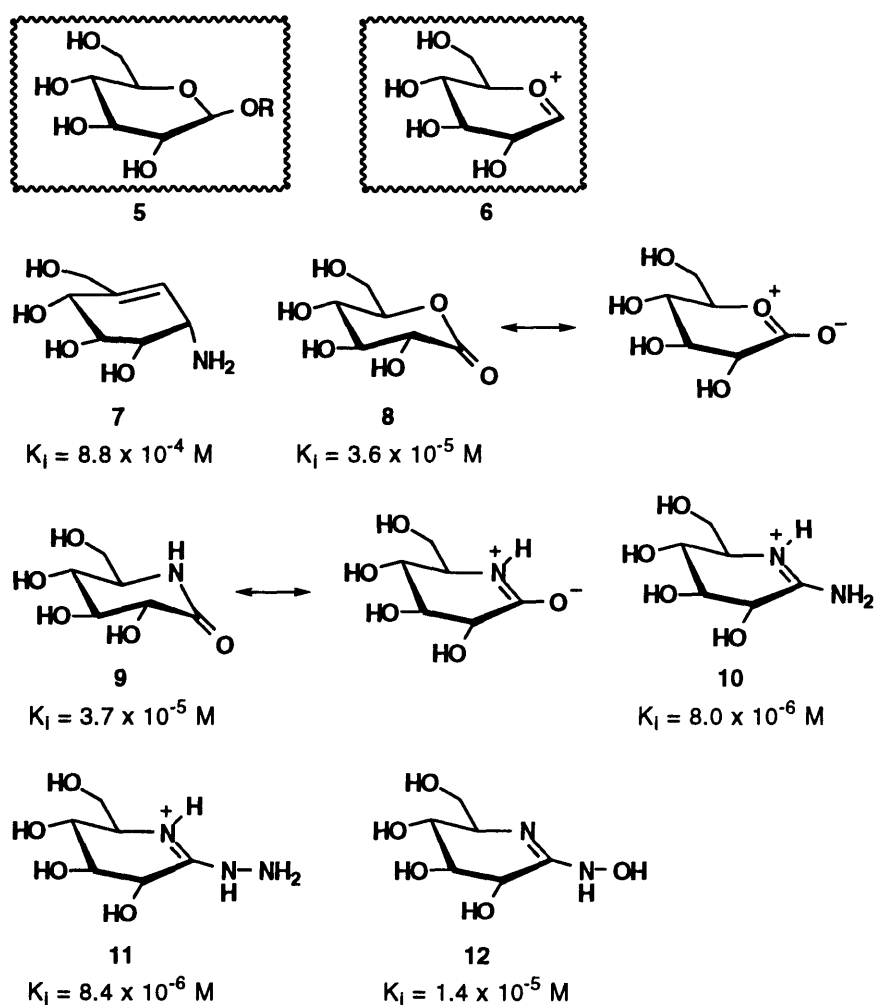
In either case, the enzyme stabilizes a half-chair conformation through specific contacts with the substrate/transition state. Conformational mimics of the half-chair distorted substrate **5** and the transition state **6** represent one class of glucosidase inhibitors (Figure 2.4).

Valienamine **7** is a moderate competitive inhibitor of β-glucosidase and a significant inhibitor of yeast α-glucosidase ($K_i = 1.8 \times 10^{-5}$ M).[53] The aminocyclitol **7** is in a half-chair conformation as a result of the double bond between C-5 and C-7. The position of the C-7 sp^2 center in **7** is corresponds in position to that of the endocyclic oxygen atoms in **5** and **6**. However, because the double bond in **7** is not ideally positioned to overlap with both sp^2 centers in **5** and **6**, valienamine **7** is an imperfect conformational mimic of **5** and **6**.

Significant competitive inhibition of β-glucosidase is observed with d-gluconolactone **8** and d-gluconolactam **9**.[56] In their uncharged resonance forms, **8** and **9** only somewhat resemble **5** and **6** with the sp^2 hybridization at C-1 corresponding to the anomeric centers in **5** and **6**. In their minor, zwitterionic resonance forms, however, **8** and **9** adopt half chair conformations analogous to that of **5** and **6**. In addition, **8** and **9** mimic the carbocation-like nature of **5** (the significance of this is detailed in Section 2.2.c.).

Amidine **10** and amidrazone **11** are strong β-glucosidase inhibitors and amidoxime **12** is a significant inhibitor.[57,58] Inhibitors **10**, **11**, and **12** are the best conformational mimics of **5** and **6** described to date; the half-chair conformation of **10**, **11** and **12** is identical to that ascribed to **5** and **6**. In addition, because both amidine **10** (pK$_a$ 10.6) and amidrazone **11** (pK$_a$ 8.7) are protonated at physiological pH, they also mimic the carbocationic nature of **6**. The importance of this feature, evidenced by the difference in the inhibitory properties of **10** and **11** compared with **12** (pK$_a$ 5.6), is discussed in Section 2.2.b.

2.2.b. Proton Acceptor Mimics

An important step in enzyme catalyzed glycoside hydrolysis involves protonation of the leaving group oxygen (**13**, Figure 2.5). An active site carboxylic acid residue has been implicated in this function in the case of several glycosidases. Compounds designed to act as proton acceptor mimics represent another class of glycosidase inhibitors (Figure 2.5).

Figure 2.5 Proton Acceptor Mimic Glucosidase Inhibitors
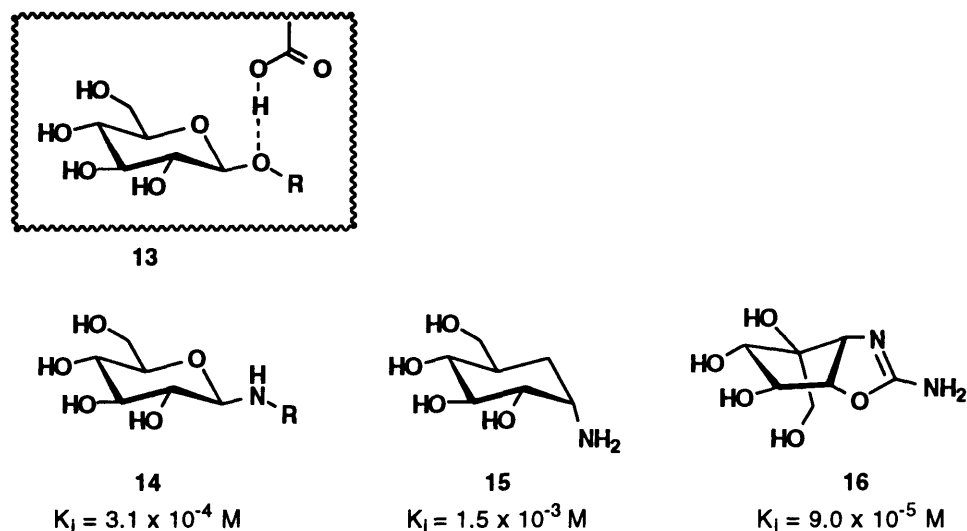
Glucosylamine **14** is a moderate inhibitor of β-glucosidase and a strong inhibitor of β-glucosidase from *Aspergillus Wenti* (K_i = 1.6 x 10^{-6} M).[59] The basic exocyclic amine in **14**, acting as a proton acceptor, supposedly forms a hydrogen bond with the active site carboxylic acid. Indeed, while N-benzylated analogs of **14** are also β-glucosidase inhibitors, N-arylated and N-acylated analogs of **14** are not inhibitors.[59] This is likely a result of the reduced basicity of the latter.
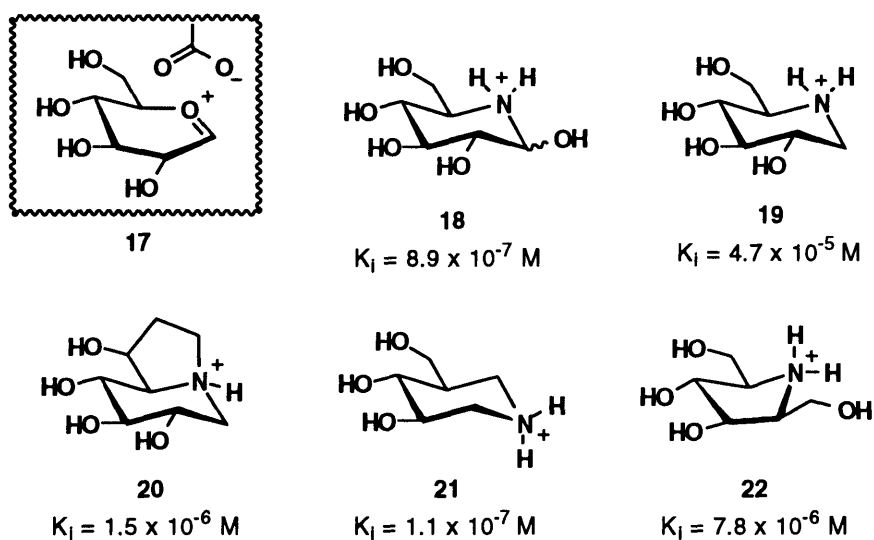
Validamine **15** is a moderate inhibitor of α-glucosidase from yeast (K_i = 5.8 x 10^{-4} M) and a weak inhibitor of β-glucosidase.[53] While the exocyclic amine may serve as a proton acceptor, replacement of the ring oxygen with a methylene group is apparently detrimental to efficient interaction with glucosidases.

3 8

Trehalamine **16** is a significant inhibitor of β-glucosidase from *Agrobacterium* despite its lack of any obvious structural similarity to pyranose **13**.[60] The oxazoline substructure in **16** is accurately positioned and sufficiently basic so as to allow for its functioning as a proton acceptor. Further, the spatial arrangement of the hydroxyl groups in **16** appears to closely resemble the positions of hydroxyl groups on the pryanosyl cation **6** (Figure 2.4).

2.2.c. Cation Mimics

Cation mimics represent a third class of glycosidase inhibitors. These compounds are designed to mimic the positive charge on the cationic oxocarbonium ion transition state (**17**, Figure 2.6) and, thereby, form an ion-pair with the active site carboxylate that stabilizes the transition state (Figure 2.6).

Figure 2.6 Cation Mimic Glucosidase Inhibitors

17

18
$K_i = 8.9 \times 10^{-7}$ M

19
$K_i = 4.7 \times 10^{-5}$ M

20
$K_i = 1.5 \times 10^{-6}$ M

21
$K_i = 1.1 \times 10^{-7}$ M

22
$K_i = 7.8 \times 10^{-6}$ M

Nojirimycin **18** is a very strong inhibitor of β-glucosidase.[59] The endocyclic amine, protonated at physiological pH (pK_a 5.3), likely forms an ion pair with the active site carboxylate. The importance of the exocyclic C-1 hydroxyl group, in terms of stabilizing enzyme-inhibitor interactions, as well as the basicity of the endocyclic amine is highlighted by a comparison of the inhibitory properties of **18** with **19** and **20**.

Deoxynojirimycin **19** is a significant inhibitor and castanospermine **20** is a strong inhibitor of β-glucosidase.[59,61] Deoxynojirimycin **19**, although structurally very similar to **18**, is, nonetheless, a less potent inhibitor. Indeed, inhibitor **19** (pK_a 6.3) lacks the exocyclic C-1 hydroxyl group as well as the amine basicity associated with **18**.

Castanospermine **20** is considered to be a derivative of deoxynojirimycin **19**. Although also lacking the exocyclic C-1 hydroxyl group in **18**, castanospermine **20** is a more potent inhibitor than deoxynojirimycin **19** because it is closer to nojirimycin **18** in terms of amine basicity (pKa 6.09).[61]

Isofagomine **21**, a recently synthesized inhibitor, is a very strong inhibitor of β-glucosidase.[62] The positively charged amine in **21**, which corresponds in position to the anomeric center in the substrate, is apparently able to interact quite favorably with the active site carboxylate residue. Notably, inhibitor **21** lacks the C-2 hydroxyl group.

The cation mimic **22** is a strong inhibitor of β-glucosidase.[63] As with the polyhydroxypyrrolidine inhibitor discussed in the preceding section, the spatial arrangement of the hydroxyl groups in **22** apparently resembles the arrangement of hydroxyl groups in the transition state **17**. Again, the inhibitory properties associated with **22** arise, primarily, as a result of the basic endocyclic amine which, presumably, ion pairs with an active site carboxylate residue.

2.2.d. Summary

Taken together, these inhibitors do not imply that there is a single superior inhibitor design. Rather, they indicate the importance of each of the three features associated with the enzyme catalyzed hydrolysis of glycosides.

2.3. Model Systems

There are three features associated with the lysozyme catalyzed hydrolysis of glycosides--distortion, protonation, and electrostatic stabilization. The question of how each of these features can serve to accelerate the rate of hydrolysis has been addressed by
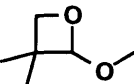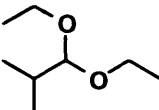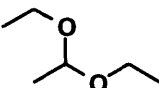
40

several investigators through the use of model systems.[64-66] The chemical models for acetal hydrolysis are briefly discussed in terms of the mechanistic feature they explore.

2.3.a. Distortion Models

The role of distortion in glycoside hydrolysis has been explored in a few model systems. The introduction of distortion in the form of ground state strain, for example, has served well to both accelerate the rate of acetal hydrolysis and to facilitate general acid catalyzed hydrolysis (Table 2.1).[67]

Strained acetal **23** is hydrolyzed approximately 10^5 times faster than its unstrained acyclic analogs **24** and **25**. This rate enhancement was attributed to the relief of strain that occurs as **23** approaches the transition state. The strain associated with **23** further serves to facilitate general acid catalyzed hydrolysis. While acetal **23** is hydrolyzed according to a general acid catalyzed mechanism, acetals **24** and **25** are hydrolyzed by a specific acid catalyzed process.

Table 2.1 Rates of Hydrolysis of Strained and Unstrained Acetals

Compound	Solvent	Temp, °C	k, $M^{-1}s^{-1}$
23	10% dioxane	30	2.24×10^5
24	50% dioxane	25	0.164
25	H_2O	30	0.490

That the hydrolysis of acetal **23** is a general acid catalyzed process is of particular note because, in analogy with the nature of the lysozyme substrate, this substrate is somewhat unreactive. The lysozyme substrate is a particularly difficult glycosidic bond to hydrolyze; the aliphatic leaving group is a relatively poor leaving group and the oxocarbonium ion produced is destabilized due to the inductive effects of the adjacent

hydroxyl groups. Similarly, acetal **23** includes an aliphatic leaving group and an unstabilized oxocarbonium ion is produced. Non-enzymatic acid catalyzed hydrolysis of unreactive acetals normally proceeds through an A-1 mechanism in which protonation is not rate-limiting (specific acid catalysis). Enzymatic acid catalyzed hydrolysis of glycosides (e.g. lysozyme), on the other hand, often occurs according to a general acid catalyzed mechanism in which protonation becomes partially rate limiting. It should be pointed out that, in fact, nearly all of the efforts to develop model systems capable of hydrolyzing similarly unreactive acetals through a general acid catalyzed mechanism have necessarily relied upon the introduction of strain (in one form or another) into the substrate. The one and only exception to this phenomena is discussed in Section 2.3.c.

The accomplishment of general acid catalyzed hydrolysis of an unreactive acetal in a chemical system speaks directly to the role of ground state distortion in lysozyme's mechanism of action. Specifically, distortion of the D subsite saccharide upon binding may be a prerequisite for the general acid catalyzed hydrolysis which ensues.

The role of distortion in facilitating glycoside hydrolysis is made evident by the results of another set of model studies. Stereoelectronic theory, the culmination of numerous model studies, dictates the reactivity of various organic compounds.[68] In terms of the hydrolysis of glycosides, stereoelectronic theory instructs that there must be a lone pair of electrons antiperiplanar to the C-O bond being cleaved in order for hydrolysis to be facile (Figure 2.7).[39,69] While the α-anomer **26** meets this requirement, the β-anomer **27**

**Figure 2.7 Orbital Overlap in α and β Glycoside Anomers**
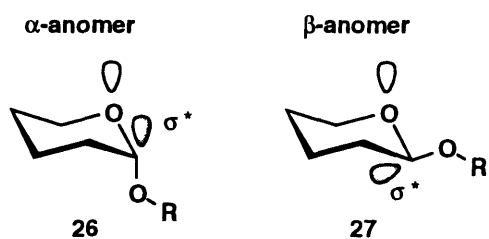
has no such orbital overlap in the ground state. Because the lysozyme substrate is a β-anomer, stereoelectronic theory suggests a role for distortion in the enzyme catalyzed hydrolysis of glycosides.

Specifically, the stereoelectronic requirement for a lone pair of electrons antiperiplanar to the C-O bond being cleaved becomes satisfied in the case of the β-anomer following any one of a number of conformational changes. These suitable conformational changes exist on a continuum of accessible alternate conformations (Figure 2.8).

Complete ring inversion ($28 \rightarrow 31$) is an unlikely solution to be utilized by lysozyme. The hexasaccharide substrate is bound tightly to the enzyme and the position of saccharides in subsites A, B, C, E, and F is interdependent on the conformation of the saccharide occupying the D subsite; the severe substrate movement associated with complete ring inversion would not be tolerated within the enzyme active site. Complete ring inversion is also precluded by the steric requirements associated with multiple axial substituents (e.g. hydroxyl groups). The intermediate conformational change ($28 \rightarrow 29$), on the other hand, is quite reasonable. The half chair conformation 29 includes substantial

**Figure 2.8 Continuum of Alternate β-Anomer Conformations**
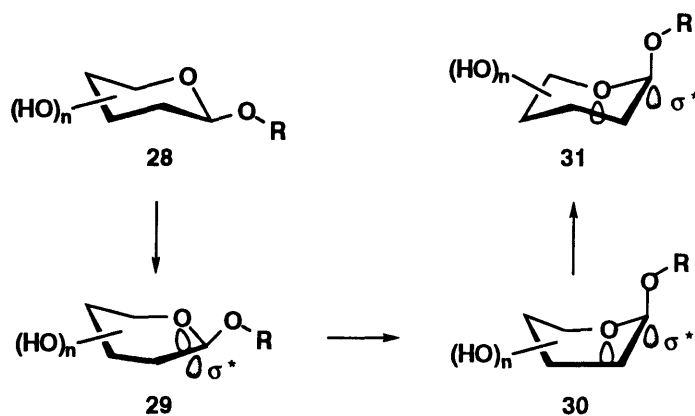
n-σ^*_{C-O} orbital overlap and is, accompanied by minimal movement of adjoining functionality. Indeed, it is a chair to half-chair conformational change which is believed to be induced in the lysozyme D subsite saccharide upon binding at the active site.

43

Stereoelectronic theory, therefore, provides further support for the role of distortion in facilitating glycoside hydrolysis.

2.3.b. Protonation Models

Several investigators have sought to probe the contribution that the lysozyme active site carboxylic acid (Glu-35) makes to catalysis through the design of model systems which incorporate a carboxylic acid in their design. The analogy between an enzyme catalyzed reaction, in which the substrate is held in close proximity to a catalytic residue in the active site, and an intramolecular reaction is exploited in these model systems.

Salicyl derivatives represent a large class of model systems in which general acid catalyzed hydrolysis of glycosides and acetals has been facilitated. Hydrolysis of salicyl derivative **32**, a general acid catalyzed process, occurs 10^4 times faster than the specific acid catalyzed hydrolysis of analog **33**, for example.[70]
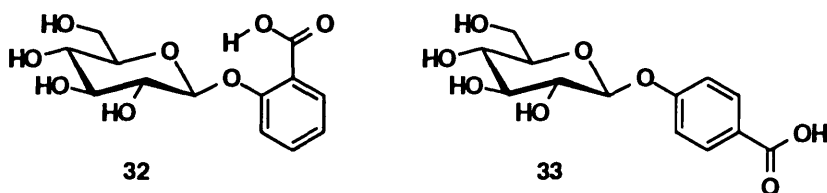
Another set of salicyl derivative model systems provide a clearer assessment of the rate enhancement provided by intra- versus intermolecular acid catalysis. Since the hydrolysis of both the salicyl derivatives **34** and **36** and their analogs **35** and **37** are
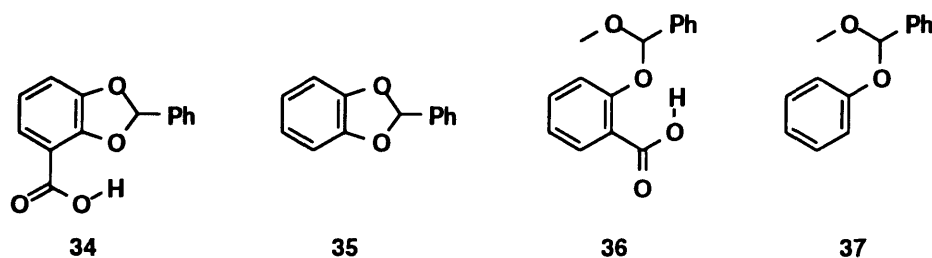
general acid catalyzed processes, a quantitative measure of the advantage of intra- over intermolecular acid catalysis is provided in terms of effective molarities.[71,72] The hydrolyses of **34** and **36**, which occur at much faster rates than then **35** and **37**,

4 4

respectively, were characterized as having effective molarities of approximately 10^2 M and 10^4 M, respectively.

These salicyl derivative model systems are quite unique, however, and their relevance to lysozyme deserves explanation. There are two features associated with the salicylic acid model systems which affect the observed high hydrolytic efficiency. First, the hydrogen bond between the carboxylic acid and the leaving group oxygen is particularly strong in salicyl derivatives. Indeed, the intramolecular hydrogen bond in salicylic acid **38** is so strong (phenol pK_a 12.95) that it persists even in water.[73]

38
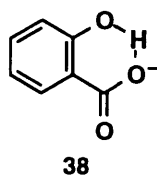
It is not unreasonable to assume that the lysozyme active site carboxylic acid (Glu-35) similarly forms a very strong hydrogen bond with the leaving group oxygen of its substrate. Second, the aryl leaving group in these salicylic systems is a particularly good leaving group. Because the C-OAr bond is relatively weak, substantial C-O bond breaking has already occurred as these compounds approach their transitions states. Indeed, C-O bond breaking must be well underway before intramolecular proton transfer can become thermodynamically favorable and, therefore, catalytically efficient. The lysozyme substrate, in contrast, includes a relatively poor aliphatic leaving group. The required substrate C-O bond weakening, which is required for protonation to become catalytically competent, is perhaps created through binding interactions with the enzyme which serve to strain the substrate (see Section 2.1.a.). Notably, there are no model system examples of efficient intramolecular general acid catalyzed hydrolysis of aliphatic acetals.

2.3.c. Electrostatic Stabilization Models

The contribution the lysozyme active site carboxylate (Asp-52) makes towards facilitating glycoside hydrolysis has been probed in a few model systems. These model

systems encourage electrostatic stabilization of the developing oxocarbonium ion by placing an ionized carboxylate in close proximity to the anomeric center.

Fife, for example, has determined that the spontaneous cleavage of mixed acetal 39

39   40
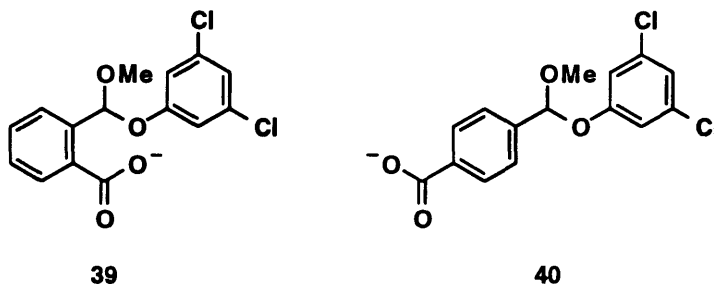
is 100 times faster than that of isomer 40 in 50% aqueous dioxane.[74] Czarnik has demonstrated the largest rate acceleration due to electrostatic stabilization to date with his conformationally restricted model system.[75] The pH-independent hydrolysis of endo acid 41 is 860 times faster than that of the reference compound 42. These model systems

41   42
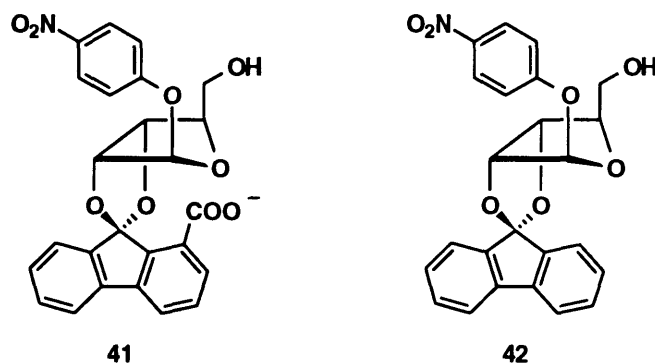
suggest that electrostatic stabilization produces modest rate enhancements in the hydrolysis of only readily hydrolyzed substrates (i.e. substrates with phenoxy leaving groups). Still, because the rate enhancements observed in these model systems are modest, several authors have concluded that electrostatic stabilization plays no role in lysozyme's catalysis of glycoside hydrolysis.

Nonetheless, some investigators still maintain that electrostatic stabilization is an important mechanistic feature in lysozyme. These authors point out that the proposed mechanism for lysozyme includes bifunctional catalysis involving the active site

46

carboxylate (Asp-52) working in concert with an active site carboxylic acid (Glu-35). Bifunctional model systems have been designed in an effort to address this issue.

Fife, for example, has demonstrated that the carboxylate and the carboxylic acid in **43** work in a synchronous fashion to facilitate acetal hydrolysis.[76] A bell-shaped pH-rate profile was observed in the hydrolysis of **43** and the rate of hydrolysis was 4×10^4 times faster than the diethyl ester **44**. This result is of particular note for two reasons. First, the leaving group in **43** is an aliphatic alcohol in analogy to the lysozyme substrate. Second, acetal **43** is hydrolyzed according to a general acid catalyzed mechanism. General acid

43   **44**   **45**
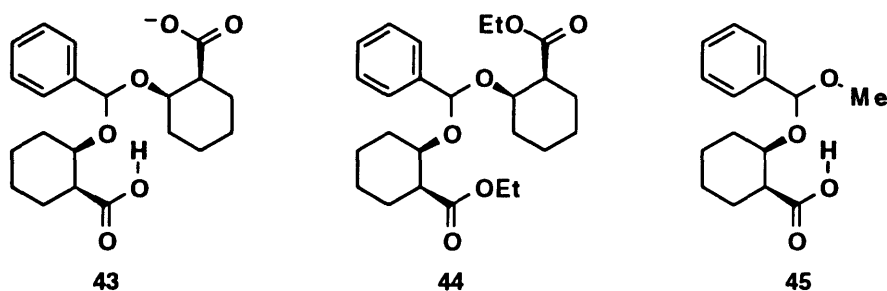
catalyzed hydrolysis is not observed in the analogous mixed acetal **45** which includes only one carboxylic acid moiety. This model system suggests that in order for electrostatic stabilization to facilitate acetal hydrolysis, the carboxylate must work in concert with protonation of the leaving group.

2.3.d.   Conclusions

Taken together, these model systems provide support for the role of distortion, protonation, and electrostatic stabilization in facilitating glycoside hydrolysis. Notably, the hydrolysis of O-alkyl, fully hydroxylated glycosides has not been achieved in any model system described to date. As has been proposed for lysozyme, the hydrolysis of such unreactive substrates may, in fact, require the combined functioning of distortion, protonation, and electrostatic stabilization
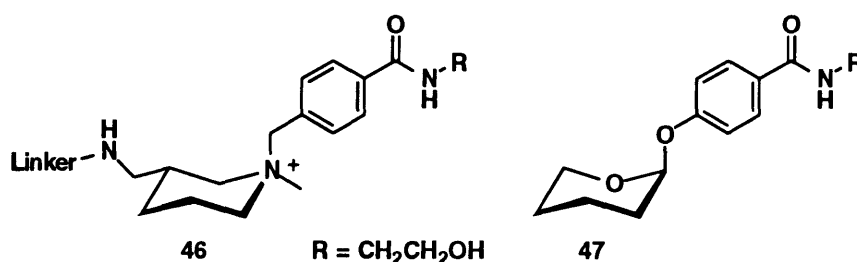
2.4.   Antibody Catalyzed Glycoside Hydrolysis

The hydrolysis of glycosides is clearly a mechanistically complex process. The relative importance of the three mechanistic features (distortion, protonation, electrostatic

stabilization) in facilitating hydrolysis remains obscured. Catalytic antibodies may provide an effective means of testing and exploiting the role of distortion, protonation, and electrostatic stabilization in glycoside hydrolysis. Jenck's prediction that antibodies raised to transition state analogs would serve to catalyze reactions in a fashion analogous to their enzyme counterparts has, indeed, been borne out by numerous catalytic antibody studies.[77,78] Glycosidase type antibodies, on the other hand, have remained a somewhat elusive achievement in catalytic antibody research. While several investigators have designed haptens for glycoside hydrolysis, the rate enhancements observed do not approach those of either enzymes or, in general, antibody catalysts. Each of the glycosidase hapten designs described to date reflects an appreciation for one or more of the aforementioned mechanistic features. A review of the published accounts of antibody-catalyzed glycoside hydrolysis is presented in this section.

2.4.a. Antibodies Induced to Quarternized Amines: The Role of Protonation

In 1991 Lerner reported the hydrolysis of substrate **47** by an antibody raised against hapten **46**.[79] The key features associated with hapten **46** are the amine and the *axial* benzylic group. The quarternized amine in the hapten **46**, which corresponds in position to the anomeric carbon on the substrate **47**, was intended to induce the formation

46   R = CH₂CH₂OH   47

Kinetic Constants at pH 5.7

$k_{cat} = 7.8 \times 10^{-5}\ s^{-1}$, $k_{cat}/k_{uncat} = 70$, $K_m = 100\ \mu M$, $K_i = 35\ \mu M$

of an active site carboxylate. The carboxylate, presumably protonated under the acidic assay conditions, was believed to function as a proton donor during the hydrolysis. The

authors determined that the rate of the antibody catalyzed reaction was completely pH-dependent while the background hydrolysis was the sum of a pH-independent reaction and a H^+-catalyzed reaction. The implication, that the antibody catalyzed reaction is a general acid catalyzed process, is viewed with caution as the pH range investigated (pH 5.2 to 7.0) was limited.

The *axial* benzylic group, corresponding to the *axial* phenoxy leaving group on the substrate, presumably provided an antibody that served to stabilize the antiperiplanar orbital overlap required for acetal hydrolysis. Indeed, haptens **48** and **49**, which include an *equatorial* benzylic group and a quarternized amine, failed to elicit antibodies that would hydrolyze the substrate **47**. Interestingly, compound **50** behaved as a potent inhibitor of the reaction (K_i = 35 μM), rather than as a substrate. The addition of the C-5 binding determinant in **50**, perhaps, disallowed the conformational change associated with formation of the half-chair transition state.

48

49

50

R = CH$_2$CH$_2$OH
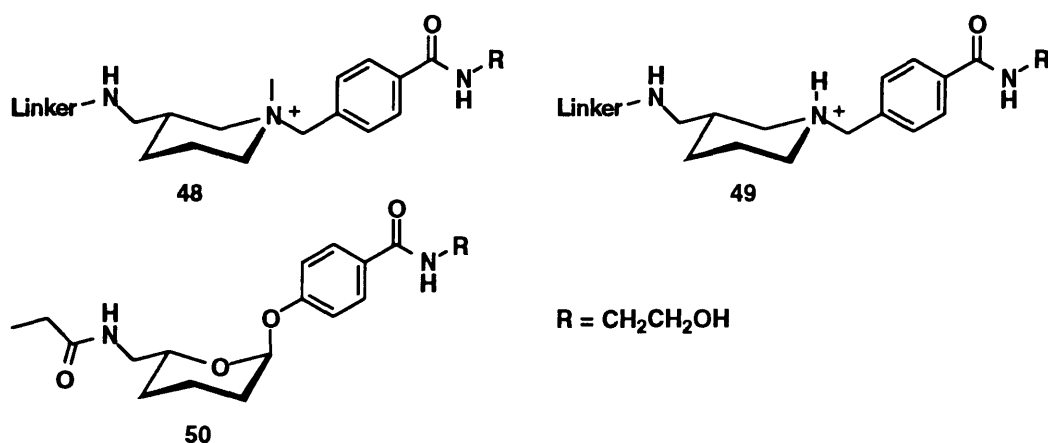
2.4.b. Antibodies Induced to Oxocarbonium Ion Mimics: The Role of Transition State Stabilization

In 1994 Schultz reported the hydrolysis of substrate **52** by an antibody raised against hapten **51**.[80] The design of hapten **51** is based on the glycosidase inhibitors nojirimycin and castanospermine. The positively charged ammonium ion was expected to

49

induce functional groups in the antibody combining site that would serve to stabilize the

charge-delocalized transition state. The position of the ammonium group corresponds to

51   52
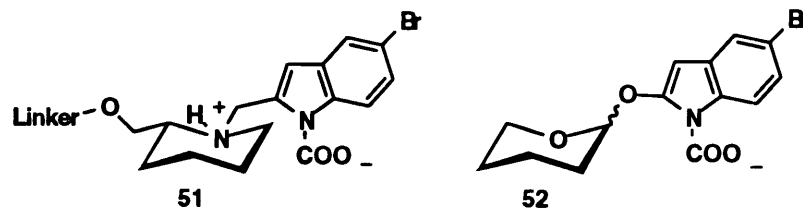
Kinetic Constants at pH 5.5

$k_{cat} = 2.5 \times 10^{-4}\ s^{-1},\ K_M = 324\ \mu M,\ K_I = 35\ \mu M,\ K_M/K_I = 9.2$
$k_{AcOH} = 3.6 \times 10^{-5}\ M^{-1}\ s^{-1}$

Kinetic Constants at pH 8.5

$k_{cat} = 2.7 \times 10^{-4}\ s^{-1},\ K_M = 178\ \mu M,\ k_{AcO^-} = 4.4 \times 10^{-6}\ M^{-1}\ s^{-1}$

that of the endocyclic oxygen in the substrate. Notably, the position of the aryl substituent

on the hapten does not exactly correspond to the position of the aryloxy leaving group on

the substrate, however.

The authors reported that the antibody catalyzed reaction was both a general acid

and general base catalyzed process under acidic and basic conditions, respectively. The

kinetic data reported is, however, difficult to interpret as the uncatalyzed rates of hydrolysis

were not reported. A value for k_{cat}/k_{uncat}, which may be estimated from the value of

K_M/K_i, indeed, suggests that the antibody described did not perform as an effective

catalyst. Furthermore, the effective molarity of the putative general acid catalyst,

approximated by the value of $k_{cat}/\ k_{AcOH}$ (7.0 M), does not provide support for the

importance of an active site catalytic residue. Nonetheless, the authors concluded that,

under acidic conditions, an active site carboxylic acid did function as a proton donor and,

thereby, facilitated hydrolysis. In support of this conclusion, the authors reported that

modification of the antibody in the absence of hapten 51 with diazoacetamide resulted in a

33% reduction in catalytic activity relative to catalysis achieved by an antibody that was

modified in the presence of hapten 51. The authors also proposed that, under basic

conditions, an active site carboxylate residue functioned to electrostatically stabilize the developing positive charge on the oxocarbonium ion transition state.

In addition to these results, Schultz also described two unsuccessful hapten designs. Hapten **53**, perhaps the best oxocarbonium ion transition state analog described to date, failed to elicit antibodies capable of catalyzing the hydrolysis of either substrate **54** or **55**. The design of hapten **53** is based on the potent amidine-containing glycosidase

53

54 n = 1, R = NH(CS)NHEt
55 n = 0, R = NO₂
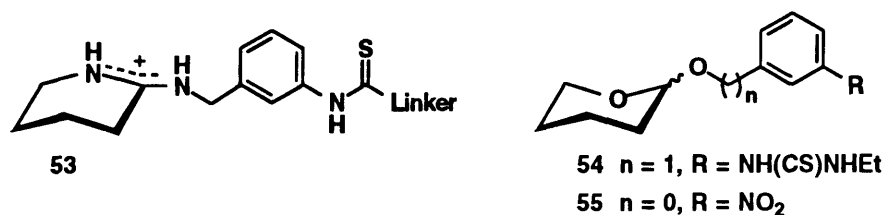
inhibitors which are thought to mimic both the half-chair conformation and the positive charge of the oxocarbonium ion transition state. It may be the case that the planar nature of the anomeric center in **53** resulted in an antibody that was incapable of accommodating the substrate which contains an sp^3 hybridized carbon at the corresponding center. The spatial location of the aryl group in hapten **53** is, indeed, different from the position of the departing aryloxy group in substrates **54** and **55**.

Hapten **56**, another distorted substrate mimic, also failed to produce antibodies capable of hydrolyzing substrate **57**. Again, the sp^2 hybridization of the hapten at the center corresponding to the anomeric center on the substrate may preclude accommodation of the substrate in the antibody binding site. In addition, substrate **57** is a fully hydroxylated glycoside and is, therefore, inherently more resistant to hydrolysis than the tetrahydropyran analog **55**.

56   **57**
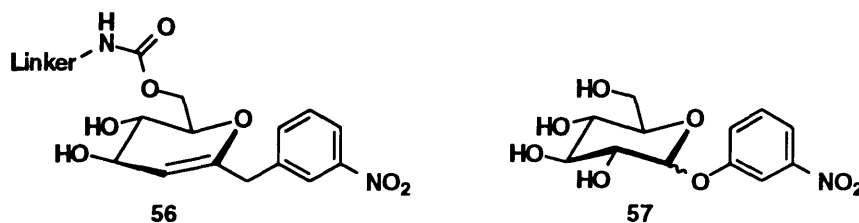
2.4.c. Antibodies Induced to Half-Chair Conformational Mimics: The Role of Distortion

Masamune has recently reported the generation of an antibody raised to hapten **58** that catalyzed the hydrolysis of substrate **59**.[81] The hapten is designed to be a conforma-

Kinetic Constants at pH 5.4

$k_{cat} = 2.5 \times 10^{-5}$ s^{-1} $k_{cat}/k_{uncat} = 375$, $K_M = 1.16$ mM, $K_i = 8.3$ μM

tional mimic of the distorted substrate/oxocarbonium ion transition state. The azetidine ring serves distort the cyclohexane ring into the half-chair conformation. The quarternized amine was included in the design in an effort to induce an active site carboxylate. The antibody catalyzed hydrolysis of **59** was pH independent over the pH range studied (pH 5.4 to 7.0). Although the pH range studied was limited, this study suggested no significant participation of an acidic residue in catalysis. The authors tentatively suggested catalysis could be attributed to distortion of the substrate upon binding to the antibody. This hapten design will be discussed again in Chapters 3 and 4, in the context of the entire Masamune group effort to generate antibodies for glycoside hydrolysis.

2.4.d. Conclusion

A number of different haptens have been designed in an effort to produce antibodies capable of catalyzing the hydrolysis of glycosides. Thus far, these efforts have met with limited success. In the following chapters, our own efforts in this area of catalytic antibody research are described.

Chapter 3

Design and Synthesis of Haptens, Inhibitors and Substrates for Glycoside Hydrolysis

3.1 Hapten Design

The three mechanistic features associated with glycoside hydrolysis (distortion, protonation, electrostatic stabilization) served as a guide for our hapten designs. Our interest in the determining the relative importance of each of these mechanistic features prompted us to design five different haptens for glycoside hydrolysis. Each hapten was specifically designed to probe the significance of a unique combination of the proposed mechanistic features associated with glycoside hydrolysis. The design and synthesis of the haptens, inhibitors and substrates for glycoside hydrolysis is discussed in this chapter.

Antibodies are characterized by high association constants with their ligands; it is believed that up to 20 kcal/mol of energy is available for ligand binding. Four of the haptens we designed are half-chair conformational mimics. Data from the lysozyme catalyzed hydrolysis of glycosides, enzyme inhibitors, and model systems suggested that the half-chair conformation plays an important role in glycoside hydrolysis. It has been postulated that the chair to half-chair conformational change first occurs in the substrate, prior to the onset of hydrolysis (ground state distortion). Once distorted into the half-chair conformation, the substrate more readily proceeds to the half-chair oxocarbonium ion transition state that accompanies hydrolysis. The half-chair conformational mimic haptens would allow us to probe the role of stabilizing the half-chair conformation in catalysis.

Antibody combining sites often include residues that will form electrostatic and/or hydrogen bonds with their ligands. We have included amine/ammonium ion functionality in all of our hapten designs in an effort to induce the formation of specific combining site residues. Protonation of the glycoside substrate leaving group and electrostatic stabilization of the positively charged oxocarbonium ion are believed to play a role in glycoside

hydrolysis. The inclusion of amine moieties in our hapten designs would allow us to probe the significance of these two mechanistic features. Specifically, the amine/ammonium ion functionality could serve to induce the formation of antibody combining site carboxylic acid/carboxylate residues that would facilitate hydrolysis.

3.2. Design and Synthesis of the Valienamine Haptens and Inhibitors

The design of haptens **V1, V2** and **V3** was based on the structure of the valienamine glycosidase inhibitor (Figure 3.1). These haptens, half-chair conformational mimics, were intended to elicit antibodies that would bind the substrate in the half-chair conformation . The double bond, which corresponds in position to the endocyclic oxygen and to C-5 in the substrate, forces the haptens to exist in the half-chair conformation. An important consideration in designing these haptens was the spatial location of the aryl functionality. The antibody binding site should accommodate the corresponding substrate aryloxy functionality along the entire hydrolytic pathway. For this reason, we designed haptens that were sp^3 hybridized at the center corresponding to the anomeric carbon in the substrate. Space in the antibody combining site would then be provided for the leaving group in the substrate and in the transition state.

Figure 3.1

Hapten V1

Hapten V2

Hapten V3

Substrate

Substrate
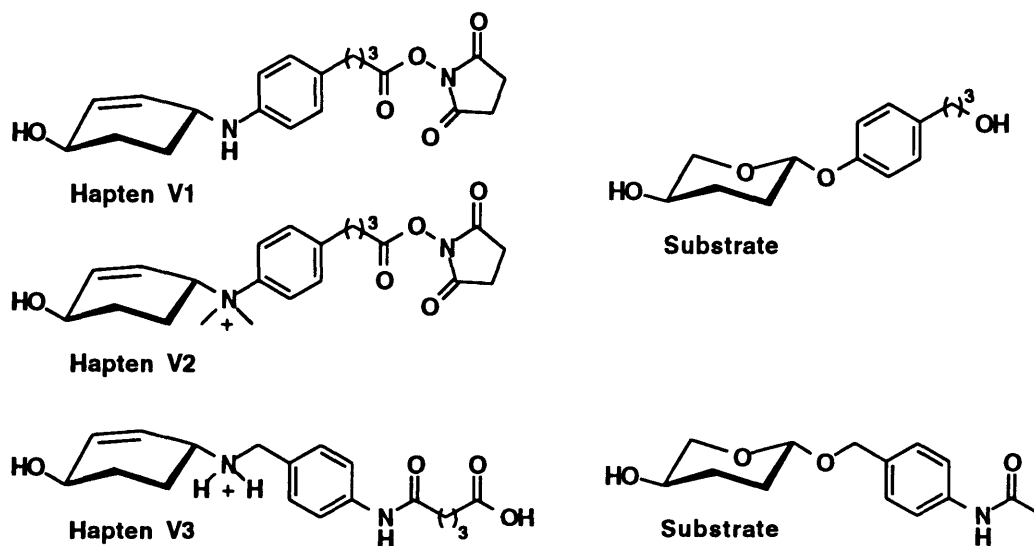
These hapten designs also provided for the generation of catalytic combining site residues. Specifically, the amine in **V1**, which is not protonated at physiological pH, could serve to induce the formation of a complementary carboxylic acid in the antibody binding site. The quarternized amine in **V2** and the ammonium residue in **V3** could serve to induce the formation of a complementary carboxylate in the antibody combining site. This carboxylate, depending upon its location and protonation state, could serve to donate a proton to the exocyclic oxygen on the substrate leaving group or to electrostatically stabilize the developing positive charge on the substrate endocyclic oxygen.

3.2.a. Synthesis of Hapten V1

Racemic cis-1-acetoxy-4-chloro-2-cyclohexene **60** was prepared according to the method of Backvall.[82,83] Coupling of allylic chloride **60** with 4-(4-aminophenyl)butyric acid under S$_N$2 conditions afforded allylic amine **61a** (Scheme 3.1). This coupling proceeded with high chemo-, regio-, and stereoselectivity; the chloro group was replaced by the amine and the resulting cyclohexene was *trans*-1,4-disubstituted. Synthesis of the *cis* diastereomer **61b** through a palladium-catalyzed coupling of allylic chloride **60** with the arylamine allowed us to confirm the stereochemical assignment (Scheme 3.1). The uncatalyzed S$_N$2 reaction and the palladium catalyzed reaction each produced single, different diastereomers.

Scheme 3.1
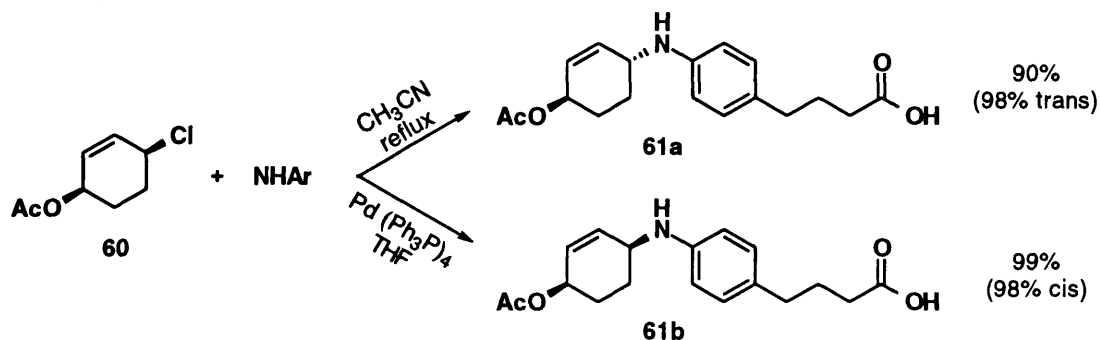
The orientation of the C-1 and C-4 substituents was assigned on the basis of steric arguments. Specifically, a consideration of 1,3 pseudoaxial-axial interactions led us to

conclude that in the *trans* isomer both substituents are pseudoequatorial and in the *cis* isomer the acetoxy group is pseudoaxial. The synthesis of hapten **V1** proceeded from the *trans* isomer **61a** according to Scheme 3.2. Hydrolysis of the acetate with lithium hydroxide and activation of the acid with N-hydroxy succinimide (NHS) provided racemic hapten **63**. The intermediate **62** could serve as an inhibitor in the antibody reactions.

Scheme 3.2

1. 1 M LiOH, THF

2. DCC, NHS, 0°C
   CH₂Cl₂/DMF

74%, 2 steps

61a

62 R=H (Inhibitor)

63 R= (Hapten V1)
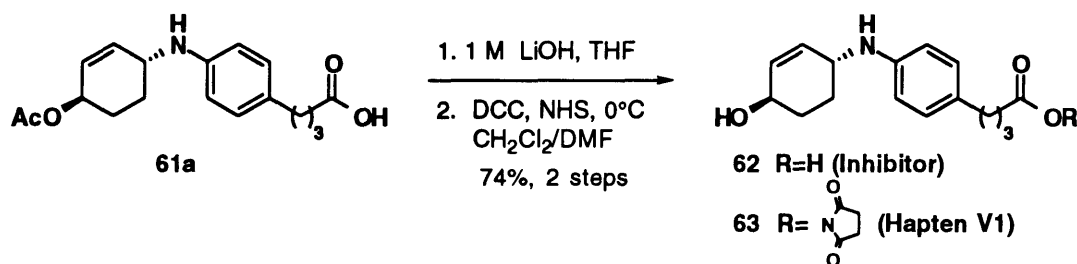
3.2.b. Synthesis of Hapten V2

Hapten **V2** was synthesized from the common intermediate **63** according to Scheme 3.3. Monomethylation of amine **63** with methyl iodide and the hindered base, 1,2,2,6,6-pentamethylpiperidine[84], followed by quarternization of the tertiary amine with methyl triflate provided racemic hapten **65**. Hapten **V2** proved to be to unstable to be used to immunize mice. In CD₃OD at room temperature, this compound had a half life of approximately 48 hours. Since the immune response occurs over a period of several days, we were forced to abandon this hapten.

Scheme 3.3

1. MeI,
   DMF, 0°C

2. MeOTf
   toluene, 0°C

45%, 2 steps

63

64 R=Me

65 R=Me₂⁺ (Hapten V2)
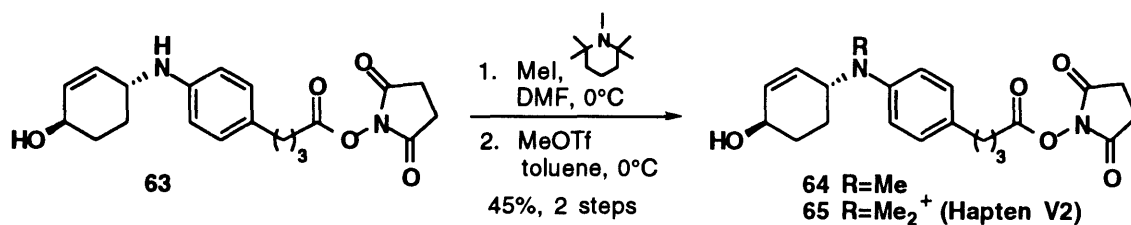
3.2.c. Synthesis of Hapten V3

The main skeleton of hapten **V3** was constructed through a coupling of cis-1-acetoxy-4-chloro-2-cyclohexene **60** with benzylamine derivative **69**. The benzylamine

56

derivative **69** was prepared from *p*-nitrobenzylamine according to Scheme 3.4. Protection of *p*-nitrobenzylamine with trifluoroacetic anhydride provided **66**. Reduction of the nitro group by hydrogenation over platinum on carbon and protection of the resulting amine **67** as the benzyloxy carbonate provided **68**. Deprotection of the trifluoracetamide **68** with potassium carbonate provided the coupling fragment **69**, which was used in subsequent couplings without purification.

Scheme 3.4
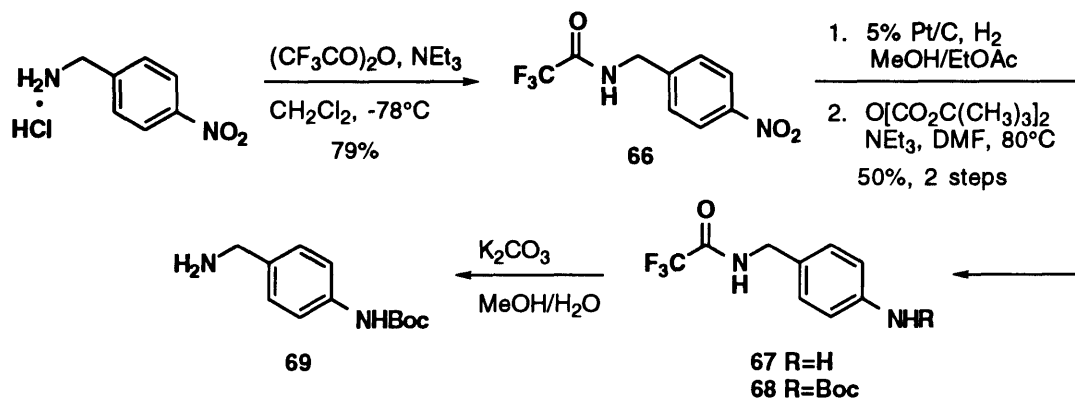
The synthesis of hapten **V3** proceeded according to Scheme 3.5. Coupling of allylic chloride **60** with crude amine **69** under S$_N$2 conditions and subsequent deprotection of the resulting amine **70** with trifluoroacetic acid provided **71**. Regioselective coupling

Scheme 3.5
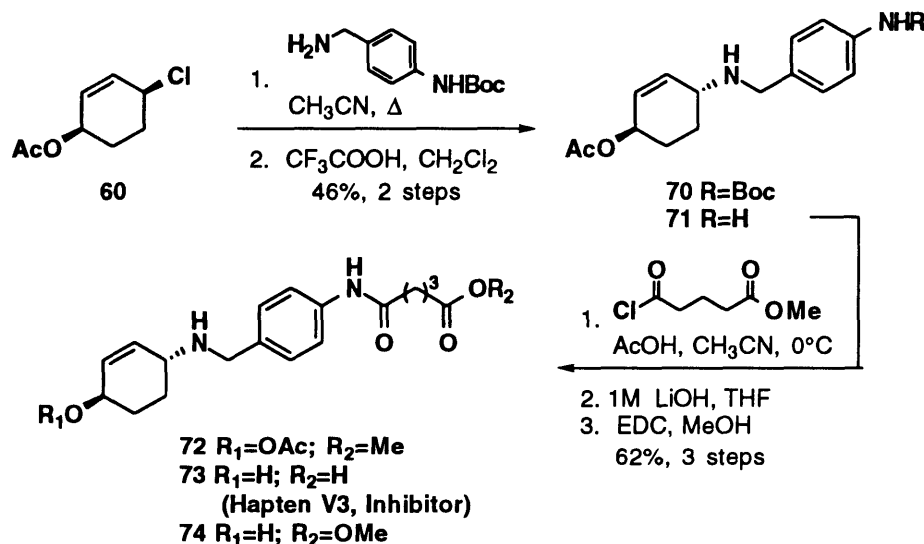
of the primary phenyl amine with methyl 4-(chloroformyl) butyrate was accomplished under acidic conditions. Due to the different pK_a values of the arylamine (pK_a 3-5) and the benzylamine (pK_a 10-11), the acid served to "protect" the arylamine from alkylation. Hydrolysis of the acetate ester and the methyl ester with lithium hydroxide provided racemic hapten **73**, which was further characterized as the methyl ester **74**. The acid **73** would serve as the antibody inhibitor.

3.3. Design and Synthesis of the Azetidine Hapten and Inhibitor

The azetidine hapten **A1** provided an additional approach to generating antibodies capable of stabilizing the half-chair conformation (Figure 3.2). The azetidine functionality forces the cyclohexane ring to adopt a half-chair conformation. Notably, the specific centers that are distorted in this hapten design are analogous to the centers that are altered in the corresponding substrate as it undergoes the chair to half-chair conformational change. Another notable difference between the azetidine hapten and the valienamine haptens design is the orientation of the C-1 substituent. In the azetidine hapten, the aryl functionality, which corresponds to the departing benzyloxy group in the substrate, is pseudoaxial.

Figure 3.2

Hapten A1   Substrate
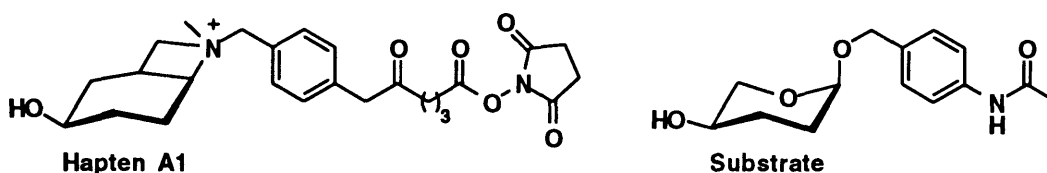
3.3.a. Synthesis of Hapten A1

The synthesis of racemic hapten **A1** was completed by Norihiko Tanimoto according to Scheme 3.6. The details of this synthesis have been described elsewhere and will, therefore, not be presented here. The inhibitor for the antibody reaction, an intermediate in the synthesis, is noted in Scheme 3.6.

5 8

Scheme 3.6
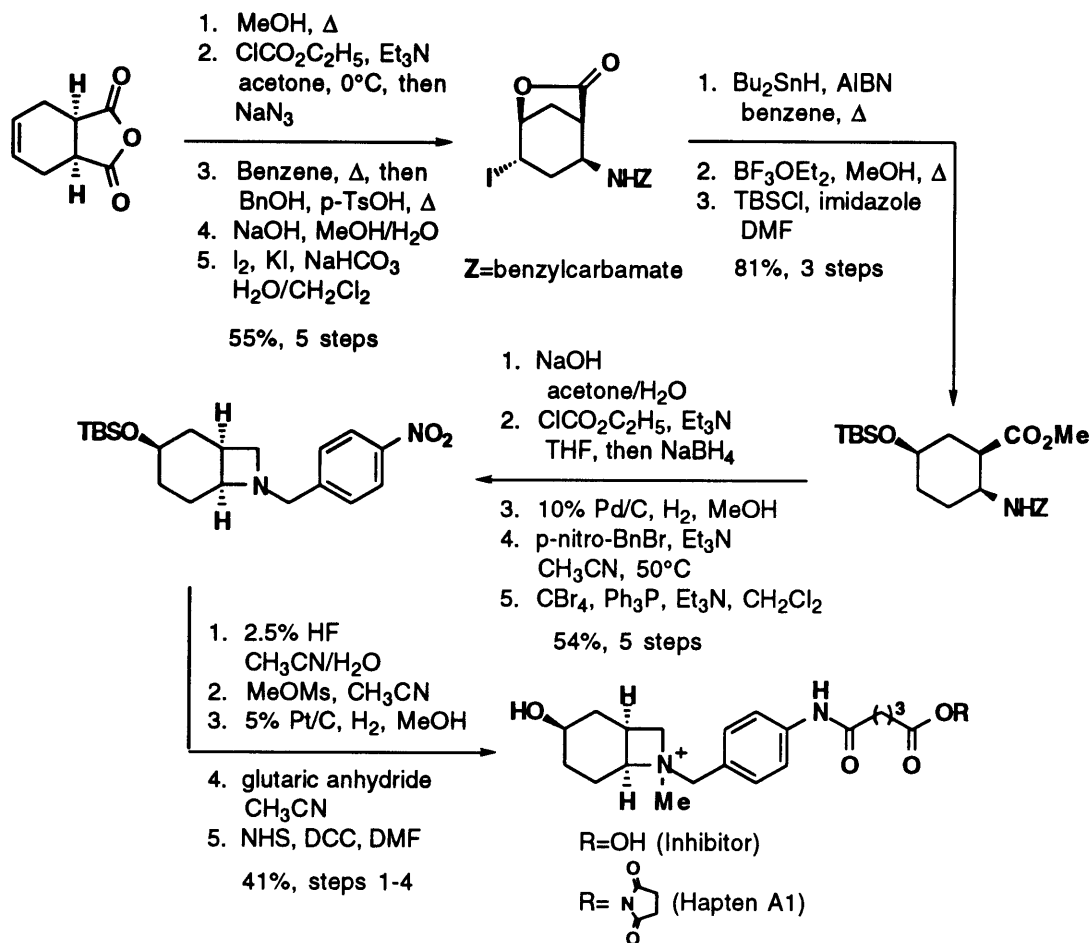
3.4. Design and Synthesis of the Glycosoamine Hapten and Inhibitor

Hapten **G1**, which also contains an amine but is not a conformational mimic of a distorted substrate, was designed to allow us to distinguish the role of distortion from the role of catalytic combining site residues (Figure 3.3). Specifically, the quarternized amine was expected to induce the formation of an antibody combining site carboxylate residue. Depending on its protonation state and location, this residue could serve to donate a proton to the substrate's leaving group oxygen, or to electrostatically stabilize the endocyclic oxygen in the transition state. Since this hapten exists in the chair conformation, it was not expected to induce an antibody that would specifically stabilize the half-chair conformation. A comparison of the catalytic properties of antibodies induced to the valienamine and

59

azetidine haptens with antibodies raised against the glycosamine hapten **G1** would provide insight into the relative importance of distortion in facilitating substrate hydrolysis.

Figure 3.3

Hapten G1   Substrate
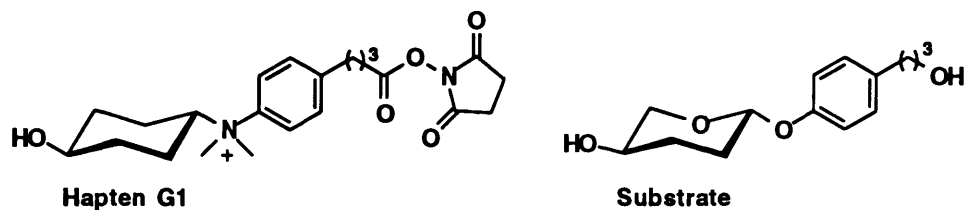
3.4.a. Synthesis of Hapten G1

Hapten **G1** was synthesized from the common intermediate **61a** according to Scheme 3.7. Hydrogenation of the double bond with rhodium on alumina provided **75**. Monomethylation of the amine with methyl iodide and hydrolysis of the acetate and methyl esters with lithium hydroxide provided **77**. The low yield associated with this sequence is due to the monomethylation step. Monomethylation was accompanied by formation of the

Scheme 3.7
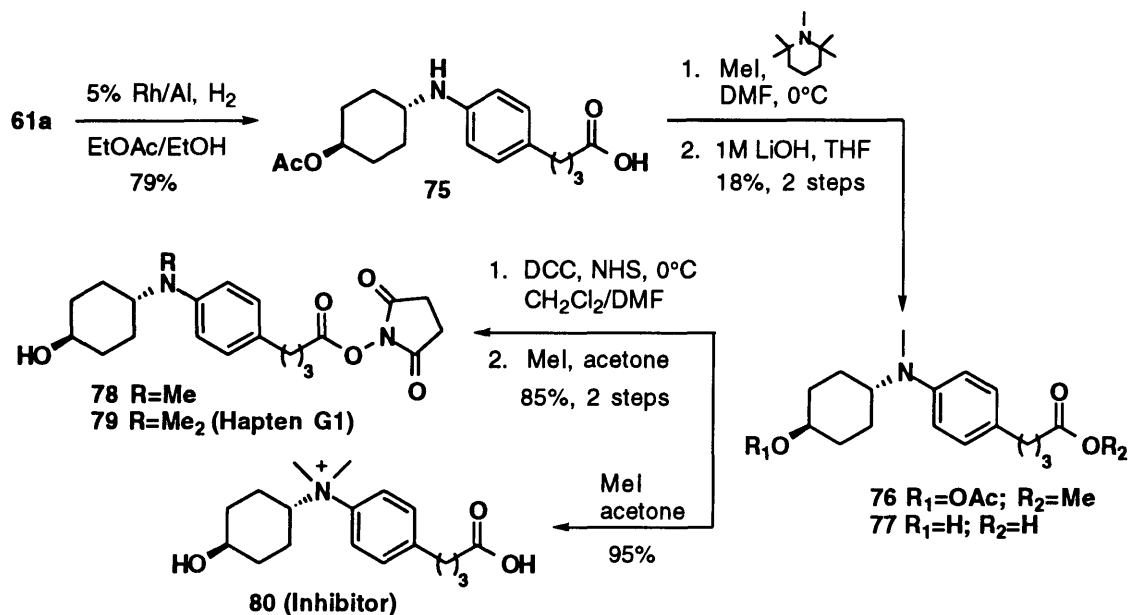
quarternized product. As the quarternized amine was, however, very difficult to work with in subsequent steps, we used the monomethylated amine and then quarternized the amine in the final step of the synthesis. Activation of the carboxylic acid with N-

60

hydroxysuccinimide and quarternization of the amine with methyl iodide provided racemic hapten **80**. Quarternization of the amine **77** provided the antibody inhibitor **80**.

3.5. Summary of Hapten Design and Synthesis

Four of the five glycosidase haptens that were designed and synthesized were stable compounds. Three (**V1, G1, A1**) of the four candidate haptens were further pursued in terms of the synthesis of substrates (following sections) and antibody production (chapter 4).

3.6. Design and Synthesis of Substrates

The synthesis of the pyranoside substrates for the antibody reactions is described in this section. Since each of the haptens used to immunize mice were racemic, both enantiomers of each of the substrates were prepared. A racemic mixture of the C-4 unsubstituted pyranoside substrates were prepared for an initial screening of the monoclonal antibodies for hydrolytic activity. Enantiomerically and diastereomerically pure C-4 hydroxylated substrates were prepared for further characterization of identified antibody catalysts. In addition to both enantiomers, we prepared both diastereomers in order to probe the stereospecificity of the antibody catalyzed reactions.

3.7. Phenoxy Substrates

The substrates for the valienamine hapten **V1** and the glucosamine hapten **G1** include a C-1 phenoxy leaving group (Figure 3.4).

Figure 3.4

(rac)-V1G1r

(1S,4R)-V1G1a
(1S,4S)-V1G1b

(1R,4S)-V1G1c
(1R,4R)-V1G1d
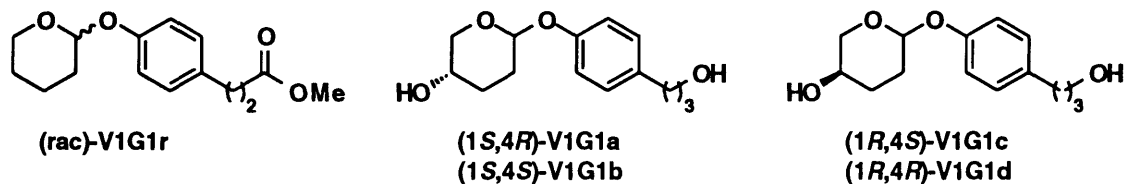
3.7.a. Synthesis of Substrate V1G1r

A racemic mixture of substrate **V1G1r** was prepared in two steps according to Scheme 3.8. The phenoxy substituent exists in the axial position in pyranoside substrate **81**.

Scheme 3.8

81 R=CO$_2$Me (V1G1r)
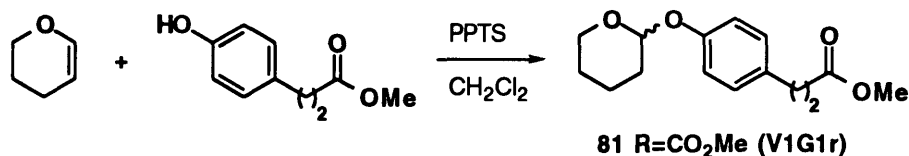
3.7.b. Synthesis of Substrates V1G1a-d

Enantiomerically and diastereomerically pure quantities of the each of the C-1,4 disubstituted pyranoside substrates were prepared from carbohydrate derived glycals, L-arabinal and D-arabinal.[85,86]

Several methods for installing C-1 *alkoxy* functionality into 3, 4, 6-substituted glycals are described in the carbohydrate literature. As the application of these methods to installing C-1 *aryloxy* functionality into 3,4-substituted glycals has not been documented, however, some discussion is warranted. In general, alkoxy groups may be installed at C-1 in either a direct[87-90] or an indirect fashion[91,92] (Figure 3.5). In the former method, the alkoxy functionality is directly coupled to the glycal in a Lewis acid catalyzed process. In the latter method, the glycal is first coupled to an activating group and, in a second step, the activating group is displaced by the desired alkoxy group.

Figure 3.5

Direct

R$_1$ = OAc, OBz
R$_2$ = CH$_3$, CH$_2$OAc, CO$_2$R
R$_3$ = alkyl

Thiopyridine Intermediate   Indirect

62
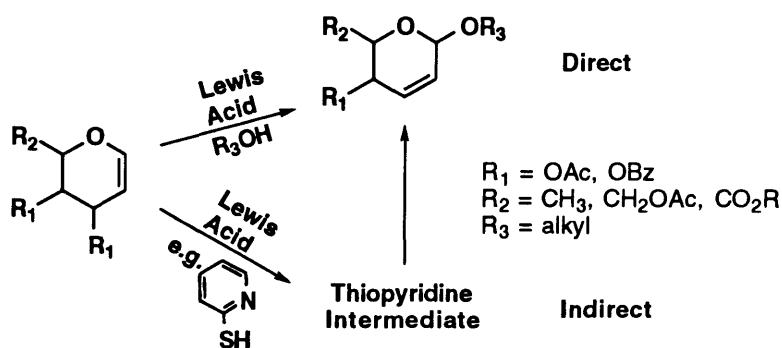
The coupling of aryloxy groups to glycals is comparatively more difficult than the coupling of alkoxy groups. Direct couplings are often complicated by the decreased nucleophilicity of phenoxy groups and the resulting increased formation of carbon coupled products.[93-95] Indeed, our efforts to directly couple the phenoxy nucleophile to arabinal under a variety of Lewis acid catalyzed conditions afforded inseparable mixtures of products. An indirect method for introducing the aryloxy functionality into arabinal was, therefore, pursued. Specifically, the glycal was first coupled to 2-thiopyridine and, in a second step, this group was activated and displaced by the desired aryloxy functionality.

Dunkerton[91] and Priebe[92] described the Lewis acid catalyzed activation of 3,4,6-substituted glycals with 2-thiopyridine. The application of Dunkerton's methodology to 3,4-substituted arabinal proved to be highly efficient (Scheme 3.10). A chromatographically stable mixture of the C-3 substituted **82a** and C-1 substituted **82b** regioisomers was prepared in high yield from D-arabinal (Scheme 3.10). The corresponding enantiomers **82c** and **82d**, respectively, were analogously prepared from L-arabinal (not shown).

Scheme 3.10

> 95% diastereofacial selectivity
71% yield (13)

> 95% diastereofacial selectivity
5.5% yield (1)
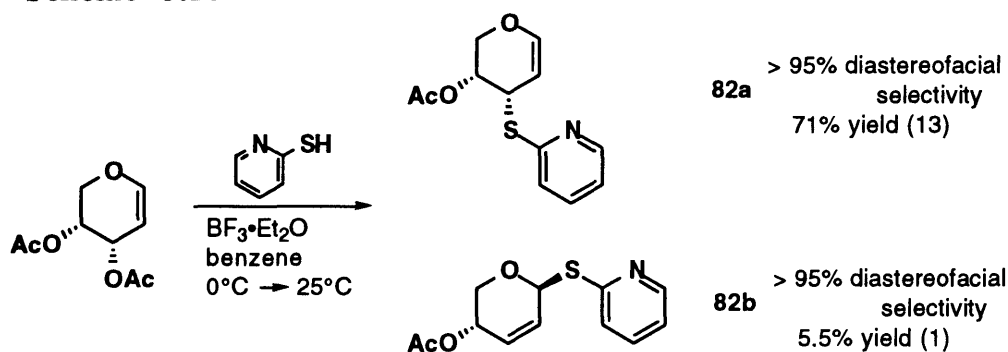
Several methods for activating 1-thio-hex-2-enopyranosides and 1-thio-pyranosides towards nucleophilic displacement have been described in the carbohydrate literature. Again, the literature is enriched with examples of alkoxy nucleophiles relative to aryloxy nucleophiles. Each of these methods (e.g. Lewis acids, MeI, NBS, Hg salts, Ag salts)

was systematically applied to the coupling of the phenoxy nucleophile with arabinal.[91,96-99] Silver triflate activation of the 3-thioglycal intermediate **82a** proved to be most efficient (Scheme 3.11). A chromatographically separable, diastereomeric mixture of 1,4-disubstituted-hex-2-enopyranosides **83a** and **83b** was prepared in reasonably high yield (Scheme 3.11). The corresponding enantiomers **83c** and **83d** were analogously prepared from 3-thioglycal **82c** (not shown).

Scheme 3.11
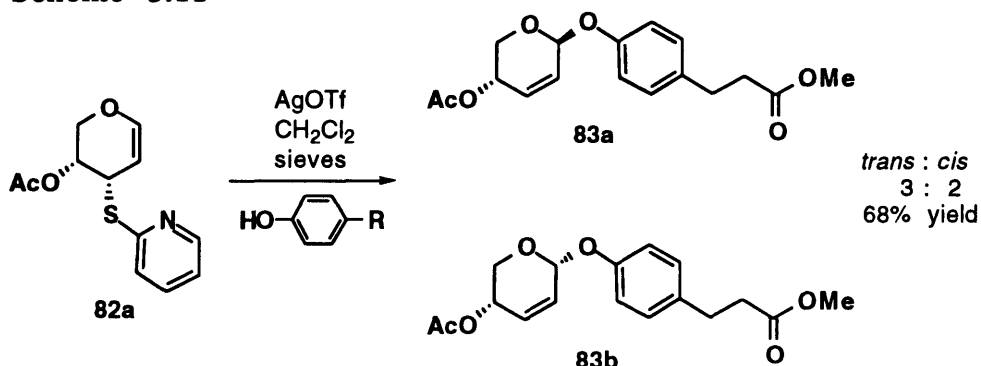
The synthesis of substrates **85a** and **85b** proceeded individually from **83a** and **83b**, respectively (Scheme 3.12). The acetate was deprotected and the ester reduced simultaneously with diisobutylaluminum hydride to provide **84a** and **84b**. Reduction of the double bond by hydrogenation over palladium on carbon provided substrates **85a** and **85b**. The corresponding enantiomers **85c** and **85d** were analogously prepared from **83c** and **83d** via **84c** and **84d**, respectively (not shown).

Scheme 3.12
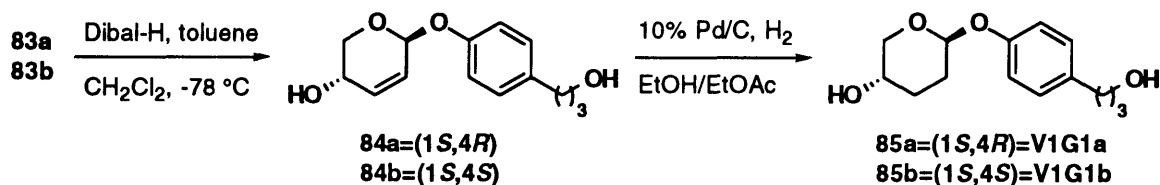
3.8. Benzyloxy Substrates

The substrates for the azetidine hapten **A1** include a benzyloxy leaving group Figure 3.6).

64

Figure 3.6

(rac)-A1r

(1S,4R)-A1a
(1S,4S)-A1b

(1R,4S)-A1c
(1R,4R)-A1d
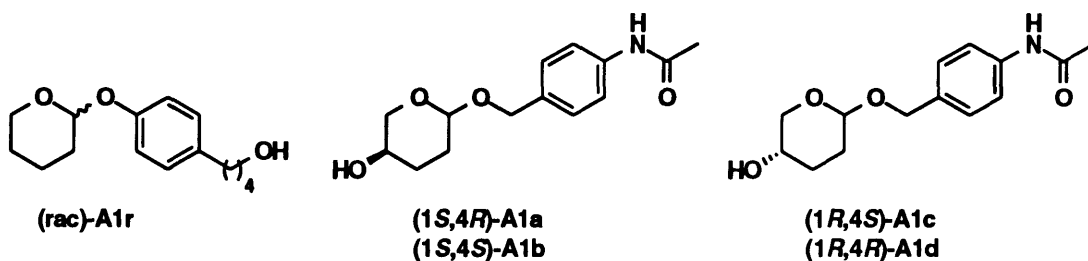
3.8.a. Synthesis of Substrate A1r

The synthesis of substrate **A1r** was carried out by Hiroaki Suga as shown in Scheme 3.13.

Scheme 3.13

PPTS, CH$_2$Cl$_2$
4 Å sieves
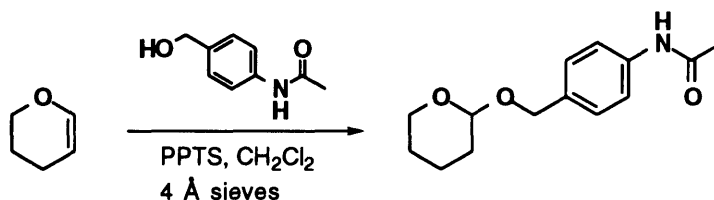
3.8.b. Synthesis of Substrates A1a-d

The synthesis of substrates **A1a-d** was carried out by Hiroaki Suga as shown in Scheme 3.14 for **A1a,b**.

Scheme 3.14

1. DHP, PPTS, CH$_2$Cl$_2$
2. LiAlH$_4$, Et$_2$O

3. TBSCl, DMAP, NEt$_3$,
   CH$_2$Cl$_2$ then
   4-Me-benzoyl chloride

70%, 3 steps

Bz=4-Me-benzolyl

1. Bu$_4$NF, THF
2. Swern

3. AcOH, THF/H$_2$O

80%, 3 steps

1. ClCO$_2$CH$_2$C$_6$H$_4$-p-NO$_2$
   NEt$_3$, CH$_2$Cl$_2$
2. 4-acetamidobenzyl alcohol
   TMSOTf, CH$_2$Cl$_2$

3. separate diasteromers
4. K$_2$CO$_3$, MeOH

49%, 3 steps

A1a=(1R, 4R)
A1b=(1S,4R)

65
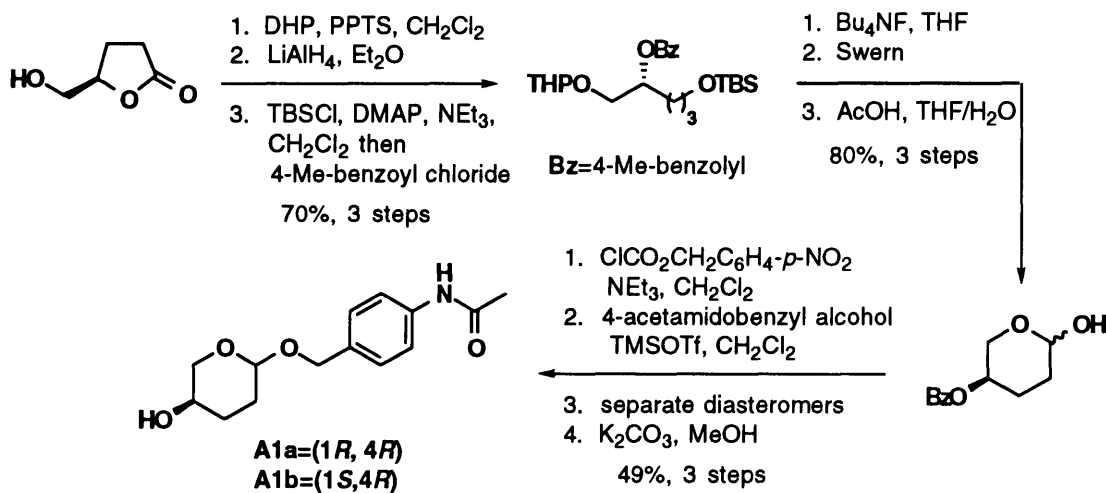
3.9. Summary

Of the five haptens designed, haptens **V1**, **A1** and **G1** were ultimately pursued for the production of monoclonal antibodies (Chapter 4). Hapten **V1** is a half-chair conformational mimic of the β-anomer of a phenoxy substrate. Hapten **A1** is a half-chair conformational mimic of the α-anomer of a benzyloxy substrate. Hapten **G1** is a chair conformational mimic of the β-anomer of a phenoxy substrate. Each of these hapten designs was also intended to provide for the induction of catalytic antibody combining site residues.

Chapter 4

Antibody Production and Assay for Catalytic Activity

Monoclonal antibody technology allows for the isolation of continuous cell lines which secrete single antibodies of predefined specificity. These monoclonal antibodies may be screened for catalytic activity and characterized in terms of observed reaction kinetics. The production, isolation, purification and screening of monoclonal antibodies raised to glucosidase haptens **V1**, **G1**, and **A1** are described in this chapter.

4.1. Protein Conjugates

The immune system is capable of recognizing and mounting an immune response to, in general, compounds with molecular weights upwards of 3000. Haptens falling below this cut off are often coupled to carrier proteins to ensure their immunogenicity. One conventional means of linking a hapten to a carrier protein is through the formation of an amide bond between a carboxylic acid on the hapten and a lysine residue on the surface of the protein. Specifically, the hapten's carboxylic acid moiety is activated towards nucleophilic attack by converting it to its N-hydroxy-succinimide ester. The activated ester is then condensed with the carrier protein. Typically, each protein carries 10-40 haptens on its surface.

4.1.a. Haptens V1, G1, and A1 Protein Conjugates

Three of our glycosidase haptens were coupled to carrier proteins according to the aforementioned method. Haptens **V1** and **G1** were individually coupled to bovine serum albumin (BSA) and fibrinogen (Fib) and **A1** was coupled to kehole limpet hemocyanin (KLH) and BSA. Each hapten was coupled to two different carrier proteins; one hapten-protein conjugate was used for immunizations and the other was used for binding assays (ELISA).

4.2. Immunization and Fusion

Standard immunization protocols for mice involve three or four immunizations before the spleen, which contains the antibody secreting B-cells, is harvested. Since B-cells are not viable in cell culture for more than one week, they are isolated and then immediately fused with myeloma cells. The resulting hybrid cells (hybridomas) are immortal cells and are, therefore, easily maintained in cell culture.

4.2.a. Hapten V1 Immunization

Four Balb/c mice each received a subcutaneous injection of **V1-BSA** emulsified in RIBI adjuvant (MPL and TDM emulsion) on day 1 (100μg) and again on day 36 (200μg). On day 44 blood serum from each of the mice was drawn and analyzed for the presence of high affinity immunoglobin class G (IgG) molecules using the standard enzyme-linked immunosorbant assay (ELISA). Three of the four mice demonstrated a strong immune response against **V1-BSA** as evidenced by the ELISA titers. One of these three mice received an intravenous (100μg, tail vein)/intraperitoneal (100μg) injection of **V1-BSA** in sterile phosphate buffered saline (PBS) on day 76. On day 79 this mouse was sacrificed, the spleen was harvested, and the B-cells were fused with 653/HGPRT⁻ myeloma cells to prepare hybridomas.

4.2.b. Hapten G1 Immunization

Four Balb/c mice each received a subcutaneous injection of **G1-BSA** emulsified in RIBI adjuvant (MPL and TDM emulsion) on day 1 (100μg) and again on day 21 (200μg). On day 28 blood serum from each of the mice was drawn and analyzed for the presence of high affinity immunoglobin class G (IgG) molecules using the standard ELISA. Two of the four mice demonstrated a moderate immune response against **G1-BSA** as evidenced by the ELISA titers. One of these two mice received an intravenous (100μg, tail vein)/intraperitoneal (100 μg) injection of **G1-BSA** in sterile phosphate buffered saline (PBS) on day 78. On day 81 this mouse was sacrificed, the spleen was harvested, and the B-cells were fused with 653/HGPRT⁻ myeloma cells to prepare hybridomas.

4.2.c. Hapten A1 Immunization

Four Balb/c mice each received a subcutaneous injection of **A1-KLH** emulsified in RIBI adjuvant (MPL and TDM emulsion) on day 1 (100μg) and again on day 14 (100μg). On day 21 blood serum from each of the mice drawn and analyzed for the presence of high affinity immunoglobin class G (IgG) molecules using the standard ELISA. On day 82, the mouse with the highest titer received an intraperitoneal injection (100μg) of **A1-KLH**. On day 85 this mouse was sacrificed, the spleen was harvested, and the B-cells were fused with 653/HGPRT⁻ myeloma cells to prepare hybridomas.

4.3. Antibody Production

Hybridomas are propagated in cell culture in such a manner as to yield monoclonal cell lines, each cell line producing a unique antibody exhibiting an affinity for the hapten. Large quantities of each of the desired monoclonal antibodies are then produced through *in vivo* propagation in mice.

4.3.a. Haptens V1 and G1 Specific Antibodies

Each fusion was treated independently according to the following protocol. Cells were suspended in media and plated into eight 96-well plates (100 μL/well). This plating media contained the selection agents hypoxanthine, aminopterine, and thymidine (HAT), and the growth supplements fetal bovine serum (20% FBS), hybridoma enhancing supplement (2% HES), and endothelial cell growth supplement (3% wt./vol. ECGS). Seven days after this initial plating, each well was supplemented with 50 μL growth media. The growth media consists of the same ingredients as the plating media, minus the toxin aminopterine. Eleven days after the fusion each well was assayed by the standard ELISA for hapten binding, and all colonies that displayed tight binding (positives) were pursued for subcloning. Following completion of the ELISA screen, indicated (positive) hapten-binding cells were pursued and non-hapten binding cells were discarded. In the case of hapten **V1**, approximately 75 wells were found to contain cell line(s) that secreted high

69

affinity hapten-binding antibodies. In the case of hapten **G1**, approximately 50 wells were found to contain cell line(s) that secreted high affinity hapten-binding antibodies.

To insure the monoclonality of the hapten-binding cell lines, each positive, growing cell line was subcloned according to the following protocol. Once confluent, each of the positive colonies from the original 96-well plate was individually serially diluted and transferred to new 96-well plates. The colonies were serially diluted in such a manner as to provide wells that theoretically contain 10, 1 and .25 cells. Cells were grown in 100 μL of growth media for seven days and were then supplemented with another 50 μL of growth media. The next day these plates were again screened by ELISA for binding to hapten. Plates containing a positive, monoclonal cell line (defined as monoclonal according to a Poissan statistical distribution) were expanded. Plates containing positive cell lines that were not statistically monoclonal were resubjected to serial dilution; the most dilute positive colony was serially diluted according to the aforementioned serial dilution protocol. Monoclonal cell lines were expanded in media containing 20% FBS and 2% HES (expansion media) through continuous growth in cell culture to a final volume of 25 mL with a density of $1\text{-}5\text{x}10^5$ cells/ml. In the case of hapten **V1**, 53 positive antibody producing cell lines were ultimately expanded. In the case of hapten **G1** 41 positive antibody producing cell lines were ultimately expanded.

To produce large quantities of each of the monoclonal antibodies, monoclonal cell lines were propagated in mice according to the following standard protocol. Each cell line was individually injected into pristane-primed Balb/c mice to produce tumors secreting high concentrations of antibody (ascites fluid). The ascites fluid was then isolated and purified. In the case of haptens **V1** and **G1**, 53 and 41 cell lines, respectively, were individually propagated in mice and the ascites fluid was isolated.

4.3.b. Hapten A1 Specific Antibodies

Monoclonal hybridomas were prepared by Hiroaki Suga according to a protocol which has been detailed elsewhere. In the end, 15 cell lines were individually propagated in mice and the ascites fluid was isolated.

4.4 Antibody Purification

Monoclonal antibodies were purified to avoid degradation by endogenous proteases and to remove any contaminating glycosidase enzymes.

4.4.a. Haptens V1, G1 and A1 Specific Antibody Purification

Antibodies raised to haptens **V1, G1** and **A1** were similarly purified to >95% homogeneity (as judged by SDS-polyacrylamide gel electrophoresis) according to a standard antibody purification protocol. First, antibodies were precipitated from ascites fluid with ammonium sulfate (45% final concentration). Precipitated antibodies were then solubilized in 50 mM Tris•HCl, pH 7.8 and exhaustively dialyzed against the same buffer. Next, antibodies were subjected to DEAE-Sephacel anion-exchange chromatography. A salt gradient (from 0 mM to 500 mM NaCl in 50 mM Tris•HCl, pH 7.8) served to elute partially purified antibodies. Finally, antibody containing fractions were concentrated, exchanged into potassium phosphate buffer (20 mM Kpi, pH 7.2), and subjected to protein G-Sepharose affinity chromatography. A low pH buffer (100 mM glycine•HCl, pH 2.7) was used to elute pure antibody (>95%) from the affinity column. Antibody containing fractions were then neutralized, concentrated and exchanged into the appropriate assay buffers.

4.5 Assays for Catalytic Activity

High performance liquid chromatography (HPLC) was used to quantitate the rates of substrate hydrolysis. Substrate hydrolysis rates in the presence and absence of substrate, as judged by product levels, provided an indication of the catalytic activity of the antibodies.

4.5.a. Haptens V1 and G1 Specific Antibodies Catalytic Activity Assays

Each antibody was individually assayed for hydrolytic activity against three substrates (V1G1r, V1G1a, V1G1c) under a variety of conditions. Since each of these

(rac)-V1G1r   (1S,4R)-V1G1a   (1R,4S)-V1G1c
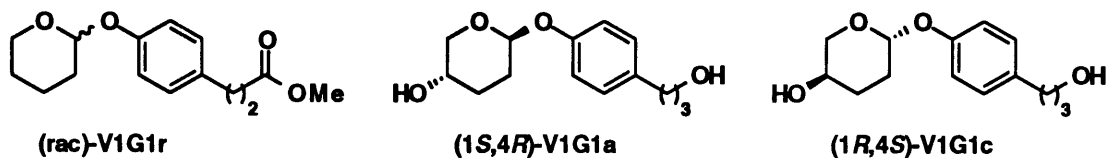
substrates was known to exist as the α-anomer, and the hapten design corresponded to a β-anomer, we anticipated a relatively high Michaelis constant (K_M) for the antibodies. In order to best observe potential catalysts, we, therefore, used substrate concentrations in the anticipated K_M range. First, antibodies (18 μM) were screened against substrate V1G1r (2.0 mM) at pH 6.0 (42 mM bis-tris, 90 mM NaCl, 10% DMF), 25°C. None of the V1 or G1 antibodies appeared to catalyze the hydrolysis of substrate V1G1r.

As it may have been the case that the C-4 hydroxyl group was an important binding determinant, each antibody was rescreened against both of the *trans* substituted substrates. Antibodies (18 μM) were screened against substrates V1G1a (1.0 mM and 3.0 mM) and substrate V1G1c (1.0 mM and 3.0 mM) at pH 5.4 (22 mM sodium citrate, 2 mM bis-tris, 98 mM NaCl, 2% DMF), 37°C. Again, no V1 or G1 catalysts were identified from these assays. Taken together, these five different assays suggested that none of the candidate monoclonal antibodies was worth pursuing further.

The failure of haptens V1 and G1 to elicit antibodies capable of hydrolyzing the glycoside substrates may be interpreted in several ways. First, as the hapten design included bis-equatorial C-1 and C-4 substituents corresponding to the axially oriented C-1 leaving group and C-4 hydroxy moiety on the substrate, the antibodies may not have been able to bind the substrates.

Alternatively, in the case of antibodies raised to hapten V1, the substrates may have been bound but were then distorted in a non-productive fashion. Recall, hapten V1 is an

imperfect half-chair conformational mimic of the putative transition state. The double bond in hapten **V1** corresponds in position to C-5 and the endocyclic oxygen in the substrates. In addition, the amine in hapten **V1** may have failed to elicit, or inappropriately positioned, the desired combining site carboxylic acid, which was intended to function as a proton donor to the departing leaving group.

In terms of hapten **G1**, the substrate may have been bound but was then rendered resistant to hydrolysis due to improper orbital overlap. According to stereoelectronic theory, in order for glycoside hydrolysis to proceed a lone pair of electrons must be positioned antiperiplanar to the C-O bond being cleaved. In the case of the β-anomer it has been postulated that this stereoelectronic requirement is satisfied if the glycoside is distorted into the half-chair conformation. Antibodies raised to hapten **G1** did not provide for such distortion, and may have, in fact, prohibited such a conformational change. In addition, the ammonium moiety in hapten **G1** may have failed to elicit, or inappropriately positioned, the desired combining site carboxylate, which was intended to electrostatically stabilize the positively charged oxocarbonium ion transition state or to donate a proton (in the case of a perturbed pK_a value) to the exocyclic oxygen of the substrate.

4.5.b. Hapten A1 Specific Antibodies Catalytic Activity Assays

These assays were conducted and analyzed by Hiroaki Suga. All assays were carried out in aqueous buffer composed of 29mM bis-tris, 11 mM succinic acid, 10 mM NaCl and 2% acetonitrile at 37°C. Each antibody was individually assayed for hydrolytic activity against five substrates (**A1r, A1a-d**). An initial assay against **A1r** (18 μM

(rac)-A1r   (1*S*,4*R*)-A1a   (1*R*,4*S*)-A1c
                       (1*S*,4*S*)-A1b   (1*R*,4*R*)-A1d

73
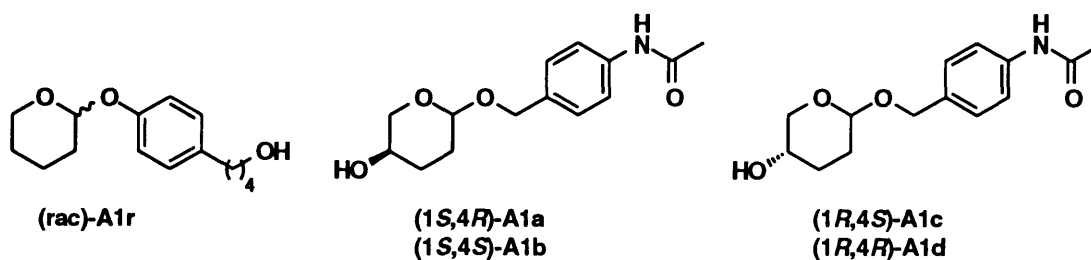
antibody, 2.0 mM **A1r**, pH 5.4) suggested that five of the monoclonal antibodies accelerated the hydrolysis of substrate **A1r**. Antibody ST-8B1, which showed the most significant activity was selected for further study. The rate of hydrolysis of substrate **A1r**, measured as a function of substrate **A1r** concentrations (0.5 mM-4.0 mM, pH 5.4), followed Michaelis-Menton kinetics. The apparent K_M value and catalytic constant k_{cat} were determined to be 1.74 mM and 3.6×10^{-2} min^{-1}, respectively. A comparison of the k_{cat} value with the uncatalyzed value ($k_{uncat} = 1.5 \times 10^{-4}$ min^{-1}) indicated a rate acceleration of 240 over background. The catalytic activity of ST-8B1 was competitively inhibited by the addition of hapten ($K_i = 8.3$ μM), indicating that the catalyzed hydrolysis proceeded in the antibody combining site (Table 4.1).

The hydrolysis of enantiomerically and diastereomerically pure substrates **A1a-d** was then examined to determine the stereospecificity of antibody ST-8B1. The rates of hydrolysis of substrates **A1a-d** were each measured as a function of substrate concentration (0.5 mM-4.0 mM, pH 5.4). The antibody catalyzed the hydrolysis of substrates **A1a** and **A1b** but not **A1c** or **A1d**. This result may be interpreted to mean the antibody catalyzed reaction is stereospecific in terms of the chirality of the C-1 benzyloxy moiety. The apparent K_M value and catalytic constant k_{cat} for substrate **A1a** were determined to be 1.16 mM and 1.5×10^{-3} min^{-1}, respectively. The apparent K_M value and catalytic constant k_{cat} for substrate **A1b** were determined to be 1.62 mM and 2.1×10^{-3} min^{-1}, respectively. A comparison of the k_{cat} values with the uncatalyzed values (**A1a** $k_{uncat} = 4.0 \times 10^{-6}$ min^{-1}, **A1b** $k_{uncat} = 2.0 \times 10^{-5}$ min^{-1}) indicated rate accelerations of

Table 4.1

Michaelis-Menten Parameters of Antibody ST-8B1*

Substrate	K_M (mM)	k_{cat} (min^{-1})	k_{cat}/k_{un}	K_i (μM)
A1r	1.74	3.6×10^{-2}	240	8.3
A1a	1.16	1.5×10^{-3}	375	9.3
A1b	1.62	2.1×10^{-3}	105	n.d.

* Taken from : Suga, H. *J. Am. Chem. Soc.* 1994, *116*, 11197.

375 with substrate **A1a** and 105 with substrate **A1b**, over background (Table 4.1). The catalytic activity of ST-8B1 was competitively inhibited by the addition of hapten, indicating that the catalyzed hydrolysis proceeded in the antibody combining site. A comparison of the apparent kinetic constants indicated that substrate **A1a** was a comparatively better substrate for the antibody catalyzed hydrolysis. This result suggested that the antibody is also able to discern the relative stereochemistry of the C-4 hydroxyl group, with the C-4 equatorial isomer being the preferred substrate. Indeed, the hapten design included C-4 equatorial and C-1 axial substituents. Taken together, antibody ST-8B1 appears to have high stereospecificity with respect to both the C-1 and C-4 stereogenic centers of the substrates, and appears to have been generated from the $(1S,4R,6S)$-hapten **A1**.

In order to begin to elucidate the mechanism of antibody ST-8B1 catalysis, the pH-dependent kinetics of antibody catalyzed hydrolysis of substrate **A1a** were determined. Hydrolysis of substrate **A1a** over the pH range from 5.4 to 7.0 indicated that k_{cat}/k_{uncat} and K_M are independent of pH. Although the pH range studied was limited, this result was interpreted to suggest that there was no significant participation of an acidic residue (ionizable in the pH region studied) in catalysis. Indeed, the observed ratio of k_{cat}/k_{uncat} and K_M/K_i, being roughly equal, led the authors to suggest that the antibody contributes only to the binding and distortion of the substrate. The lack of general acid catalysis by ST-8B1 may be interpreted to mean the quaternary ammonium ion moiety on hapten **A1** is not appropriate for the generation of an acidic residue in close proximity to the exo-oxygen of the substrate.

4.6. Summary and Conclusions

The combined efforts of the Masamune, Schultz and Lerner groups to generate glycosidase type antibodies have, thus far, met with only moderate success. The best catalyst (Masamune) provides a 375-fold rate enhancement over the uncatalyzed reaction. This rate enhancement falls far below the corresponding enzyme catalyzed rates, as well as

the rates generally observed in antibody catalyzed reactions. Indeed, glycoside bond hydrolysis is a particularly difficult reaction for which to develop catalytic antibodies. The lack of success in generating efficient glycosidase antibodies is a reflection of the mechanistic complexity and energetic barriers associated with glycoside hydrolysis. Nonetheless, important information, in terms of future efforts to generate glycosidase antibodies, may be gleaned from these preliminary efforts.

It should be noted, for each of the glycosidase antibody catalysts reported to date, the substrate that has been hydrolyzed was an α-anomer. Mechanistically, in terms of catalytic antibodies, the hydrolysis of α-glycosides is, perhaps, less demanding than the hydrolysis of β-glycosides. According to stereoelectronic theory, the α-anomer need not undergo a conformational change in order for hydrolysis to proceed; a lone pair of electrons is positioned antiperiplanar to the C-O bond being cleaved in the ground state. Following protonation of the exocyclic oxygen, hydrolysis is then accompanied by the formation of the half-chair oxocarbonium ion transition state. In contrast, the β-anomer must undergo a conformational change *prior* to the onset of hydrolysis. This conformational change serves to position a lone pair of electrons antiperiplanar to the C-O bond being cleaved and, thereby, satisfy the stereoelectronic requirement for hydrolysis. Once this stereochemical requirement has been met, hydrolysis, and the accompanied formation of the half-chair oxocarbonium ion transition state, may proceed. In terms of glycosidase enzymes, this is perhaps a subtle distinction. β-Glucosidases are able to hydrolyze β-glycosides with rates comparable to those produced by α-glucosidases with α-glycosides. In terms of the rational design of glucosidase type antibodies, however, this distinction should not be overlooked. In essence, to hydrolyze an α-glycoside, the antibody combining site should be complementary to the putative transition state. To hydrolyze a β-anomer, on the other hand, the antibody combining site must be capable of distorting the substrate such that the requisite orbital overlap is achieved and then must also accommodate the transition state structure. Future efforts to design glycosidase antibodies might, therefore, best be focused

on the hydrolysis of α-glycosides until the specific hapten features needed to induce the formation of efficient catalysts have been elucidated.

It is also important to note that the glycosidase antibodies generated thus far have hydrolyzed relatively labile substrates. Fully hydroxylated glycosides are approximately 10^7 times less reactive towards hydrolysis than the unsubstituted and C-4 substituted glycosides studied in the antibody experiments. In order to overcome the energetic barrier associated with the hydrolysis of fully hydroxylated glycosides, it is likely that the hapten designs will have to be improved. Specifically, it is likely that all three mechanistic features (distortion, protonation, electrostatic stabilization) will have to be accommodated for in a single antibody combining site. To achieve this goal, hapten designs will be required to include residues that will induce the formation of both a combining site acid and base. In addition, the hapten design must provide for a combining site that will distort the substrate and/or accommodate the half-chair conformation of the transition state. Although antibody combining sites are capable of providing up to 20 kcal/mol towards ligand binding, this magnitude of binding energy may not be raised to the relatively small haptens used in catalytic antibody research. In order to generate antibodies endowed with more binding energy, larger haptens may need to be utilized. Disaccharide type haptens, for example, would provide a greater number of binding determinants. Indeed, the lysozyme substrate, a hexasaccharide, may be distorted in the D subsite as a result of the binding energy provided by the saccharide contacts in the remaining five binding sites.

Although only one of the three haptens studied in the Masamune group succeeded in generating antibodies capable of hydrolyzing a glycosidic bond, all three of the haptens served to provide information that will serve as a guide in subsequent glucosidase hapten designs.

Chapter 5

Experimental

5.1. Synthesis of Haptens and Substrates

5.1.a. General Methods

All anhydrous reactions were carried out in flame-dried glassware under an argon atmosphere. Aqueous reactions required no special handling. Column chromatography was performed using 230-400 mesh silica gel (Merck). Proton (^{1}H NMR) and fully decoupled carbon (^{13}C NMR) were recorded on a Bruker AC-250 (^{1}H 250 MHz, ^{13}C 62.9 MHz), Varian VXR-500 (^{1}H 500 MHz, ^{13}C 125.7 MHz), Varian VXR-501 (^{1}H 501 MHz, ^{13}C 125.0 MHz), or Varian UN-300 (^{1}H 300 MHz, ^{13}C 75.4 MHz). ^{1}H NMR chemical shifts are reported in ppm (δ) from the center peak of the solvent peak(s): CDCl$_3$ (7.26), C$_6$D$_6$ (7.15), CD$_3$OD (3.30), CD$_3$COCD$_3$ (2.04). ^{13}C NMR chemical shifts are reported in ppm (δ) from the center peak of the solvent peak(s): CDCl$_3$ (77.0), C$_6$D$_6$ (128.0), CD$_3$OD (49.07), CD$_3$COCD$_3$ (29.8). 1H NMR peak multiplicities are indicated by s (singlet), d (doublet), t (triplet), q (quartet), quint (quintuplet), m (multiplet). Coupling constants (J) are reported in Hz. Infrared spectra (IR) were recorded on a Perkin-Elmer 283B spectrophotometer with polystyrene (1601 cm^{-1}) as the reference. High resolution mass spectra (HRMS) were obtained using a Finnegan MAT 8200 spectrophotometer. Melting points were not corrected.

5.1.b. Hapten Synthesis

60
(racemic)

CH₃CN, reflux

61a
(racemic)
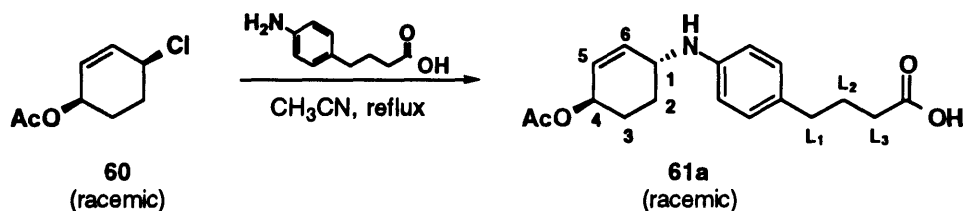
Preparation of allylic amine 61a

To a room temperature solution of allylic chloride **60** (526 mg, 3.0 mmol) in CH-3CN (11mL) was added 4-(4-aminophenyl)butyric acid (1.52 g, 8.5 mmol). The mixture was heated at reflux for 16.5 hours, cooled to 25° C and concentrated in vacuo to 25% volume. The resulting suspension was diluted with EtOAc (25 mL), filtered, and concentrated in vacuo. The residual oil was purified by flash silica gel column chromatography to yield **61a** (823 mg, 89.5%) as a colorless oil.

Physical data for 61a:

^{1}H NMR (250 MHz, CDCl$_3$) δ 1.50-1.75 (m, 2H, H$_3$, H$_3$'), 1.90 (quint, 2H, L$_2$), 2.06

(s, 3H, OAc), 2.10 (m, 2H, H$_2$, H$_2$'), 2.34 (t, J=7.4 Hz, 2H, L$_3$), 2.55 (t, J=7.4

Hz, 2H, L$_1$), 4.03 (m, 1H, H$_1$), 5.32 (m, 1H, H$_4$), 5.78 (dd, J=10.1, 2.1 Hz,

1H, H$_6$), 5.96 (d broad, J=10.1 Hz, 1H, H$_5$), 6.58 (d, J=8.4 Hz, 2H, Ar), 6.99

(d, J=8.4 Hz, 2H, Ar)

^{13}C NMR (125.0 MHz, CDCl$_3$) d 21.26, 26.47, 26.64, 27.00, 33.24, 34.03, 48.43,

68.56

IR (film) 3700-2500 (acid O-H), 3370 (amine N-H), 3025 (=C-H), 1710 (acid C=O), 1610 (Ar, C=C), 1510 (Ar, C=C)

HRMS (EIMS) calculated for C$_{18}$H$_{23}$NO$_4$ 317.1627, found 317.1625

60
(racemic)

$Pd(Ph_3P)_4$, THF

61b
(racemic)
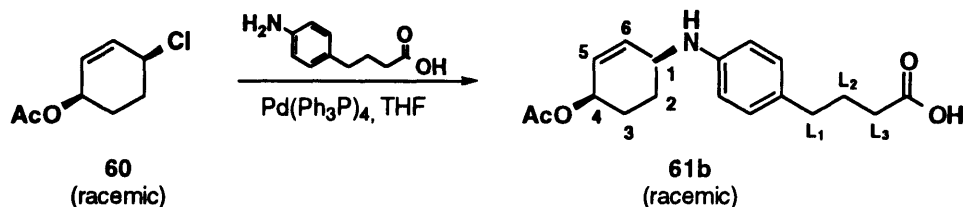
Preparation of allylic amine 61b

To a room temperature solution of allylic chloride **60** (75 mg, 0.43 mmol) in THF (1.5 mL) was added 4-(4-aminophenyl)butyric acid (233 mg, 1.3 mmol) followed by $Pd(Ph_3P)_4$. After stirring for 3.5 hours the mixture was filtered, poured into saturated NaCl (5 mL) and extracted with EtOAc (1x10 mL), dried over anhydrous Na_2SO_4, and concentrated in vacuo. The residual oil was purified by flash silica gel column chromatography to yield **61b** (136 mg, 100%) as a white solid.

Physical data for 61b

^{1}H NMR (250 MHz, $CDCl_3$) δ 1.74-1.83 (m, 2H, H_2, $H_{2'}$), 1.83-1.90 (m, 2H, H_3,

$H_{3'}$), 1.91 (m, 2H, L_2), 2.06 (s, 3H, OAc), 2.36 (t, J=7.4 Hz, 2H, L_3), 2.55 (t,

J=7.4 Hz, 2H, L_1), 3.95 (m, 1H, H_1), 5.24 (m, 1H, H_4), 5.84 (ddd, J=10.0,

3.4, 1.7 Hz, 1H, H_6), 6.01 (dd, J=10.0, 2.5 Hz, 1H, H_5), 6.65 (d, J=8.2Hz,

2H, Ar), 7.02 (d, J=8.2 Hz, 2H, Ar)

HRMS (EIMS) calculated for $C_{18}H_{23}NO_4$ 317.1627, found 317.1625

Melting point 85-88°C

61a
(racemic)

62
(racemic)
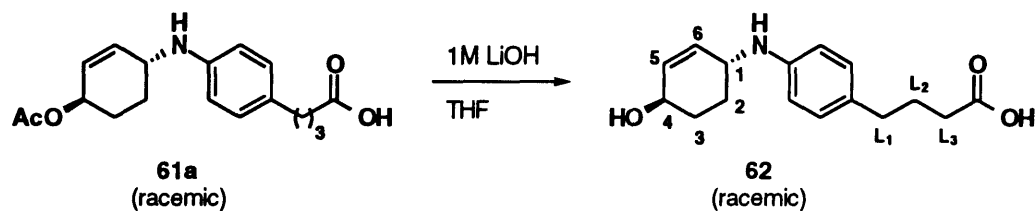
Preparation of acid 62

To a room temperature solution of esters **61a** (130 mg, 0.4 mmol) in THF (3.7 mL) was added LiOH (3.7 mL, 1.0 M). After stirring for 2.5 hours the solution was neutralized with 10% HCl and concentrated in vacuo. The residual oil was purified by flash silica gel column chromatography to yield **62** (101 mg, 89.7%) as a colorless oil.

Physical data for 62

^{1}H NMR (250 MHz, CDCl$_3$) δ 1.42-1.65 (m, 2H, H$_3$, H$_3$'), 1.91 (quint, J=7.5 Hz, 2H, L$_2$), 2.15 (m, 2H, H$_2$, H$_2$'), 2.35 (t, J=7.5 Hz, 2H, L$_3$), 2.56 (t, J=7.5 Hz, 2H, L$_1$), 4.01 (m, 1H, H$_1$), 4.28 (m, 1H, H$_4$), 4.79 (s broad, 1H, OH), 5.82 (d, J=11.2 Hz, 1H, H$_6$), 5.86 (d J=11.2 Hz, 1H, H$_5$), 6.58 (d, J=8.3 Hz, 2H, Ar), 6.99 (d, J=8.3 Hz, 2H, Ar)

^{13}C NMR (125.0 MHz, CDCl$_3$) δ 26.53, 27.54, 30.73, 33.30, 34.06, 48.93, 66.29, 113.86, 129.31, 130.58, 131.38, 132.20, 144.87, 179.07

IR (film) 3500-2500 (acid O-H, alcohol O-H, amine N-H), 3020 (=C-H), 1700 (acid C=O), 1610 (Ar, C=C), 1510 (Ar, C=C)

HRMS (EIMS) calculated for C$_{16}$H$_{21}$NO$_3$ 275.1521, found 275.1521

8 1

62
(racemic)

63
(racemic)

Preparation of N-hydroxysuccinimate ester 63 (Hapten V1)

To a $0°$ C solution of acid **62** (167 mg, 0.61 mmol) in CH_2Cl_2:DMF (4.0 mL:1.0 mL) was added N-Hydroxysuccinimide (119 mg, 1.04 mmol) followed by DCC (252 mg, 1.22 mmol). After stirring for 3.5 hours at $0°$ C the mixture was filtered and concentrated in vacuo. The residual oil was purified by flash silica gel column chromatography to yield **63** (187 mg, 82.4%) as a viscous oil.
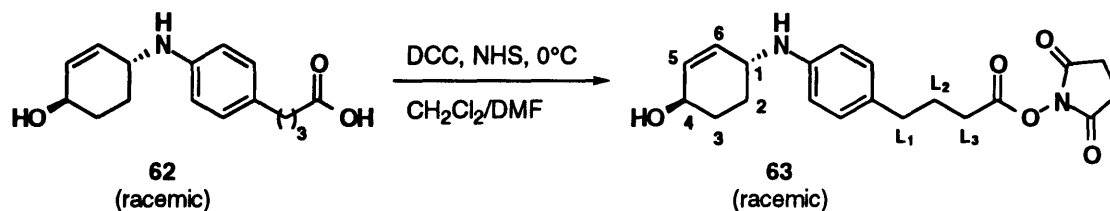
Physical data for 63

^1H NMR (250 MHz, $CDCl_3$) δ 1.42-1.63 (m, 2H, H_3, H_3'), 2.00 (quint, J=7.5 Hz, 2H, L_2), 2.13 (m, 2H, H_2, H_2'), 2.58 (t, J=7.5 Hz, 2H, L_3), 2.61 (t, J=7.5 Hz, 2H, L_1), 2.83 (s, 4H, CH_2, CH_2), 4.00 (m, 1H, H_1), 4.27 (m, 1H, H_4), 5.81 (d, J=11.2 Hz, 1H, H_6), 5.86 (d J=11.2 Hz, 1H, H_5), 6.59 (d, J=8.2 Hz, 2H, Ar), 7.00 (d, J=8.2 Hz, 2H, Ar)

^{13}C NMR (125.0 MHz, $CDCl_3$) δ 25.47, 26.36, 27.49, 29.99, 30.73, 33.52, 48.70, 66.09, 113.59, 129.28, 131.16, 132.29, 145.08, 168.49, 169.14

IR (film) 3600-3200 (alcohol O-H, amine N-H), 3020 (C=C), 1810 (imide C=O), 1780 (imide C=O), 1730 (succinimate ester C=O), 1610 (Ar, C=C), 1510 (Ar, C=C)

HRMS (EIMS) calculated for $C_{20}H_{24}N_2O_5$ 372.1685, found 372.1683

82

63
(racemic)

64
(racemic)
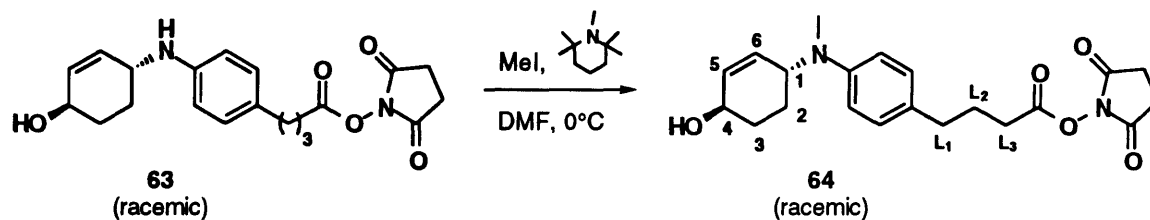
Preparation of monomethylamine 64

To a 0° C solution of amine **63** (215 mg, 0.58 mmol) in DMF (5.0 mL) was added 1,2,2,6,6-pentamethylpiperidine (0.20 mL, 1.16 mmol) followed by methyl iodide (0.90 mL, 14.5 mmol). After stirring at 0° C for 5 hours the mixture was poured into water (10 mL) and extracted with Et_2O (20 mL). The organic phase was washed with water (1x10 mL) and saturated NaCl (1x10 mL), dried over anhydrous Na_2SO_4, and concentrated in vacuo. The residual oil was purified by flash silica gel column chromatography to yield **64** (101 mg, 45.1%) as a colorless oil.

Physical data for 64

^{1}H NMR (250 MHz, $CDCl_3$) δ 1.61 (m, 2H, H_3, $H_{3'}$), 1.98 (m, 1H, H_2), 2.02 (m, 2H, L_2), 2.17 (m, 1H, $H_{2'}$), 2.56-2.66 (m, 4H, L_1, L_3), 2.72 (s, 3H, Me), 2.83 (s, 4H, CH_2, CH_2), 4.32 (m, 1H, H_1), 4.45 (m, 1H, H_4), 5.72 (d, J=10.0 Hz, 1H, H_6), 5.89 (d J=10.0 Hz, 1H, H_5), 6.74 (d, J=8.2 Hz, 2H, Ar), 7.06 (d, J=8.2 Hz, 2H, Ar)

HRMS (EIMS) calculated for $C_{21}H_{26}N_2O_5$ 386.1842, found 386.1844

8 3
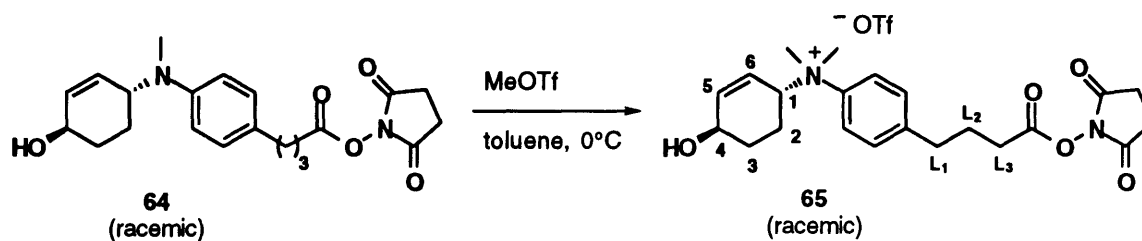
Preparation of quartenized amine 65

To a $0°$ C solution of **64** (10 mg, 26 μmol) in toluene (1.0 mL) was added methyl triflate (6.0 μL, 52 μmol). After standing at $0°C$ for 22 hours volatiles were removed by vacuum transfer. Anhydrous toluene was added to the flask and removed by vacuum transfer (3x1 mL). The residual white solid was identified as >95% **65** by ^{1}HNMR.

Physical data for 65

^{1}H NMR (250 MHz, CD_3OD) δ 1.51 (m, 2H, H_3), 1.79 (m, 1H, H_3') 1.91 (m, 1H, H_2), 2.03-2.21 (m, 3H, H_2', L_2), 2.66 (t, 2H, J=7.1 Hz, L_1), 2.83 (t, J=7.1 Hz, 2H, L_3), 2.83 (s, 4H, CH_2, CH_2), 3.49 (s, 3H, Me), 3.56 (s, 3H, Me), 4.21 (m, 1H, H_4), 4.86 (m, 1H, H_4), 5.71 (dd broad, J=10.6, 2.0 Hz, 1H, H_5), 6.19 (dd broad J=10.6, 1.7 Hz, 1H, H_6), 7.52 (d, J=9.0 Hz, 2H, Ar), 7.75 (d, J=9.0 Hz, 2H, Ar)

8 4
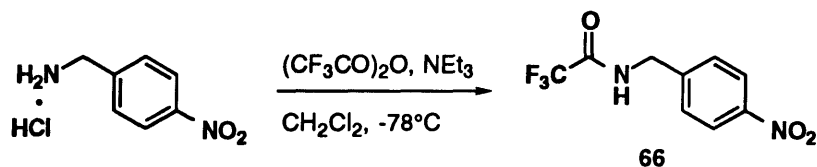
Preparation of acetamide 66

To a room temperature solution of 4-nitrobenzylamine hydrochloride (5.0 g, 26.5 mmol) in CH_2Cl_2 (100 mL) was added triethylamine (13.3 mL, 95.4 mmol). After stirring for 20 minutes the solution was cooled to -78°C and trifluoroacetic anhydride (6.7 mL, 47.7 mmol) was added dropwise. After 40 minutes the solution was poured into saturated NH_4Cl (100 mL) and extracted with CH_2Cl_2 (3x150 mL). The organic phase was washed with saturated NH_4Cl (1x100 mL), dried over anhydrous Na_2SO_4, and concentrated in vacuo. The residual oil was purified by flash silica gel column chromatography to yield 66 (5.24g, 79.1%) as an orange solid.

Physical data for 66

^1H NMR (501 MHz, CD_3OD) δ 4.57 (s, 2H, CH_2), 7.53 (dm, J=8.7 Hz, 2H, Ar), 8.22

(dm, J=8.7 Hz, 2H, Ar)

^{13}C NMR (125.0 MHz, CD_3OD) δ 38.55, 119.73, 124.54, 141.02

IR (film) 3280, broad (amine N-H), 3080 (=C-H), 1700 (amide C=O), 1510 (nitro,

N=O), 1340 (nitro, N=O)

HRMS (EIMS) calculated for $C_9H_7F_3N_2O_3$ 248.0409, found 248.0410

Melting point 85-88°C
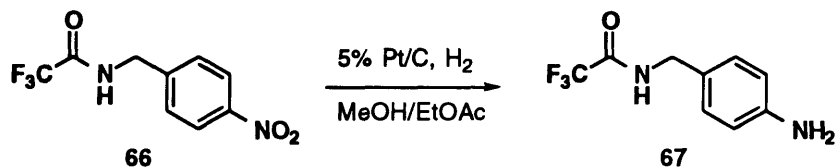
Preparation of amine 67

To a room temperature solution of **66** (5.10 g, 20.4 mmol) in EtOAc:MeOH (1:1, 240 mL) was added 5% platinum on activated carbon (780 mg, 2.0 mmol). Argon, followed by hydrogen, was bubbled through the suspension. After stirring for 3 hours argon was bubbled through the suspension. The mixture was filtered through celite eluting with hot EtOAc:MeOH (1:1, 300 mL) and concentrated in vacuo. The residual oil was purified by flash silica gel column chromatography to yield **67** (3.05 g, 70.0%) as an orange solid.

Physical data for 67

^{1}H NMR (300 MHz, CD$_3$OD) δ 4.30 (s, 2H, CH$_2$), 6.68 (d, J=8.1 Hz, 2H, Ar), 7.04

(d, J=8.1 Hz, 2H, Ar)

^{13}C NMR (125.0 MHz, CD$_3$OD) δ 39.05, 111.54, 122.71, 124.91, 143.36

IR (film) 3420 (amine N-H), 3340 (amine N-H), 3180 (amide N-H), 3020 (=C-H) 1700

(amide C=O)

HRMS (EIMS) calculated for C$_9$H$_9$F$_3$N$_2$O 218.0667, found 218.0710

Melting point 109°C
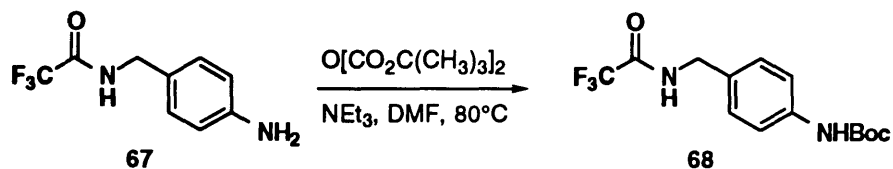
Preparation of carbamate 68

To a room temperature solution of amine **67** (700 mg, 3.18 mmol) in DMF (20 mL) was added NEt$_3$ (1.7 mL, 12.4 mmol) followed by di-*tert*-butyl dicarbonate (0.95 mL, 4.13 mmol). The solution was warmed to 80°C for 30 minutes, cooled to room temperature, poured into water (40 mL) and extracted with Et$_2$O (2x80 mL). The organic phase was washed with saturated NaCl (1x100 mL), dried over anhydrous Na$_2$SO$_4$, and concentrated in vacuo. The residual oil was purified by flash silica gel column chromatography to yield **68** (726 mg, 71.1%) as a white solid.

Physical data for 68

^{1}H NMR (300 MHz, CD$_3$OD) δ 1.50 (s, 9H, t-bu), 4.38 (s, 2H, CH$_2$), 7.19 (d, J=8.7

   Hz, 2H, Ar), 7.36 (d, J=8.7 Hz, 2H, Ar)

^{13}C NMR (125.0 MHz, CD$_3$OD) δ 23.69, 38.84, 75.87, 114.92, 124.30, 127.58,

   135.09, 150.22

IR (film) 3340 (amide N-H), 3280 (carbamate N-H), 3080 (=C-H), 1690 (amide,

   carbamate C=O)

HRMS (EIMS) calculated for C$_{14}$H$_{17}$F$_3$N$_2$O$_3$ 318.1191, found 318.1196

Melting point 153°C

F_3C ... NHBoc **68** → K$_2$CO$_3$ / MeOH/H$_2$O → H$_2$N ... NHBoc **69**
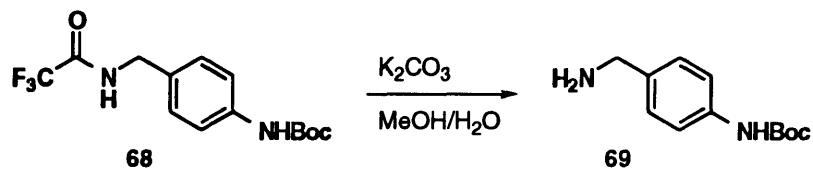
Preparation of benzyl amine 69

To carbamate **68** (1.85 g, 5.76 mmol) was added a solution of K$_2$CO$_3$ (3.98 g, 28.8 mmol) dissolved in MeOH:H$_2$0 (25 mL:10 mL) at room temperature. After stirring for 12 hours, the solution was poured into saturated NaHCO$_3$ (50 mL) and extracted with EtOAc (3x75 mL), dried over anhydrous Na$_2$SO$_4$, and concentrated in vacuo. The crude oil **69** was used without further purification.

Physical data for 69

^{1}H NMR (300 MHz, CD$_3$OD) δ 1.50 (s, 9H, t-bu), 3.70 (s, 2H, CH$_2$), 7.21 (d, J=8.5

Hz, 2H, Ar), 7.34 (d, J=8.5 Hz, 2H, Ar)

^{13}C NMR (125.0 MHz, CD$_3$OD) δ 23.73, 40.85, 75.79, 114.96, 123.54, 124.05,

131.43, 134.63, 150.25

IR (film) 3500-3100 (amine N-H), 1690 (carbamate C=O), 1595 (Ar C=C), 1520 (Ar

C=C)

HRMS (EIMS) calculated for C$_{12}$H$_{18}$N$_2$O$_2$ 222.1368, found 222.1364
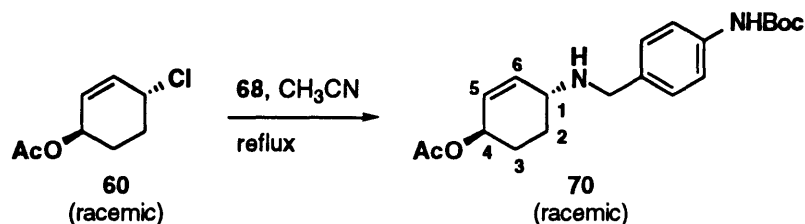
Prepartation of allylic amine 70

To allylic chloride **60** (350 mg, 2.0 mmol) was added a room temperature solution of amine **69** (1.26 g, 5.7 mmol) in CH$_3$CN (7.5 mL). The solution was heated at reflux for 12.5 hours, cooled to room temperature, filtered, and concentrated in vacuo. The residual oil was purified by flash silica gel chromatography to yield **70** (332 mg, 46.1%) as an orange oil.

Physical data for 70

^{1}H NMR (501 MHz, CD$_3$OD) δ 1.50 (s, 9H, t-bu), 1.59-1.46 (m, 2H, H$_3$, H$_3$'), 2.00

(s, 3H, OAc), 2.07 (m, 1H, H$_2$), 2.12 (m, 1H, H$_2$'), 3.25 (m, 1H, H$_1$), 3.69 (d,

J=13.3 Hz, 1H, Bn), 3.73 (d, J=13.3 Hz, 1H, Bn), 5.27 (m, 1H, H$_4$), 5.70 (dm,

10.2 Hz, 2H, H$_6$, H$_5$), 7.23 (d, J=8.6 Hz, 2H, Ar), 7.35 (d, J=8.6 Hz, 2H, Ar)

^{13}C NMR (125.0 MHz, CD$_3$OD) δ 21.14, 27.88, 28.04, 28.73, 50.76, 53.30, 70.72,

80.76, 119.79, 129.33, 130.00, 134.22, 136.62, 139.64, 155.20, 172.40

IR (film) 3320 broad (amine N-H), 3100 (=C-H), 1725 (ester C=O), 1690 (carbamate

C=O), 1590 (Ar C=C), 1540 (Ar C=C)

HRMS (EIMS) calculated for C$_{20}$H$_{28}$N$_2$O$_4$ 360.2049, found 360.2046
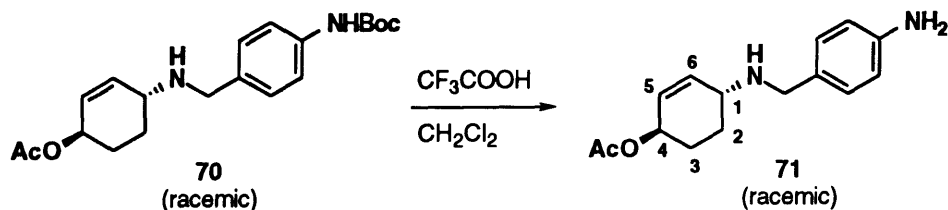
Preparation of amine 71

To a room temperature solution of carbamate **70** (67 mg, 0.18 mmol) in CH$_2$Cl$_2$ (1.0 mL) was added CF$_3$COOH (1.0 mL). After 5 minutes the solution was poured into saturated NaHCO$_3$ (5 mL), extracted with EtOAc (3x10 mL), dried over anhydrous Na$_2$SO$_4$, and concentrated in vacuo. The crude oil **71** was used without further purification.

Physical data for 71

^{1}H NMR (501 MHz, CD$_3$OD) δ 1.63 (m, 1H, H$_3$), 1.78 (m, 1H, H$_3$') 2.03 (s, 3H,

OAc), 2.18-2.95 (m, 2H, H$_2$, H$_2$'), 3.80 (dd, J=8.5, 5.5 Hz, 1H, H$_1$), 4.00 (d,

J=13.3 Hz, 1H, Bn), 4.02 (d, J=13.3 Hz, 1H, Bn), 5.32 (dd, J=8.0, 5.5 Hz, 1H,

H$_4$), 5.95 (d, 11.8 Hz, 1H, H$_6$), 5.97 (d, J=11.8 Hz, 1H, H$_5$), 6.72 (d, J=8.5

Hz, 2H, Ar), 7.18 (d, J=8.5 Hz, 2H, Ar)

^{13}C NMR (125.0 MHz, CD$_3$OD) δ 21.09, 27.50, 27.95, 50.74, 53.28, 70.59, 116.56,

128.71, 129.93, 130.69, 133.36, 148.72, 172.48

IR (film) 3420 broad (amine N-H), 3330 broad (amine N-H), 3210 broad (amine N-H),

3010 (=C-H), 1720 (ester C=O), 1615 (Ar C=C), 1510 (Ar C=C)

HRMS (EIMS) calculated for C$_{15}$H$_{21}$N$_2$O$_2$ 260.1525, found 260.1527
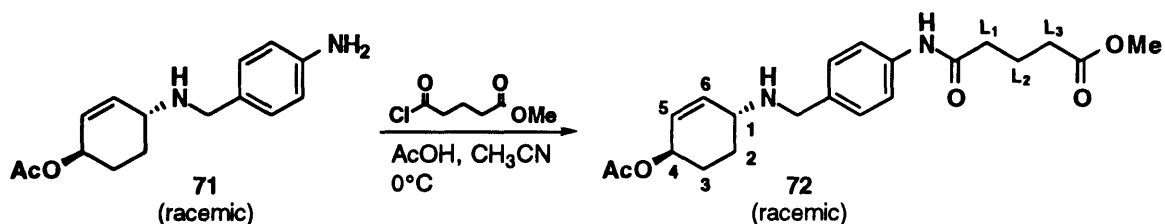
Preparation of amide 72

To a 0° C solution of crude amine **71** (0.18 mmol) in CH3CN (5.0 mL) was added acetic acid (21 μL, 0.36 mmol) followed by a solution of methyl 4-(chloroformyl) butyrate (0.21 mL, 1.0 M) in CH2Cl2 dropwise. After 20 minutes the mixture was poured into saturated NaHCO3 (10 mL), extracted with EtOAc (3x15 mL), dried over anhydrous Na2SO4, and concentrated in vacuo. The residual oil was purified by flash silica gel chromatography (10% MeOH, 90% EtOAc) to yield **72** (56.9 mg, 79.4% over two steps) as an amorphous solid.

Physical data for 72

^{1}H NMR (501 MHz, CD3OD) δ 1.60–1.63 (m, 2H, H3, H3'), 1.97 (quint, J=7.3 Hz, 2H, L2), 2.02 (s, 3H, OAc), 2.14-2.20 (m, 2H, H2, H2'), 2.41 (t, J=7.3 Hz, 4H, L1, L3), 3.50 (m, 1H, H1), 3.65 (s, 3H, OMe), 3.89 (d, J=13.5 Hz, 1H, Bn), 3.93 (d, J=13.5 Hz, 1H, Bn), 5.30 (m, 1H, H4), 5.84 (d, 10.3 Hz, 1H, H6), 5.94 (d, J=10.3 Hz, 1H, H5), 7.34 (d, J=8.8 Hz, 2H, Ar), 7.56 (d, J=8.8 Hz, 2H, Ar)

^{13}C NMR (125.0 MHz, CD3OD) δ 16.10, 17.00, 22.84, 23.03, 29.00, 31.79, 45.73, 47.04, 48.38, 65.69, 116.20, 124.27, 125.03, 129.06, 131.10, 133.95, 167.42, 168.48, 170.16

IR (film) 3600-3100 (amine N-H, amide N-H), 3020 (=C-H), 1725 (ester C=O), 1660 (amide C=O), 1590 (Ar C=C), 1510 (Ar C=C)

HRMS (EIMS) calculated for C21H28N2O5 388.1998, found 388.1994

9 1
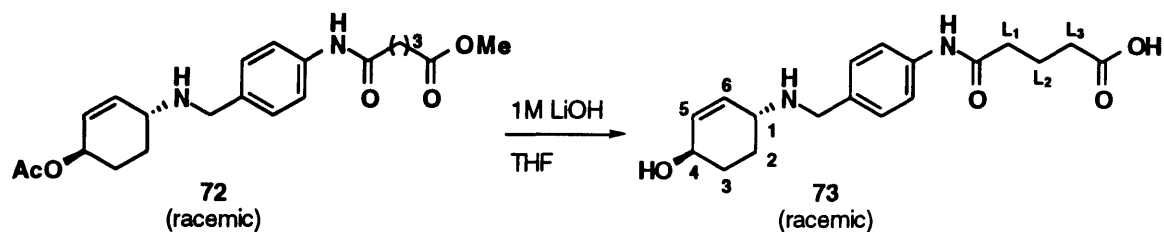
Preparation of acid 73 (Hapten V3/Inhibitor V3)

To a room temperature solution of esters **72** (80.3 mg, 0.21 mmol) in THF (2.0 mL) was added LiOH (2.0 mL, 1.0 M). After 2 hours the mixture was concentrated in vacuo. The residual oil was purified by flash ^{18}C gel column chromatography (80% CH_3CN, 20% H_2O) to yield **73** (64.1 mg, 78.7%) as a white solid.

Physical data for 73

^{1}H NMR (501 MHz, CD_3OD) δ 1.41–1.45 (m, 2H, H_3, $H_{3'}$), 1.95 (quint, J=7.5 Hz, 2H, L_2), 2.05-2.10 (m, 2H, H_2, $H_{2'}$), 2.24 (t, J=7.5 Hz, 2H, L_3), 2.38 (t, J=7.5 Hz, 2H, L_1) 3.24 (m, 1H, H_1), 3.72 (d, J=13.0 Hz, 1H, B_n), 3.76 (d, J=13.0 Hz, 1H, B_n), 4.18 (m, 1H, H_4), 5.74 (d, 11.1 Hz, 1H, H_6), 5.77 (d, J=11.1 Hz, 1H, H_5), 7.28 (d, J=8.5 Hz, 2H, Ar), 7.52 (d, J=8.5 Hz, 2H, Ar)

^{13}C NMR (125.0 MHz, CD_3OD) δ 19.07, 23.54, 25.74, 27.02, 32.95, 33.33, 45.70, 48.86, 62.50, 116.21, 124.96, 129.07, 131.17, 134.02, 169.44, 176.81

HRMS (FAB) calculated for $C_{18}H_{24}N_2O_4$ (M + H) 333.1814, found 333.1812

Melting point (decomposed) 222°C

9 2
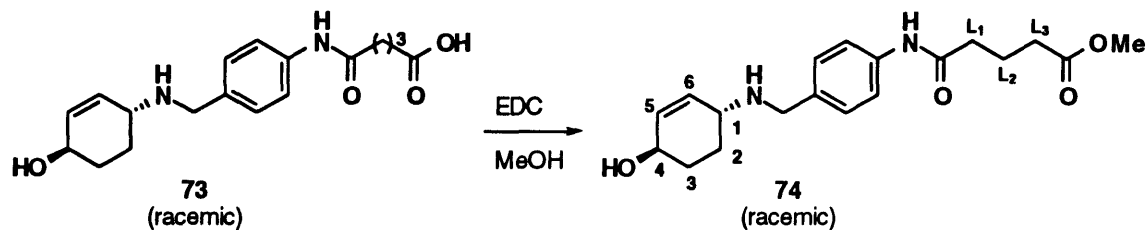
Preparation of methyl ester 74

To a room temperature solution of carboxylate **73** (5.4 mg, 14.0 μmol) in MeOH (1 mL) was added 1-(3-dimethylaminopropyl)-3-ethylcarbodiimide hydrochloride (10.8 mg, 56 μmol). After standing for 12 hours the solution was diluted with EtOAc (10 mL), extracted against saturated $NaHCO_3$ (5 mL), dried over anhydrous Na_2SO_4, and concentrated in vacuo. The residual film was identified as >95% **74** by ^{1}HNMR.

Physical data for 74

^{1}H NMR (501 MHz, CD_3OD) δ 1.43–1.47 (m, 2H, H_3, $H_{3'}$), 1.97 (quint, J=7.3 Hz, 2H, L_2), 2.06-2.12 (m, 2H, H_2, $H_{2'}$), 2.41 (t, J=7.3 Hz, 4H, L_3, L_1) 3.29 (m, 1H, H_1), 3.76 (d, J=12.8 Hz, 1H, Bn), 3.80 (d, J=12.8 Hz, 1H, Bn), 4.18 (m, 1H, H_4), 5.77 (s, 2H, H_5,H_6), 7.30 (d, J=8.3 Hz, 2H, Ar), 7.52 (d, J=8.3 Hz, 2H, Ar)

^{13}C NMR (125.0 MHz, CD_3OD) δ 17.02, 23.28, 25.75, 26.94, 29.01, 31.81, 45.56, 47.05, 49.01, 62.40, 116.26, 126.01, 129.63, 168.90

IR (film) 3600-2600 (amine N-H, alcohol N-H), 3010 (=C-H), 1725 (ester C=O), 1655 (amide C=O), 1595 (Ar C=C), 1510 (Ar C=C)

HRMS (EIMS) calculated for $C_{19}H_{26}N_2O_4$ 346.1893, found 346.1887

5% Rh/Al, H₂

EtOAc/EtOH

61a
(racemic)

75
(racemic)
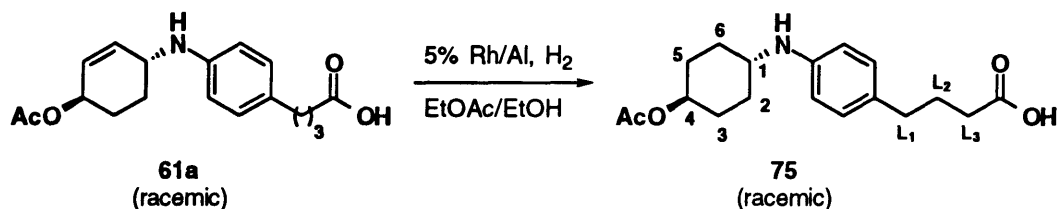
Preparation of cyclohexane 75

To a room temperature solution of olefin **61a** (2.92 g, 9.2 mmol) in EtOAc:EtOH (1:1, 250 mL) was added 5% rhodium on alumina powder (189 mg, 0.9 mmol). Argon, followed by hydrogen, was bubbled through the suspension. After stirring for 18 hours argon was bubbled through the suspension. The mixture was filtered through celite eluting with hot EtOAc:EtOH (1:1, 250 mL) and concentrated in vacuo. The residual oil was purified by flash silica gel column chromatography to yield **75** (2.31 g, 78.7%) as a pink solid.

Physical data for 75

^{1}H NMR (250 MHz, CDCl₃) δ 1.05-1.79 (m, 6H, H$_2$, H$_2$', H$_3$, H$_3$', H$_6$, H$_6$'), 1.89

(m, 2H, L$_2$), 2.04 (s, 3H, OAc), 2.02-2.18 (m, 2H, H$_5$, H$_5$'), 2.33 (t, J=7.4 Hz, 2H, L$_3$), 2.54 (t, J=7.4 Hz, 2H, L$_1$), 3.23 (m, 1H, H$_1$), 4.73 (m, 1H, H$_4$), 6.53 (d, J=8.4 Hz, 1H, Ar), 6.54 (d, J=8.4 Hz, 1H, Ar), 6.96 (d, J=8.4 Hz, 1H, Ar), 6.98 (d, J=8.4 Hz, 1H, Ar)

^{13}C NMR (125.0 MHz, CDCl₃) δ 21.33, 26.51, 30.08, 30.79, 33.29, 34.03, 51.23, 72.32, 113.59, 129.24, 130.16, 145.17, 170.65, 179.34

IR (film) 3500-2500 (acid O-H), 3380 (amine N-H), 1720 broad (acid C=O, ester C=O), 1610 (Ar C=C), 1510 (Ar C=C)

HRMS (EIMS) calculated for C$_{18}$H$_{25}$NO$_4$ 319.1784, found 319.1786

Melting point 82-85°C
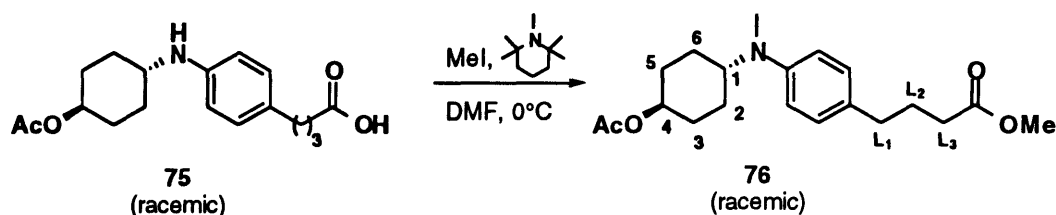
Preparation of monomethyl amine **76**

To a 0° C solution of amine **75** (1.80 g, 5.64 mmol) in DMF (40 mL) was added 1,2,2,6,6-pentamethylpiperidine (2.8 mL, 16.9 mmol) followed by methyl iodide (5.3 mL, 84.6 mmol). After standing at 0° C for 24 hours the mixture was poured into water (50 mL) and extracted with Et_2O (100 mL). The organic phase was washed with water (1x50 mL) and saturated NaCl (1x50 mL), dried over anhydrous Na_2SO_4, and concentrated in vacuo. The residual oil was purified by flash silica gel column chromatography to yield **76** (585.2 mg, 31.0%).

Physical data for **76**

^{1}H NMR (300 MHz, $CDCl_3$) δ 1.44 (dd, J= 12.9, 3.3 Hz, 1H, H_3), 1.52 (dd, J=12.9,

2.4 Hz, 1H, H_3'), 1.58 (dm, J=13.2 Hz, 1H, H_2), 1.66 (dm, J=13.2, 3.0, H_2'),

1.78-1.85 (m, 2H, H_6), 1.91 (m, 2H, L_2), 2.04 (s, 3H, OAc), 2.03-2.12 (m, 2H,

H_5), 2.32 (t, J=7.5 Hz, 2H, L_3), 2.55 (t, J=7.4 Hz, 2H, L_1), 2.73 (s, 3H, Me),

3.56 (tt, J=11.4, 3.9 Hz, 1H, H_1), 3.66 (s, 3H, OMe), 4.68 (m, J=11.1, 4.5 Hz,

1H, H_4), 6.72 (d, J=8.6 Hz, 2H, Ar), 7.04 (d, J=8.6 Hz, 2H, Ar)

^{13}C NMR (125.0 MHz, $CDCl_3$) δ 21.30, 26.71, 27.14, 31.01, 31.43, 34.00, 34.10,

51.36, 57.50, 72.44, 113.90, 129.04, 148.1, 170.48, 173.99

IR (film) 1730 broad (ester C=O), 1610 (Ar C=C), 1510 (Ar C=C)

HRMS (EIMS) calculated for $C_{20}H_{29}NO_4$ 347.2097, found 347. 2096

76
(racemic)

77
(racemic)
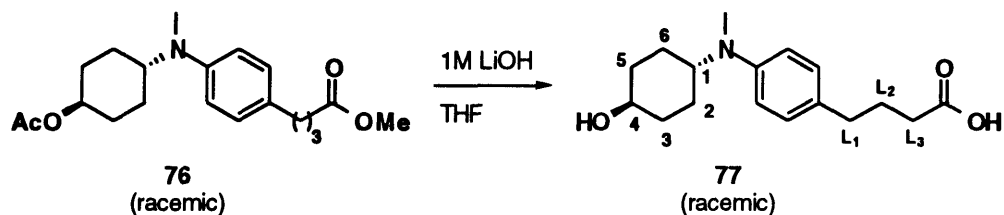
Preparation of acid 77

To a room temperature solution of esters **76** (540 mg, 1.62 mmol) in THF (15 mL) was added LiOH (15.0 mL, 1 M). After stirring for 3 hours the solution was neutralized with 10% HCl and concentrated in vacuo. The residual oil was purified by flash silica gel column chromatography to yield **77** (273 mg, 57.9%) as a colorless oil.

Physical data for 77

^{1}H NMR (501 MHz, CD$_3$OD) δ 1.37 (m, 2H, H$_3$, H$_3$'), 1.56 (m, 2H, H$_2$, H$_2$'), 1.73 (m, 2H, H$_6$, H$_6$'), 1.85 (m, 2H, L$_2$), 1.97-2.00 (m, 2H, H$_5$, H$_5$'), 2.25 (m, 3H, L$_3$), 2.53 (m, 2H, L$_1$), 2.71 (s, 3H, Me), 3.50-3.53 (m, 2H, H$_1$, H$_4$), 6.79 (m, 2H, Ar), 7.03 (m, 2H, Ar)

^{13}C NMR (125.0 MHz, CDCl$_3$) δ 21.30, 26.71, 27.14, 31.01, 31.43, 34.00, 34.10, 51.36, 57.50, 72.44, 113.90, 129.04, 148.1, 170.48, 173.99

IR (film) 3600-2400 (acid O-H), 1710 (acid C=O), 1610 (Ar C=C), 1510 (Ar C=C)

HRMS (EIMS) calculated for C$_{17}$H$_{25}$NO$_3$ 291.1834, found 291.1838

DCC, NHS, 0°C
CH2Cl2/DMF

77
(racemic)

78
(racemic)
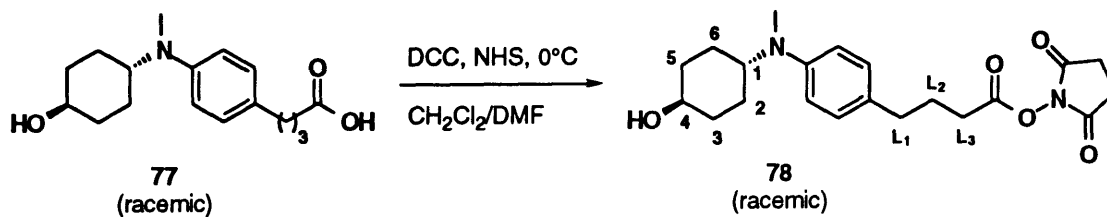
Preparation of N-hydroxysuccinimate ester **78**

To a 0° C solution of acid **77** (17 mg, 58 μmol) in CH_2Cl_2:DMF (1.0 mL:0.2 mL) was added N-Hydroxysuccinimide (11.5 mg, 100 μmol) followed by DCC (24.3 mg, 118 μmol). After stirring for 4 hours at 0° C the mixture was filtered and concentrated in vacuo. The residual oil was purified by flash silica gel column chromatography to yield **78** (19 mg, 85.3%).


Physical data for **78**

^{1}H NMR (250 MHz, $CDCl_3$) δ 1.35 (dm, J=13.2 Hz, 1H, H_3), 1.45 (dm, J=13.2 Hz,

1H, H_3'), 1.51 (d broad, 1H, H_2), 1.54 (d broad, J=10.4 Hz, 1H, H_2'), 1.80 (m,

2H, H_6, H_6'), 1.96-2.08 (m, 4H, H_5, H_5',L_2), 2.56-2.67 (m, 4H, L_1,L_3), 2.74

(s, 3H, Me), 2.83 (s, 4H, CH_2, CH_2), 3.50-3.68 (m, 2H, H_1, H_4), 6.73 (d,

J=8.2 Hz, 2H, Ar), 7.06 (d, J=8.2 Hz, 2H, Ar)

IR (film) 3600-3200 (alcohol O-H), 1810 (imide C=O), 1780 (imide C=O), 1610 (Ar

C=C), 1510 (Ar C=C)

HRMS (EIMS) calculated for $C_{21}H_{28}N_2O_5$ 388.1998, found 388.1997

78
(racemic)

79
(racemic)
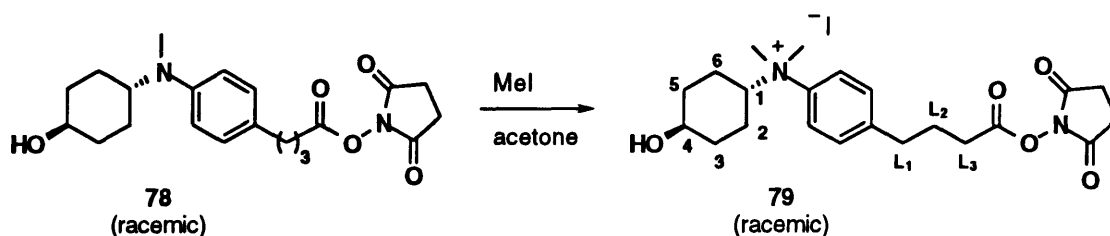
Preparation of quartenized amine 79 (Hapten G1)

To a room temperature solution of **78** (16.7 mg, 43 µmol) in acetone (2.0 mL) was added methyl iodide (0.5 mL, 8.0 mmol). The flask was covered with foil and left to stand. After 5 days volatiles were removed in vacuo, the residual oil triturated with EtOAc:CH$_2$Cl$_2$ (1:1) and filtered. The quartenized amine **79** was isolated (17.2 mg, 99.2%) as an orange solid.

Physical data for 79

^{1}H NMR (250 MHz, CD$_3$OD) δ 1.31 (dm, J=10.2 Hz, 1H, H$_3$), 1.40 (dm, J=10.2 Hz,

1H, H$_3$'), 1.61 (dd, J=12.3, 2.6 Hz, 1H, H$_2$), 1.71 (dd, J=12.3, 2.6 Hz, 1H,

H$_2$'), 1.90 (m, 2H, H$_6$, H$_6$'), 2.00-2.09 (m, 4H, H$_5$, H$_5$', L$_2$), 2.66 (t, J=7.4

Hz, 2H, L$_3$), 2.84 (t, J=7.4 Hz, 2H, L$_1$), 3.54 (m, 1H, H$_4$), 3.56 (s, 6H, Me,

Me), 3.99 (tt, J=11.9, 3.2 Hz, 1H, H$_1$), 6.73 (d, J=8.2 Hz, 2H, Ar), 7.06 (d,

J=8.2 Hz, 2H, Ar)

HRMS (FAB) calculated for C$_{22}$H$_{31}$N$_2$O$_5$ 403.2233, found 403.2234

Melting point (decomposed) 98-103°C

9 8

77
(racemic)

Mel
acetone

80
(racemic)
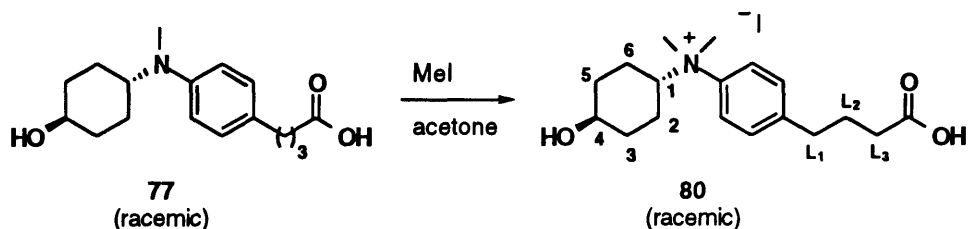
Prepartion of quartenized amine **80** (Inhibitor G1)

To a room temperature solution of amine **77** (5.0 mg, 17 μmol) in acetone (0.5 mL) was added methyl iodide (0.5 mL, 8.0 mmol). The flask was covered with foil and left to stand. After 7 days volatiles were removed in vacuo. The residual film was identified as >95% **80** by ^{1}HNMR.

Physical data for **80**

^{1}H NMR (501 MHz, CD3OD) δ 1.34 (d broad, J=12.8 Hz, 1H, H3), 1.39 (d broad,

J=12.8 Hz, 1H, H3'), 1.64 (d broad, J=12.5, 2.6 Hz, 1H, H2), 1.69 (d broad,

J=12.5, 2.6 Hz, 1H, H2'), 1.90 (m, 2H, H5, H5'), 1.92 (quin, J=7.5 Hz, 2H,

L2), 2.03 (d broad, J=12.0 Hz, 2H, H6, H6'), 2.32 (t, J=7.5 Hz, 2H, L3), 2.75

(t, J=7.5 Hz, 2H, L1), 3.54 (m, 1H, H4), 3.56 (s, 6H, Me, Me), 3.40 (tt, J=11.5,

3.0 Hz, 1H, H1), 7.48 (d, J=9.0 Hz, 2H, Ar), 7.76 (d, J=9.0 Hz, 2H, Ar)

HRMS (FAB) calculated for C18H28NO3 306.2069, found 306.2065

5.1.c. Substrate Synthesis
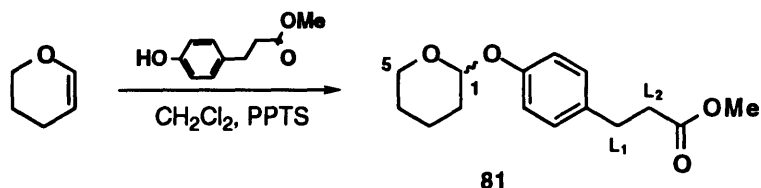
Preparation of acetal 81 (V1G1r)

To a room temperature solution of methyl 3-(4-hydroxyphenyl)-propionate (4.0 g, 22.2 mmol) in CH_2Cl_2 (100 mL) was added 3,4-dihydro-2H-pyran (2.42 mL, 24.4 mmol) followed by pyridinium p-toluenesulfonate (80 mg, 0.32 mmol). After 10 hours the mixture was concentrated in vacuo and purified by flash silica gel chromatography to yield 81 as a colorless oil (5.31 g, 90.3%).

Physical data for 81

^{1}H NMR (501 MHz, C_6D_6) δ 1.12 (m, 1H), 1.22-1.35 (m, 2H), 1.50 (m, 1H), 1.63 (m, 1H), 2.31 (t, J=7.5 Hz, 2H, L_2), 2.74 (t, J=7.5 Hz, 2H, L_1), 3.25 (s, 3H, OAc), 3.32 (m, 1H, H_5), 3.72 (ddd, J=10.5, 10.5, 3.0 Hz, 1H, $H_{5'}$), 5.22 (t, J=3.0 Hz, 1H, H_1), 6.92 (d, J=8.5 Hz, 2H, Ar), 7.08 (d, J=8.5 Hz, 1H, Ar)

^{13}C NMR (62.9 MHz, C_6D_6) δ 18.86, 25.50, 30.47, 30.62, 36.02, 50.93, 61.44, 96.45, 116.94, 129.48, 133.94, 156.37, 172.59

IR (film) 1735 (ester C=O), 1610 (Ar C=C), 1510 (Ar C=C), 1435 (C-O), 1355 (C-O)

HRMS (EIMS) calculated for $C_{15}H_{20}O_4$ 264.1362, found 264.1363

100
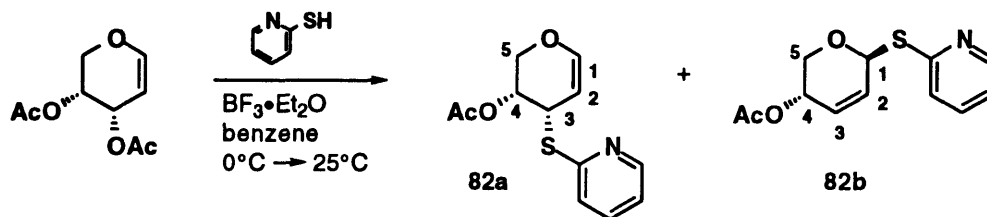
Preparation of 3-thioglycals 82a and thioglycoside 82b

To a 0°C solution of D-arabinal (5.10 g, 25.5 mmol) and 2-thiopyridine (5.7 g, 51.0 mmol) in benzene (80 mL) was added freshly distilled boron trifluoride etherate (3.14 mL, 25.5 mmol) dropwise. Upon complete addition, the mixture was allowed to warm to room temperature. After stirring for 3 hours, the solution was poured into saturated $NaHCO_3$ (200 mL) and extracted with EtOAc. The organic phase was washed with saturated NaCl, dried over anhydrous Na_2SO_4, and concentrated in vacuo. The residual oil was purified by flash silica gel column chromatography to yield 82a (4.58 g, 70.7%) and its regioisomer 82b (354 mg, 5.5%) as colorless oils.

Physical data for 82a

^{1}H NMR (250 MHz, $CDCl_3$) δ 4.14 (dt, J=12.2, 2.3, 2.3 Hz, 1H, H_5 equatorial), 4.21
(d, J=12.2 Hz, 1H, H_5 axial), 4.41 (m, 1H, H_3), 4.86 (m, 1H, H_2), 5.10 (s broad, 1H, H_4), 6.54 (dd, J=6.3, 0.8 Hz, 1H, H_1), 6.98 (m, 1H, Ar-2), 7.16 (d, J=7.8 Hz, 1H, Ar-4), 7.48 (dt, J=7.8, 7.8, 1.9 Hz, 1H, Ar-3), 8.38 (d broad, J=4.2 Hz, 1H, Ar-1)

^{13}C NMR (75.4 MHz, $CDCl_3$) δ 21.03, 37.68, 63.25, 65.59, 96.93, 120.01, 122.00, 36.14, 146.30, 149.52, 156.82, 169.95

IR (film) 3060 (=C-H), 3040 (=C-H), 1735 (ester C=O), 1635 (Ar C=C), 1570 (Ar C=C)

HRMS (EIMS) calculated for $C_{12}H_{13}NO_3S$ 251.0616, found 251.0619

Physical data for **82b**

^{1}H NMR (250 MHz, CDCl$_3$) δ 3.93 (d, J=13.3 Hz, 1H, H$_5$), 4.28 (dd, J=13.3, 2.7 Hz, 1H, H$_5$'), 5.02 (dd, J=5.2, 2.7 Hz, 1H, H$_4$), 6.09 (ddt broad, J=9.9, 5.2, 1.6, 1.6 Hz, 1H, H$_3$), 6.24 (dd, J=9.9, 3.4 Hz, 1H, H$_2$), 6.72 (dd broad, J=3.3, 1.8 Hz, 1H, H$_1$), 7.04 (m, 1H, Ar), 7.28 (d, J=7.6 Hz, 1H, Ar), 7.52 (dt, J=7.7, 7.7, 1.8 Hz, 1H, Ar), 8.46 (d broad, J=4.6 Hz, 1H, Ar)
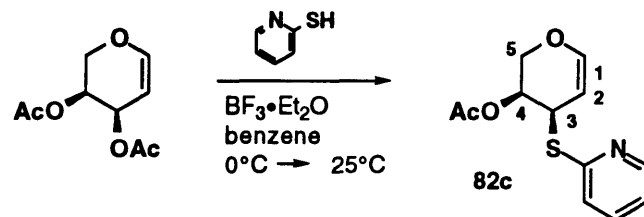
Preparation of 3-thioglycal 82c

To a 0°C solution of L-arabinal (1.55 g, 7.75 mmol) and 2-thiopyridine (1.72 g, 15.5 mmol) in benzene (25 mL) was added freshly distilled boron trifluoride etherate (0.95 mL, 7.75 mmol) dropwise. Upon complete addition, the mixture was allowed to warm to room temperature. After stirring for 5.25 hours, the solution was poured into saturated $NaHCO_3$ (50 mL) and extracted with EtOAc. The organic phase was washed with saturated NaCl, dried over anhydrous Na_2SO_4, and concentrated in vacuo. The residual oil was purified by flash silica gel column chromatography to yield 82c (1.53 g, 77.7%) as a colorless oil.

Physical data for 82c

^1H NMR (250 MHz, $CDCl_3$) δ 4.16 (dt, J=12.2, 2.3, 2.3 Hz, 1H, H_5 equatorial), 4.23
(d, J=12.2 Hz, 1H, H_5 axial), 4.42 (m, 1H, H_3), 4.88 (m, 1H, H_2), 5.12 (s
broad, 1H, H_4), 6.55 (d, J=5.6 Hz, 1H, H_1), 7.00 (m, 1H, Ar-2), 7.18 (d,
J=8.1 Hz, 1H, Ar-4), 7.50 (dt, J=7.7, 7.7, 1.8 Hz, 1H, Ar-3), 8.40 (dd fine,
J=4.2, 1.1 Hz, 1H, Ar-1)

^{13}C NMR (125.7 MHz, CD_3OD) δ 20.93, 39.26, 64.14, 71.05, 97.75, 121.70, 123.68,
138.16, 147.61, 150.61, 158.39, 171.79

IR (film) 3060 (=C-H), 3040 (=C-H), 1735 (ester C=O), 1640 (Ar C=C), 1575 (Ar
C=C)

HRMS (EIMS) calculated for $C_{12}H_{13}NO_3S$ 251.0616, found 251.0618
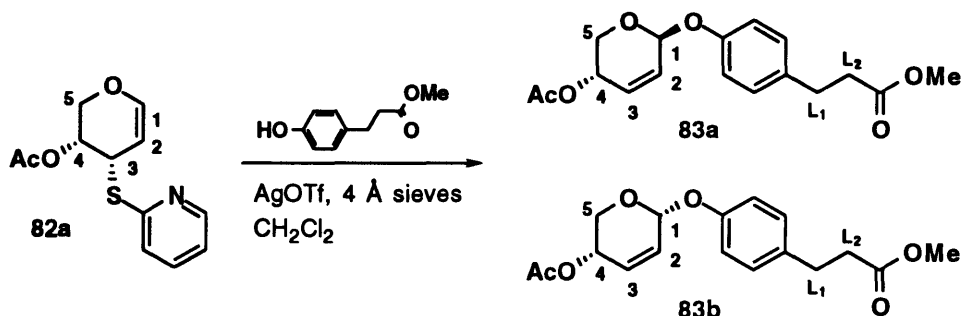
Preparation of 83a and 83b

To a room temperature solution of 3-thioarabinal **82a** (4.54 g, 17.9 mmol) and methyl 3-(4-hydroxyphenyl)-propionate (7.51g, 26.8 mmol) in CH_2Cl_2 (150 mL) was added 4 Å crushed molecular sieves (200 mg) followed by silver triflate (5.05 g, 19.7 mmol). After stirring for 3.5 hours, additional silver triflate (2.0 g, 7.8 mmol) was added to the mixture. After stirring for an additional 1.5 hours, a final portion of silver triflate (2.5 g, 9.7 mmol) was added to the mixture. After stirring for a final 1.5 hours the mixture was filtered through celite and concentrated in vacuo. The residual oil was subjected to reaction with chlorotriethlysilane (4.7 mL, 27.8 mmol) in pyridine (50 mL) at room temperature to facilitate removal of unreacted methyl 3-(4-hydroxyphenyl)-propionate, which co-elutes with **83a** and **83b** on silica gel as the free alcohol but is separable as the triethylsilyl ether. The reaction mixture was concentrated in vacuo after 20 minutes and the residual oil was purified by flash silica gel column chromatography to yield **83a** (2.34 g, 40.9%) and **83b** (1.54 g, 26.9%) as a separable mixture of diastereomers. Compound **83a** was a solid and **83b** was an oil.

Physical data for 83a

^{1}H NMR (501 MHz, CDCl$_3$) δ 2.12 (s, 3H, OAc), 2.60 (t, J=7.5 Hz, 2H, L$_2$), 2.90 (t,

2H, J=7.5 Hz, L$_1$), 3.67 (s, 3H, OMe), 3.92 (dd, J=13.5, 1.0 Hz, 1H, H$_5$ axial),

4.26 dd, J=13.5, 2.5 Hz, 1H, H$_5$ equatorial), 5.03 (dd, J=5.0, 2.5 Hz, 1H, H$_4$),

5.71 (d, J=3.0 Hz, 1H, H$_1$), 6.17 (dd, J=10.5, 3.0 Hz, 1H, H$_2$), 6.22 (dd broad,

104

J=10.5, 5.5 Hz, 1H, H$_3$), 7,02 (dm, J=8.3 Hz, 2H, Ar), 7.13 (dm, J=8.3 Hz, 2H, Ar)

^{13}C NMR (75.4 MHz, CDCl$_3$) δ 21.03, 30.12, 35.84, 51.54, 61.96, 63.00, 91.50, 116.68, 125.70, 129.25, 134.30, 155.58, 170.47, 173.24

IR (film) 1730 (ester C=O), 1610 (Ar C=C), 1580 (Ar C=C), 1505 (Ar C=C), 1435 (C-O)

HRMS (EIMS) calculated for C$_{17}$H$_{20}$O$_6$ 320.1260, found 320.1261

Melting point 60-61°C

Physical data for 83b

^{1}H NMR (300 MHz, CDCl$_3$) δ 2.09 (s, 3H, OAc), 2.60 (t, J=7.5 Hz, 2H, L$_2$), 2.90 (t, 2H, J=7.5 Hz, L$_1$), 3.66 (s, 3H, OMe), 3.87 (dd, J=10.5, 9.0 Hz, 1H, H$_5$ axial), 3.94 ddd, J=10.5, 5.7, 0.9 Hz, 1H, H$_5$ equatorial), 5.38 (m, 1H, H$_4$), 5.61 (s broad, 1H, H$_1$), 5.99 (ddd, J=10.2, 2.4, 1.8 Hz, 1H, H$_3$), 6.08 (dm, J=10.2 Hz, 1H, H$_2$), 6.99 (dm, J=8.7 Hz, 2H, Ar), 7.12 (dm, J=8.7 Hz, 2H, Ar)

^{13}C NMR (75.4 MHz, CDCl$_3$) δ 20.92, 30.12, 35.85, 51.51, 60.22, 64.71, 92.46, 116.79, 127.90, 129.22, 130.06, 134.33, 155.61, 170.33, 173.23

IR (film) 1735 (ester C=O), 1640 (C=C), 1610 (Ar C=C), 1580 (Ar C=C), 1510 (Ar C=C), 1435 (C-O)

HRMS (EIMS) calculated for C$_{17}$H$_{20}$O$_6$ 320.1260, found 320.1258
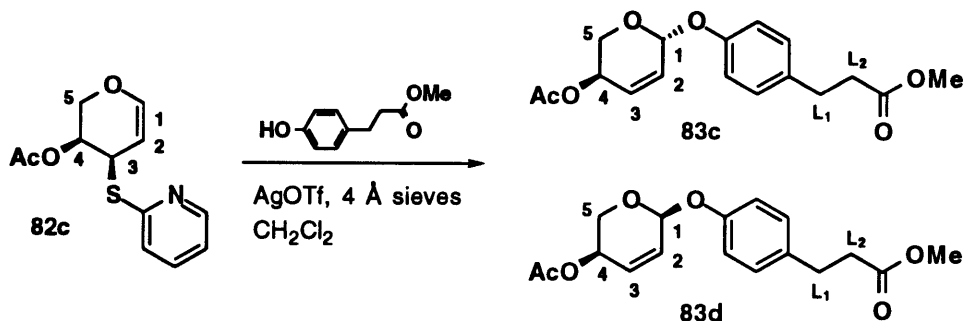
Preparation of 83c and 83d

To a room temperature solution of 3-thioarabinal **82c** (1.3 g, 5.2 mmol) and methyl 3-(4-hydroxyphenyl)-propionate (1.4 g, 7.8 mmol) in CH_2Cl_2 (40 mL) was added 4 Å crushed molecular sieves (100 mg) followed by silver triflate (1.35 g, 5.2 mmol). After stirring for 1.5 hours, additional silver triflate (1.35 g, 5.2 mmol) was added to the mixture. After stirring for an additional 1.5 hours the mixture was filtered through celite and concentrated in vacuo. The residual oil was subjected to reaction with chlorotriethlysilane (0.8 mL, 4.7 mmol) in pyridine (40 mL) at room temperature to facilitate removal of unreacted methyl 3-(4-hydroxyphenyl)-propionate, which co-elutes with **83c** and **83d** on silica gel as the free alcohol but is separable as the triethylsilyl ether. The reaction mixture was concentrated in vacuo after 30 minutes and the residual oil was purified by flash silica gel column chromatography to yield a mixture of **83c** and **83d** (847 mg, 50.9%) which was used without separation in the following step.

Physical data for 83c and 83d

^{1}H NMR (300 MHz, C_6D_6) Comparison with the individual spectra of **83a** and **83b**, indicates a mixture **83c** and **83d**. Material was used as a mixture in the following step.

106
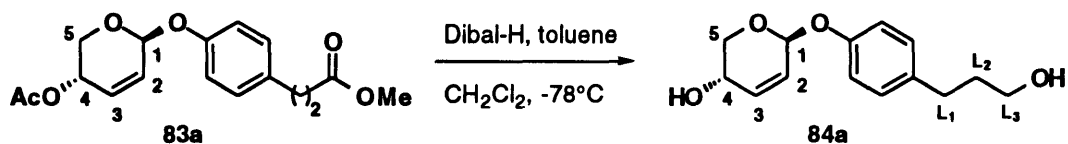
Preparation of 84a

To a -78°C solution of ester **83a** (250 mg, 0.78 mmol) in toluene (3.5 mL) and CH_2Cl_2 (1.0 mL) was added diisobutylaluminum hydride (3.9 mL, 3.9 mmol, 1.0 M solution in hexane). After stirring for 1 hour, the reaction was quenched by inverse addition to a rapidly stirred biphasic solution of saturated sodium potassium tartrate and EtOAc (1:1, 100 mL). After stirring for 30 minutes, the aqueous phase was extracted with EtOAc (2x50 mL) and concentrated in vacuo. The residual oil was purified by flash silica gel chromatography to yield **84a** (141 mg, 72.3%) as a white solid.

Physical data for 84a

^{1}H NMR (500 MHz, CD3OD) δ 1.79 (m, 2H, L_2), 2.61 (t, J=7.0 Hz, 2H, L_1), 3.54 (t, 2H, J=7.0 Hz, L_3), 3.76 (dt, J=12.5, 1.5, 1.5 Hz, 1H, H_5), 3.86 (m, 1H, H_4), 4.14 (dd, J=12.5, 2.5 Hz, 1H, $H_{5'}$), 5.63 (d broad, J=3.0 Hz, 1H, H_1), 6.01 (dd, J=10.0, 3.0 Hz, 1H, H_2), 6.16 (dd, J=10.0, 5.5 Hz, 1H, H_3), 6.97 (dt, J=8.5, 2.5 Hz, 2H, Ar), 7.10 (dt, J=8.5, 2.5 Hz, 2H, Ar)

^{13}C NMR (125.0 MHz, CD3OD) δ 32.24, 35.65, 61.85, 62.19, 66.03, 93.44, 118.01, 128.61, 130.25, 130.49, 136.98, 156.88

IR (film) 3650-3100 (alcohol O-H), 3015 (=C-H), 1605 (Ar C=C), 1580 (Ar C=C), 1500 (Ar C=C), 1390 (C-O)

HRMS (EIMS) calculated for $C_{14}H_{18}O_4$ 250.1205, found 250.1207

Melting point 80-82°C
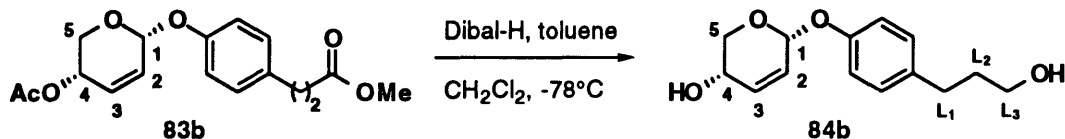
Preparation of 84b

To a -78°C solution of ester **83b** (290 mg, 0.91 mmol) in toluene (4.0 mL) and CH$_2$Cl$_2$ (1.0 mL) was added diisobutylaluminum hydride (4.5 mL, 4.5 mmol, 1.0 M solution in hexane). After stirring for 40 minutes, the reaction was quenched by inverse addition to a rapidly stirred biphasic solution of saturated sodium potassium tartrate and EtOAc (1:1, 100 mL). After stirring for 30 minutes, the aqueous phase was extracted with EtOAc (3x50 mL) and concentrated in vacuo. The residual oil was purified by flash silica gel chromatography to yield **84b** (204 mg, 90.1%) as a colorless oil.

Physical data for 84b

^{1}H NMR (500 MHz, CD$_3$OD) δ 1.79 (m, 2H, L$_2$), 2.61 (t, J=6.5 Hz, 2H, L$_1$), 3.54 (t, 2H, J=6.5 Hz, L$_3$), 3.66 (t, J=10.6 Hz, 1H, H$_5$), 3.76 (ddd, J=10.6, 5.9, 1.2 Hz, 1H, H$_5$'), 4.25 (m, 1H, H$_4$), 5.57 (s with fine coupling, J=1.25 Hz, 1H, H$_1$), 5.87 (dt, J=10.3, 2.3, 2.3 Hz, 1H, H$_2$), 6.08 (dm, J=10.3 Hz, 1H, H$_3$), 6.95 (dt, J=8.7, 2.1 Hz, 2H, Ar), 7.10 (d broad, J=8.7, 2H, Ar)

^{13}C NMR (125.0 MHz, CD$_3$OD) δ 32.24, 35.64, 62.19, 63.49, 64.08, 93.90, 117.92, 126.90, 130.25, 135.71, 136.96, 156.92

IR (film) 3650-3100 (alcohol O-H), 3020 (=C-H), 1635 (C=C), 1605 (Ar C=C), 1500 (Ar C=C)

HRMS (EIMS) calculated for C$_{14}$H$_{18}$O$_4$ 250.1205, found 250.1207
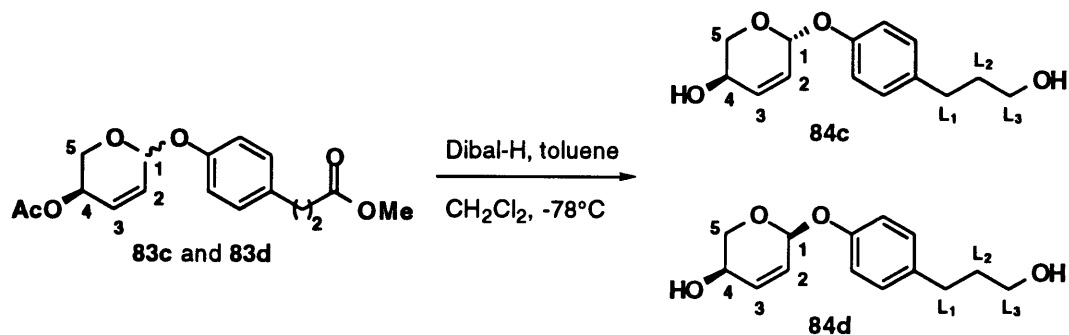
Preparation of 84c and 84d

To a -78°C solution of esters **83c** and **83d** (830 mg, 2.59 mmol) in toluene (12.0 mL) and CH_2Cl_2 (3.0 mL) was added diisobutylaluminum hydride (13.0 mL, 13.0 mmol, 1.0 M solution in hexane). After stirring for 1 hour, the reaction was quenched by inverse addition to a rapidly stirred biphasic solution of saturated sodium potassium tartrate and EtOAc (1:1, 200 mL). After stirring for 30 minutes, the aqueous phase was extracted with EtOAc (3x100 mL) and concentrated in vacuo. The residual oil was purified by flash silica gel chromatography to yield **84c** (258 mg, 39.8%) as a white solid and **84d** (190.4 mg, 29.4%) as a colorless oil.

Physical data for 84c

^{1}H NMR (250 MHz, CD_3OD) δ 1.78 (m, 2H, L_2), 2.61 (t, J=6.5 Hz, 2H, L_1), 3.54 (t, 2H, J=6.5 Hz, L_3), 3.75 (d broad, J=12.2 Hz, 1H, H_5), 3.86 (m, 1H, H_4), 4.13 (dd, J=12.2, 2.3 Hz, 1H, $H_{5'}$), 5.62 (d, J=3.0 Hz, 1H, H_1), 6.00 (dd, J=10.0, 3.0 Hz, 1H, H_2), 6.17 (dd, J=10.0, 5.2 Hz, 1H, H_3), 6.97 (d broad, J=8.5 Hz, 2H, Ar), 7.10 (d, J=8.5 Hz, 2H, Ar)

^{13}C NMR (125.0 MHz, CD_3OD) δ 32.21, 35.61, 61.81, 62.18, 66.01, 93.39, 118.00, 128.61, 130.26, 130.49, 137.00, 156.86

IR (film) 3600-3100 (alcohol O-H), 3015 (=C-H), 1605 (Ar C=C), 1580 (Ar C=C), 1500 (Ar C=C)

HRMS (EIMS) calculated for $C_{14}H_{18}O_4$ 250.1205, found 250.1207

Melting point 80-82°C

Physical data for **84d**

^{1}H NMR (501 MHz, CD$_3$OD) δ 1.79 (m, 2H, L$_2$), 2.61 (t, J=6.5 Hz, 2H, L$_1$), 3.51 (t,

2H, J=6.5 Hz, L$_3$), 3.67 (t, J=10.5 Hz, 1H, H$_5$), 3.76 (ddd, J=10.5, 6.0, 1.2

Hz, 1H, H$_5'$), 4.25 (m, 1H, H$_4$), 5.57 (s broad, 1H, H$_1$), 5.87 (dt, J=10.5, 2.5,

2.5 Hz, 1H, H$_2$), 6.08 (dm, J=10.5 Hz, 1H, H$_3$), 6.95 (d broad, J=8.5 Hz, 2H,

Ar), 7.09 (d broad, J=8.5, 2H, Ar)

^{13}C NMR (125.0 MHz, CD$_3$OD) δ 32.24, 35.65, 62.20, 63.50, 64.09, 93.91, 117.93,

126.93, 130.27, 135.93, 136.92, 156.96

IR (film) 3620-3100 (alcohol O-H), 3020 (=C-H), 1640 (C=C), 1605 (Ar C=C), 1580 (Ar

C=C), 1500 (Ar C=C)

HRMS (EIMS) calculated for C$_{14}$H$_{18}$O$_4$ 250.1205, found 250.1207
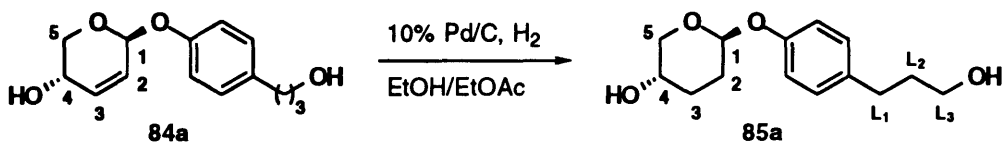
Preparation of 85a

To a room temperature solution of olefin **84a** (122 mg, 0.49 mmol) in EtOH:EtOAc (15 mL:20 mL) was added 10% palladium on activated carbon (10 mg). Argon, followed by hydrogen was bubbled through the suspension. After stirring for 2.5 hours argon was bubbled through the suspension. The mixture was filtered through celite eluting with hot EtOH:EtOAc (1:1, 100 mL) and concentrated in vacuo. The residual oil was purified by flash silica gel column chromatography to yield **85a** (113 mg, 91.9%) as a white solid.


Physical data for 85a

^{1}H NMR (501 MHz, CD$_3$OD) δ 1.65-1.73 (m, 2H, H$_3$, H$_{3'}$), 1.79 (m, 2H, L$_2$), 2.15-2.22 (m, 2H, H$_2$, H$_{2'}$), 2.60 (t, J=6.5 Hz, 2H, L$_1$), 3.45 (ddd, J=12.0, 4.0, 1.5 Hz, 1H, H$_5$), 3.54 (t, 2H, J=6.5 Hz, L$_3$), 3.76 (m, 1H, H$_4$), 3.93 (dd, J=12.0, 3.0 Hz, 1H, H$_{5'}$), 5.39 (t broad, J=3.0 Hz, 1H, H$_1$), 6.94 (dt, J=9.0, 2.5 Hz, 2H, Ar), 7.09 (dt, J=9.0, 2.5 Hz, 2H, Ar)

^{13}C NMR (125.0 MHz, CD$_3$OD) δ 26.80, 26.93, 32.24, 35.66, 62.22, 65.45, 66.93, 97.60, 117.52, 130.24, 136.66, 156.55

IR (film) 3450-3100 (alcohol O-H), 1500 (Ar C=C), 1440 (C-O), 1225 (C-O)

HRMS (EIMS) calculated for C$_{14}$H$_{20}$O$_4$ 252.1362, found 252.1365

Melting point 99°C
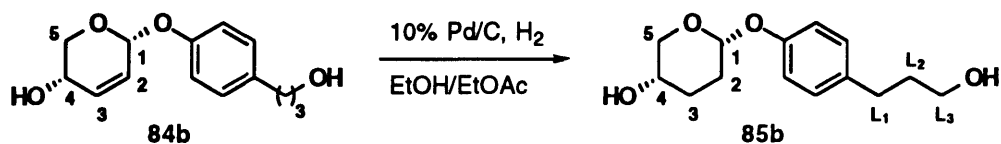
Preparation of 85b

To a room temperature solution of olefin **84b** (177 mg, 0.71 mmol) in EtOH:EtOAc (15 mL:20 mL) was added 10% palladium on activated carbon (15 mg). Argon, followed by hydrogen was bubbled through the suspension. After stirring for 4.0 hours argon was bubbled through the suspension. The mixture was filtered through celite eluting with hot EtOH:EtOAc (1:1, 100 mL) and concentrated in vacuo. The residual oil was purified by flash silica gel column chromatography to yield **85b** (156 mg, 87.3%).

Physical data for 85b

^{1}H NMR (501 MHz, CD$_3$OD) δ 1.76-1.95 (m, 5H, H$_2$, L$_2$, H$_3$, H$_3$'), 2.01 (m, 1H,

H$_2$'), 2.61 (t, J=7.5 Hz, 2H, L$_1$), 3.50-3.56 (m, 3H, H$_5$, L$_3$), 3.58 (ddd, 1H,

J=11.0, 4.5, 1.5 Hz, H$_5$'), 3.68 (m, J=4.5 Hz, 1H, H$_4$), 5.38 (t broad, J=3.0

Hz, 1H, H$_1$), 6.94 (d broad, J=8.5 Hz, 2H, Ar), 7.09 (d braod, J=8.5 Hz, 2H,

Ar)

^{13}C NMR (125.0 MHz, CD$_3$OD) δ 28.35, 29.68, 32.23, 35.66, 62.20, 66.13, 66.36,

96.07, 117.56, 130.22, 136.65, 156.35

IR (film) 3600-3000 (alcohol O-H), 1600 (Ar C=C), 1580 (Ar C=C), 1500 (Ar C=C),

1350 (C-O)

HRMS (EIMS) calculated for C$_{14}$H$_{20}$O$_4$ 252.1362, found 252.1365

Melting point 81-82°C
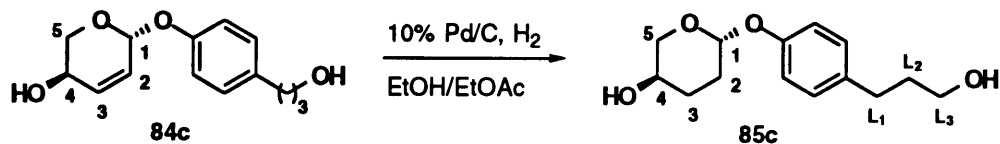
Preparation of 85c

To a room temperature solution of olefin **84c** (95 mg, 0.38 mmol) in EtOH:EtOAc (15 mL:20 mL) was added 10% palladium on activated carbon (9 mg). Argon, followed by hydrogen was bubbled through the suspension. After stirring for 5.0 hours argon was bubbled through the suspension. The mixture was filtered through celite eluting with hot EtOH:EtOAc (1:1, 100 mL) and concentrated in vacuo. The residual oil was purified by flash silica gel column chromatography to yield **85c** (83 mg, 86.7%) as a white solid.

Physical data for 85c

^{1}H NMR (501 MHz, CD$_3$OD) δ 1.65-1.73 (m, 2H, H$_3$, H$_3$'), 1.79 (m, 2H, L$_2$), 2.14-
2.22 (m, 2H, H$_2$, H$_2$'), 2.60 (t, J=6.5 Hz, 2H, L$_1$), 3.45 (ddd, J=11.5, 4.0, 1.5
Hz, 1H, H$_5$), 3.54 (t, 2H, J=6.5 Hz, L$_3$), 3.76 (m, 1H, H$_4$), 3.93 (dd, J=12.5,
2.5 Hz, 1H, H$_5$'), 5.39 (t, J=3.0 Hz, 1H, H$_1$), 6.94 (dt, J=9.0, 2.5 Hz, 2H, Ar),
7.09 (dt, J=9.0, 2.5 Hz, 2H, Ar)

^{13}C NMR (125.0 MHz, CD$_3$OD) δ 26.79, 26.92, 32.23, 35.70, 62.21, 65.46, 66.92,
97.62, 117.53, 130.25, 136.69, 156.59

IR (film) 3500-3100 (alcohol O-H), 1600 (Ar C=C), 1580 (Ar C=C), 1500 (Ar C=C),
1430 (C-O), 1225 (C-O)

HRMS (EIMS) calculated for C$_{14}$H$_{20}$O$_4$ 252.1362, found 252.1365

Melting point 99°C

113
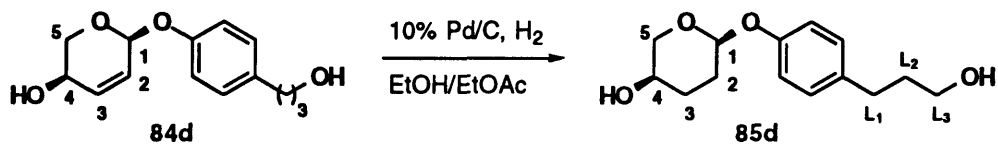
Preparation of 85d

To a room temperature solution of olefin **84d** (71.9 mg, 0.28 mmol) in EtOH:EtOAc (15 mL:20 mL) was added 10% palladium on activated carbon (7.0 mg). Argon, followed by hydrogen was bubbled through the suspension. After stirring for 5.0 hours argon was bubbled through the suspension. The mixture was filtered through celite eluting with hot EtOH:EtOAc (1:1, 100 mL) and concentrated in vacuo. The residual oil was purified by flash silica gel column chromatography to yield **85d** (61.7 mg, 87.4%) as a white solid.


Physical data for 85d

^{1}H NMR (501 MHz, CD$_3$OD) δ 1.76-1.94 (m, 5H, H$_2$, L$_2$, H$_3$, H$_3$'), 2.01 (m, 1H,

   H$_2$'), 2.61 (t, J=7.5 Hz, 2H, L$_1$), 3.50-3.56 (m, 3H, H$_5$, L$_3$), 3.59 (ddd, 1H,

   J=11.0, 4.5, 1.5 Hz, H$_5$'), 3.68 (m, J=4.5 Hz, 1H, H$_4$), 5.38 (t, J=3.0 Hz, 1H,

   H$_1$), 6.94 (d broad, J=8.5 Hz, 2H, Ar), 7.09 (d braod, J=8.5 Hz, 2H, Ar)

^{13}C NMR (125.0 MHz, CD$_3$OD) δ 28.33, 29.66, 32.21, 35.62, 62.20, 66.10, 66.35,

   96.05, 117.56, 130.24, 136.64, 156.35

HRMS (EIMS) calculated for C$_{14}$H$_{20}$O$_4$ 252.1362, found 252.1365

Melting point 81-82°C

5.2. Biological Methods

5.2.a. Preparation of Hapten-Protein Conjugates

Hapten-protein conjugate reactions were performed at room temperature with stirring in 5 mL covered vials. Conjugate reactions containing insoluble materials were initially purified on Sephadex G-25 M columns (Pharmacia PD-10). Protein containing fractions were collected and exhaustively dialyzed against phosphate buffered saline (PBS) at 4 °C. Exhaustive dialysis is defined as a minimum of 10^6-fold dilution of the sample buffer.

Protein assays were performed according to the method of Bradford using the Bradford Assay solution (Bio-Rad) diluted 1/4 (v/v) with H_2O. BSA was used for the standard curve. Quantitation of the hapten/protein ratios was determined through a comparison of the U.V. spectra of the protein-hapten conjugate and the free hapten.

5.2.a.1. V1-Protein Conjugates

A solution of hapten **V1** (7.1 mg) in DMF (90 μL) was added to 0.2 M Kpi (130 μL, pH 7.2) at room temperature. To a solution of BSA (5 mg) in 0.2 M Kpi (800 μL, pH 7.2) was added 100 μL of the hapten solution. After stirring gently for 1 hour at room temperature, the reaction was loaded onto a G-25 column and the protein was eluted with Kpi (0.2 M, pH 7.2). Protein containing fractions were collected and exhaustively dialyzed against PBS at 4 °C. The V1/BSA ratio was determined to be 46.

A solution of hapten **V1** (5.0 mg) in DMF (90 μL) was added to 0.2 M Kpi (130 μL, pH 7.2) at room temperature. To a solution of Fib (15 mg) in 0.2 M Kpi (2400 μL, pH 7.2) was added 30 μL of the hapten solution. After stirring gently for 5 minutes at room temperature, the reaction was loaded onto a G-25 column and the protein was eluted with Kpi (0.2 M, pH 7.2). Protein containing fractions were collected and exhaustively dialyzed against PBS at 4 °C. The V1/Fib ratio was determined to be 23.

5.2.a.2. G1-Protein Conjugates

A solution of hapten **G1** (5.6 mg) in DMF (90 μL) was added to 0.2 M Kpi (130 μL, pH 7.2) at room temperature To a solution of BSA (5 mg) in 0.2 M Kpi (800 μL, pH 7.2) was added 100 μL of the hapten solution. After stirring gently for 1 hour at room temperature, the reaction was loaded onto a G-25 column and the protein was eluted with Kpi (0.2 M, pH 7.2). Protein containing fractions were collected and exhaustively dialyzed against PBS at 4 °C. The G1/BSA ratio could not be accurately determined.

A solution of hapten **G1** (5.6 mg) in DMF (90 μL) was added to 0.2 M Kpi (130 μL, pH 7.2) at room temperature To a solution of Fib (5 mg) in 0.2 M Kpi (800 μL, pH 7.2) was added 10 μL of the hapten solution. After stirring gently for 10 minutes at room temperature, the reaction was loaded onto a G-25 column and the protein was eluted with Kpi (0.2 M, pH 7.2). Protein containing fractions were collected and exhaustively dialyzed against PBS at 4 °C. The G1/Fib ratio could not be accurately determined.

5.2.b. Immunizations

Subcutaneous injections were performed using an 25 G 5/8 gauge needle and were given at two sites on the backs of mice. For these immunizations, the hapten-protein conjugate in PBS was combined with an equal volume of RIBI adjuvant (MPM and TDM emulsion) at room temperature and vortexed vigorously for 2-3 minutes to provide the emulsified antigen solution. RIBI is a commonly accepted alternative to Freund's adjuvant. Intravenous injections were performed using an 29 G 1/2 gauge needle and were given through a tail vein. The mouse was first warmed to dilate its blood vessels by shining a heat lamp directly into the open cage (from a distance of about 1 foot) until the mouse began to rub its face with its front paws (about 3-5 minutes). The mouse was then removed, placed in a mouse restraint, and one of the four blood vessels running laterally through the tail was injected with a solution of the hapten-protein conjugate. For these immunizations, the hapten-protein conjugate in PBS was used. Intraperitoneal injections,

used to complement the intravenous injections, were given using the same syringe/needle and hapten solution that was used for the I.V. injections.

Test bleeds from the immunized mice were performed by Chris Hues (Division of Comparative Medicine); blood was obtained from anesthetized mice from their eyes. An alternative to this procedure is to obtain blood from one of the tail veins of heat lamp-warmed mouse by nicking one of the veins with a razor blade. After standing at room temperature for 30 minutes, test bleeds were centrifuged to pellet the blood clot. The straw-colored supernatant serum was isolated, used to determine the titer of the immunized mouse, and was subsequently stored at 4°C. The serum titer is defined as the maximum serum dilution at which an above background ELISA signal is observed.

Antibody affinities (e.g. titers) for the immunizing hapten were determined using the standard enzyme-linked immunosorbant assay (ELISA). The standard ELISA protocol requires the following buffers:

Buffer	Components
Coating Buffer	0.5 M $NaCO_3$ (pH 9.0)
Washing Buffer	PBS: 0.8 g NaCl, 0.2 g KCl, 0.2 g KH_2PO_4, 1.15 g Na_2HPO_4 in 1 L dd H_2O
Blocking Buffer	PBS containing 10 µg/mL of protein (BSA or Fib)
PBS-Tween	PBS containing tween 20 (1:1000 dilution)
Substrate Solution	0.1 M Sodium citrate (pH 5.0) containing 1,2-phenylenediamine (4 mg/10 mL) and 30% hydrogen peroxide (1:1000 dilution).

The ELISA protocol is as follows.

1.   To the each of the wells of a 96-well plate (flexible vinyl) was added 100 µL of a 1 µg/mL solution of the hapten-protein conjugate[†] in coating buffer and the plate was allowed to stand at 4°C overnight or at room temperature for 2 hours.

2.   The plate was emptied, each well was filled with 200 µL of blocking buffer, and the plates were allowed to stand at room temperature for 1 hour.

3.   Blocking solution was removed and the plates were washed 3 times with 200 µL of PBS-Tween, and 1 time with water.

4.   Antibody containing solutions* (100 µL/well) were added to the antigen coated plates and the plates were allowed to stand at room temperature for 1 hour.

5.   Antibody containing solutions were removed and the plates were washed 3 times with 200 µL of washing buffer and 1 time with water.

6.   Goat anti-mouse IgG-HRP conjugate, diluted in washing buffer (1:1000 dilution), was added to each well (100 µL/well) and the plates were allowed to stand at room temperature for 1 hour.

7.   Anti-mouse antibody solutions were removed and the plates were washed 3 times with 200 µL of washing buffer and 1 time with water.

8.   Substrate solution (prepared just prior to use) was added to each well (100 µL/well) and the plates were allowed to stand at room temperature in the dark for approximately 5 minutes (until the wells began to turn yellow).

9.   Reactions were ended by adding 1.0 M H_2SO_4 to each well (100 µL/well).

10.   Absorbance readings at 405 nM are obtained using a microtiter plate reader.

*The antibody solutions prepared from test bleeds are obtained by serially diluting a stock solution of the antibody serum (1:200 dilution in PBS) 2-fold 12-times across the 96-well plate (from 1:200 to 1:409600).

*The antibody solutions prepared from hybridomas in cell culture are used without dilution.

†In the case of test bleeds, some of the wells were coated with 100 µL of a 1 µg/mL solution of BSA or a 100 µL of a 1 µg/mL solution of Fib. These wells served as controls.

118

5.2.b.1. V1-BSA Immunizations

Four Balb/c mice each received a subcutaneous injection of **V1-BSA** on day 1 (100µg) and again on day 36 (200µg). On day 44 blood serum from each of the mice was drawn and analyzed for the presence of high affinity immunoglobin class G (IgG) molecules using the standard enzyme-linked immunosorbant assay (ELISA). Three of the four mice demonstrated a strong immune response against **V1-BSA** as evidenced by the ELISA titers (1/12800). One of these three mice received a intravenous (100µg, tail vein)/intraperitoneal (100µg) injection of **V1-BSA** on day 76. On day 79 this mouse was sacrificed, the spleen was harvested, and the B-cells (approximately $5x10^7$ cells) were fused with $5x10^7$ 653/HGPRT- myeloma cells to prepare hybridomas.

5.2.b.2. G1-BSA Immunizations

Four Balb/c mice each received a subcutaneous injection of **G1-BSA** on day 1 (100µg) and again on day 21 (200µg). On day 28 blood serum from each of the mice was drawn and analyzed for the presence of high affinity immunoglobin class G (IgG) molecules using the standard ELISA. Two of the four mice demonstrated a moderate immune response against **G1-BSA** as evidenced by the ELISA titers (1/6400). One of these two mice received a intravenous (100µg, tail vein)/intraperitoneal (100 µg) injection of **G1-BSA** on day 78. On day 81 this mouse was sacrificed, the spleen was harvested, and the B-cells were fused with $5x10^7$ 653/HGPRT- myeloma cells to prepare hybridomas.

5.2.c. Monoclonal Antibody Production

Mice were sacrificed by CO asphyxiation and the spleens were immediately isolated by dissection. All dissections were carried out in a hood that had been thoroughly washed with an EtOH/water solution and irradiated with U.V. light. Dissection instruments were wrapped in aluminum foil, placed in a covered container, and autoclaved prior to use. Dissections proceeded as follows. The skin above the left posterior of each mouse was cut and then removed by tearing it back towards the head of the mouse, exposing the peritoneal

cavity along its entire left side. The peritoneal lining directly above the spleen was lifted free of the viscera with forceps and then cut away. The spleen was gently drawn out of the body cavity with dull tweezers and the fatty and connective tissue attached to it was removed with a second pair of tweezers.

All tissue culture work was carried out using Dulbecco's modified Eagles' medium with glucose (DME, Sigma). Stock solutions of DME containing the following supplements (sterile filtered) were prepared in a sterile laminar flow hood.

Supplement/1L DME	Components
OP (10 mL)	1.5 g oxaloacetic acid, 0.5 g pyruvic acid, 100 mL dd H_2O, pH 7.4
Glutamine (19 mL)	200 mM in dd H_2O
Insulin (1 mL)	50 mg insulin in 10 mL of 1.0 M HCl
Gentamicin (1 mL)	50 mg/mL (Sigma)

This stock media was then supplemented with Fetal Bovine Serum (FBS, Sigma), Endothelial Cell Growth Supplement (ECGS, Collaborative Research), Hybridoma Enhancing Supplement (HES, Sigma), Hypoxanthine/Amimopterine/Thymidine (HAT, Sigma), and Hypoxanthine/Thymidine (HT, Sigma) to provide the following tissue culture media:

Media	Supplements/1 L Stock DME
Myeloma selection media	5% FBS, 2 x 10^{-5} M 8-azaguanine
Myeloma growth media	5% FBS
Feeder layer	B-cells from two un-immunized mice (see fusion protocol steps 1-3) in plating media
Fusion media	30 mg ECGS
Plating media	20% FBS, 30 mg ECGS 2% HES, 2 bottles 50X HAT
Growth media	20% FBS, 2 bottles 50X HT, 2% HES
Expansion media	20% FBS, 2% HES

HGPRT$^-$ myeloma cells were initially grown in a 24-well plate from frozen stocks using the myeloma selection media. The media supplement 8-azaguanine is a toxic purine

analog which gets incorporated into the DNA of cells via their salvage pathway and, thereby, kills myeloma cells which are HGPRT$^+$ revertants. Following this selection, HGPRT$^-$ cells were expanded in the myeloma growth media until 100 mL of media containing 6 x 10^{-5} cells/mL were obtained. Myeloma cells are considered healthy, a prerequisite for successful fusions, when they are in log phase growth (cell density is between 3.5 x 10^5 and 1.0 x 10^6 cells/mL) and less than 2% of the population is dead.

Cell densities were determined by trypan blue staining as follows. To a 20 µL aliquot of a thoroughly suspended cell sample in a small test tube was added 20 µL of trypan blue stain and the resulting suspension was thoroughly mixed. The cells were slowly pipetted into the sample groove of a clean hemacytometer until the observation window was completely covered. The hemacytometer was placed on an inverted phase microscope and the living cells (no blue stain in the interior of the cells) in the four counting grids were counted, divided by four and multiplied by 1 x 10^4. This number was then multiplied by two, to account for the trypan blue dilution, to afford the number of cells/mL.

The following fusion protocol was used for the production of hybridomas from each of the sacrificed mice:

1.   The spleen was placed in a sterile 50 mL conical tube containing 25 mL of prewarmed (37°C) fusion media.

2.   In a sterile laminar flow hood, the spleen and the media were transferred to a 35 mm tissue culture dish. The spleen was washed by successive transfer through three 35 mm tissue culture dishes each containing 20 mL of fusion media. In the final dish, the spleen was cut into three pieces using a sterile razor blade and each piece was then teased between two sterile glass slides to provide the B-cells (approximately 5 x 10^7 cells).

3.   The B-cells were transferred to a 50 mL sterile centrifuge tube and spun for 5 minutes at 1300 rpm. The supernatant* was aspirated off, the pellet was loosened and

resuspended in 25 mL of serum free media, and the mixture was again centrifuged for 5 minutes at 1300 rpm.

4.   The supernatant was aspirated off, the pellet was loosened and resuspended in 25 mL of serum free media containing 5 x 10^7 myeloma cells (653/HGPRT-). The suspension of B-cells and myeloma cells was spun for 5 minutes at 1900 rpm.

5.   The supernatant was aspirated off, the pellet was loosened, and 1 mL of prewarmed (37°C) polyethylene glycol (PEG 1500, Boheinger-Mannhaim) was added with gentle swirling over a period of 1 minute at room temperature.

6.   Follwing complete addition, the 50 mL tube was sealed and the fusion mixture was immersed in a 37°C bath and swirled for 90 seconds.

7.   To end the fusion, fusion media was added to the mixture according to the following schedule: 1 mL over a period of 30 seconds, then 3 mL over a period of 30 seconds, then 20 mL over a period of 1 minute. The centrifuge bottle was then topped to a final volume of 40 mL with fusion media and allowed to stand for 10 minutes at room temperature.

8.   The mixture was centrifuged for 10 minutes at 1300 rpm, the supernatant was removed, and the pellet was loosened and then resuspended in 25 mL of plating media. The cell suspension was combined with 20 mL of feeder media (prepared the day before and stored in 20 mL of plating media at 37°C in a CO_2 incubator), the resulting mixture was divided between two 35 mm tissue culture dishes, and 16 mL more plating media was added to each culture dish.

9.   Cells were dispensed into 8 96-well sterile plates (100 μL per well) and left to stand at 37°C in a CO_2 incubator for 7 days. After 7 days each well was supplemented with 50 μL of plating media.

*For the preparation of the Feeder layer the supernatant was transferred to a tissue culture flask and left to stand at 37°C in a CO_2 incubator until the next day when it was used in the fusion.

To insure the monoclonality of the hapten-binding cell lines, each positive, growing cell line was subcloned by limited dilution using the Poisson distribution: $f_{(0)}$ is the fraction of wells on the plate with growth and λ is the average number of cells/well. When $\lambda = 1$ (monoclonal), 35% of the wells on the plate have growth. Eleven days after the fusion the plates were screened for binding to hapten (positive) according to the standard ELISA. Media removed for the assay was immediately replaced with growth media. Colonies identified as positive, and growing at such a rate as to have slightly discolored the media, were stirred and the plates were returned to the incubator. Approximately 50% of the positive colonies reached this stage at days 11-14, 40% at days 15-20, and 10% at days 20-31. After being stirred, colonies became confluent between 12-24 hours if they were healthy. Once a positive, healthy colony had approached confluency ($>10^4$ cells/mL) it was serial diluted according to the following subcloning procedure:

1.   The number of viable cells/mL was determined using trypan blue staining.

2.   Three thousand cells were placed in 300 uL of growth media in one well of a 24-well tissue culture plate.

3.   Thirty microliters of media (300 cells) were removed from the 24-well tissue culture plate and placed into a tissue culture dish containing 3 mL of growth media. Using an eight channel multipipeter, 100 uL of media was placed in each of 24 wells of a 96-well tissue culture plate (10 cells/well). The 24-well tissue culture plate was placed in the incubator and the cell lines maintained in case the limiting dilution failed.

4.   The remaining 0.6 mL of media in the tissue culture dish was diluted with 5.4 mL of growth media (10x dilution). Using an eight channel multipipeter, 100 uL of media was placed in each of 32 wells of the aforementioned 96-well tissue culture plate (1 cell/well).

5.   The remaining 2.8 mL media in the tissue culture dish was diluted with 8.4 mL of growth media (4x dilution). Using an eight channel multipipeter, 100 uL of media was placed in each of the remaining 40 wells of the 96-well tissue culture plate (0.25 cells/well).

6. After seven days 50 uL of growth media is added to each of the wells in the 96-well tissue culture plate.

7. After eight days, wells containing viable colonies were usually discolored. Plates were again screened for hapten binding according to the standard ELISA protocol. Plates containing positive cell lines, defined as monoclonal according to the Poisson statistical distribution, were expanded in expansion media. Cells from one of the monoclonal wells were grown until confluent, transferred to a 24-well sterile tissue culture plate, grown until confluent, transferred to a 35 mm tissue culture plate, and grown in 25 mL of expansion media for the production of ascites.

8. Plates containing positive cell lines that were not statistically monoclonal were subjected to serial dilution again; the most dilute positive colony was serially diluted in growth media according to the serial dilution protocol described above.

In order to generate large quantities of monoclonal antibodies, cell lines were propagated *in vivo* in pristane primed mice. Mice were intraperitoneally injected with pristane (0.5 mL per mouse) at least 1 week prior to the injection of hybridoma cell lines. Each monoclonal hybridoma cell line was individually prepared for injection into a mouse by growing the healthy cell line in 25 mL of expansion media in a 35 mm tissue culture dish to a final density of 5 x 10^5 to 1 x 10^6 cells/mL. The cells were washed from the surface of the plate and centrifuged in a 50 mL conical tube for 5 minutes at 1000 rpm. The supernatant was aspirated off, the pellet was resuspended in 0.5 mL of sterile PBS, and the suspension injected intraperitoneally into a pristane primed mouse. Only one monoclonal hybridoma cell line was injected per mouse. Within one to two weeks abdominal swelling was observed in the injected mice. Each mouse was "tapped" for the ascites fluid by draining the swelled area into a sterile tube using an 18-gauge needle. Mice were tapped 1-3 times (depending on their health) prior to being sacrificed.

Monoclonal hybridoma cell lines were frozen according to the following protocol. Each healthy cell line was grown in 25 mL of expansion media in a 35 mm tissue culture

124

dish to a final density of 5 x 10^5 to 1 x 10^6 cells/mL. The cells were washed from the surface to the plate and centrifuged in a 50 mL conical tube for 5 minutes at 1000 rpm. The supernatant was aspirated off and the pellet was resuspended in 1 mL of ice-cold freezing solution (4% DMSO, 96% FBS). The resulting suspension was then aliquoted between four freezing vials (250 μL/vial) and the vials were immediately placed in a -78°C freezer. Cell lines were transferred to a liquid nitrogen storage container for long-term storage no sooner than 24 hours after the initial freezing.

5.2.c.1. Hapten V1 Specific Monoclonal Antibodies

On day 79, three days after the final injection, the immunized mouse was sacrificed, the spleen was harvested, and the B-cells were fused with 5x10^7 653/HGPRT- myeloma cells to prepare hybridomas. Eleven days after the fusion each of the fusion plates were screened for the presence of hapten-binding antibodies using the standard ELISA assay. Approximately 75 wells were found to contain antibodies which bound hapten V1 with a high affinity, and 55 of these wells were found to contain viable cell lines. All of these viable, high affinity cell lines were subcloned according to the aforementioned subcloning protocol. A total of 53 cell lines survived the subcloning and were ultimately used for the production of ascites.

5.2.c.2. Hapten G1 Specific Monoclonal Antibodies

On day 81, three days after the final injection, the immunized mouse was sacrificed, the spleen was harvested, and the B-cells were fused with 5x10^7 653/HGPRT- myeloma cells to prepare hybridomas. Eleven days after the fusion each of the fusion plates were screened for the presence of hapten-binding antibodies using the standard ELISA assay. Approximately 50 wells were found to contain antibodies which bound hapten G1 with a high affinity, and 45 of these wells were found to contain viable cell lines. All of these viable, high affinity cell lines were subcloned according to the aforementioned subcloning protocol. A total of 41 cell lines survived the subcloning and were ultimately used for the production of ascites.

5.2.d. Purification of Monoclonal Antibodies

Monoclonal antibodies were purified to >95% homogeneity (as judged by SDS-polyacrlamide gel electrophoresis) in three steps from the ascites fluid according to the following protocol. Freshly collected ascites fluid was centrifuged at 4000 rpm for 30 minutes at 4°C to pellet red blood cells. The supernatant was collected and an equal volume of saturated ammonium sulfate was added dropwise with stirring 4°C to precipitate the antibodies. Approximately 1 hour following complete addition of the ammonium sulfate, the samples were centrifuged at 8000 rpm for 20 minutes. The supernatant was discarded and the precipitates were stored at -20°C until they were further purified.

Precipitated antibodies were solubilized in and exhaustively dialyzed against 50 mM Tris•HCl (pH 7.8) at 4°C. Dialyzed samples were filtered through 0.45 μm filter and then individually loaded onto a DEAE-Sephacel anion-exchange column (XK26) attached to a Pharmacia FPLC at 4°C. A salt gradient (from 0 mM to 500 mM NaCl in 50 mM Tris•HCl, pH 7.8) served to elute partially purified antibodies. The running program was as follows: 0-50 mL (0% NaCl), 50-51 mL (10% NaCl), 51-90 mL (10% NaCl), 90-170 mL (30% NaCl), 170-171 mL (100% NaCl), 171-210 mL (100% NaCl), 210-211 mL (0% NaCl), 211-260 mL (0% NaCl) at a rate of 2 mL/min, collecting 10 mL fractions. Antibody containing fractions were collected, concentrated using an Amicon filtration apparatus to a final volume of approximately 10 mL, and exhaustively dialyzed against 20 mM Kpi (pH 7.2) at 4°C.

Samples were filtered through a 0.22 μm filter and loaded onto a protein G-Sepharose affinity column (HR 10/2) attached to a Pharmacia FPLC 4°C. A low pH buffer (100 mM glycine•HCl, pH 2.7) was used to elute pure antibody (>95%) from the affinity column (equilibrated with 20 mM Kpi at pH 7.2). Antibody containing fractions were immediately neutralized with 1 M Tris•HCl (pH 9) and buffered with 1 M Kpi (pH 7.2). The running program was as follows: 0-100 mL (0% glycine), 100-101 mL (100% glycine), 101-160 mL (100% glycine), 160-161 mL (0% glycine), 161-220 mL (0%

126

glycine) at a rate of 2 mL/min, collecting 6 mL fractions. Antibody concentrations were determined using the absorbance at 280 nm and an extinction coefficient of 1.35. Antibody containing fractions were stored without concentration at -20°C until the assays for catalytic activity were performed.

5.2.d.1. Purification of Hapten V1 Specific Antibodies

Ascites fluid from 53 mice was purified and 46 of the mice yielded enough monoclonal antibody for the catalytic assays.

5.2.d.2. Purification of Hapten G1 Specific Antibodies

Ascites fluid from 41 mice was purified and 31 of the mice yielded enough monoclonal antibody for the catalytic assays.

5.2.e. Assays for Catalytic Activity

Antibody containing solutions (i.e., fractions from the protein G column) were thawed, concentrated, exchanged into 20 mM bis-tris containing 0.1% NaN_3 (pH 7.2), diluted to a final concentration of 180 μM, and stored at 4°C in preparation for catalytic assays. High performance liquid chromatography (HPLC) was used to quantitate the rates of substrate hydrolysis. A Waters Nova-Pak [18]C column and isocratic CH_3CN/H_2O gradients (no TFA was added to the solvents) provided efficient separation of the internal standard, the product, and the substrates. In the assays performed with substrate **V1G1r** (retention time 2.6 minutes), 2-(1-acetamidoethyl) napthalene was used as an internal standard (retention time = 4.4 minutes) and chromatography was performed on a Waters 510 HPLC running a 67:23 ($H_2O:CH_3CN$) isocratic gradient at 1.5 mL/min. In the assays performed with substrates **V1G1a** and **V1G1c** (retention time = 2.4 min), acetanilide (retention time 3.3 minutes) was used as an internal standard and chromatography was performed on a Hewlett Packard 1050 HPLC running a 85:15 ($H_2O:CH_3CN$) isocratic gradient at 1.5 mL/min. In all of the assays, product production was monitored at $\lambda = 274$ nm. The hydrolysis rates, in the presence and absence of substrate, were determined by quantitating the amount of product produced over time. For each reaction, product levels

127

were determined six times over a period of eight hours. A product standard curve was prepared to allow for the conversion of integration values to product quantities. An internal standard was used to normalize all integration values. Each antibody (46 antibodies specific for hapten V1 and 31 antibodies specific for hapten G1) was individually assayed for hydrolytic activity against three substrates (**V1G1r, V1G1a, V1G1c**) under a variety of conditions (see below).

5.2.e.1. Hapten V1 and G1 Specific Antibodies Catalytic Activity Assays

Antibodies (18 μM) were initially screened against substrate **V1G1r** (2.0 mM) at pH 6.0 (42 mM bis-tris, 90 mM NaCl, 10% DMF), 25°C. None of the **V1** or **G1** antibodies appeared to catalyze the hydrolysis of substrate **V1G1r**. The uncatalyzed rate of hydrolysis of **V1G1r** under these conditions was determined to be 3.2×10^{-5} min^{-1}.

Antibodies (18 μM) were next screened against substrate **V1G1a** (1.0 mM and 3.0 mM) and substrate **V1G1c** (1.0 mM and 3.0 mM) at pH 5.4 (22 mM sodium citrate, 2 mM bis-tris, 98 mM NaCl, 2% DMF), 37°C. Again, no **V1** or **G1** catalysts were identified from these assays. The uncatalyzed rate of hydrolysis of **V1G1a** and **V1G1c** under there conditions was found to be 1.4×10^{-4} min^{-1}.

References

1. Park, T. K.; Feng, Q.; Rebek, J., Jr., Synthetic Replicators and Extrabiotic Chemistry. *J. Am. Chem. Soc.* **114**, 4529-4532, (1992).

2. Wintner, E. A.; Conn, M.; Rebek, J., Jr., Studies in Molecular Recognition. *Acc. Chem. Res.* **27**, 198-203, (1994).

3. Dougherty, D. A.; Stauffer, D. A., Acetylcholine Binding by a Synthetic Receptor: Implications for Biological Recognition. *Science* **250**, 1558-1560, (1990).

4. Breslow, R., Biomimetic Chemistry and Artificial Enzymes: Catalysis by Design. *Acc. Chem. Res.* **28**, 146-153, (1995).

5. Kohler, G.; Milstein, C., Continuous Cultures of Fused Cells Secreting Antibody of Predefined Specificity. *Nature* **256**, 495-497, (1975).

6. Pauling, L., Molecular Architecture and Biological Reactions. *Chem. Eng. News* **24**, 1375-1377, (1946).

7. Pauling, L., Chemical Achievement and Hope for the Future. *Am. Sci.* **36**, 51-58, (1948).

8. Jencks, W. P., Catalysis in Chemistry and Enzymology. In ; Ed.; McGraw-Hill: New York, 1969; pp Pages, (1969).

9. Raso, V.; Stollar, B. D., The Antibody-Enzyme Analogy: Characterization of Antibodies to Phosphopyridoxyltyrosine Derivatives. *Biochemistry* **14**, 584-591, (1975).

10. Raso, V.; Stollar, B. D., The Antibody-Enzyme Analogy. Comparison of Enzymes and Antibodies Specific for Phosphopyridoxyltyrosine. *Biochemistry* **14**, 591-599, (1975).

11. Tramontano, A.; Janda, K. D.; Lerner, R. A., Catalytic Antibodies. *Science* **234**, 1566-1570, (1986).

12. Pollack, S. J.; Jacobs, J. W.; Schultz, P. G., Selective Chemical Catalysis by an Antibody. *Science* **1570-1573**, (1986).

13. Thomas, N. R., Hapten Design for the Generation of Catalytic Antibodies. *Appl. Biochem. Biotech.* **47**, 345-372, (1994).

14. Lerner, R. A.; Benkovic, S. J.; Schultz, P. G., At the Crossroads of Chemistry and Immunology: Catalytic Antibodies. *Science* **252**, 659-667, (1991).

15. Jackson, D. Y.; Jacobs, J. W.; Sugasawara, R.; Reich, S. H.; Bartlett, P. A.; Schultz, P. G., An Antibody-Catalyzed Claisen Rearrangement. *J. Am. Chem. Soc.* **110**, 4841-4842, (1988).

16. Jackson, D. Y.; Liang, M. N.; Bartlett, P.; Schultz, P. G., Activation Parameters and Sterochemistry of an Antibody-Catalyzed Claisen Rearrangement. *Angew. Chem. Int. Ed. Engl.* **31**, 182-183, (1992).

17. Hilvert, D.; Nared, K. D., Sterospecific Claisen Rearrangement Catalyzed by an Antibody. *J. Am. Chem. Soc.* **110**, 5593-5594, (1988).

18. Hilvert, D.; Carpenter, S. H.; Nared, K. D.; Auditor, M.-T. M., Catalysis of Concerted Reactions by Antibodies: The Claisen Rearrangement. *Proc. Natl. Acad. Sci. USA* **85**, 4953-4955, (1988).

19. Shokat, K. M.; Leumann, C. J.; Sugasawara, R.; Schultz, P. G., A New Strategy for the Generation of Catalytic Antibodies. *Nature* **338**, 269-271, (1989).

20. Shokat, K.; Uno, T.; Schultz, P. G., Mechanistic Studies of an Antibody-Catalyzed Elimination Reaction. *J. Am. Chem. Soc.* **116**, 2261-2270, (1994).

21. Lewis, C.; Kramer, T.; Robinson, S.; Hilvert, D., Medium Effects in Antibody-Catalyzed Reactions. *Science* **253**, 1019-1022, (1991).

22. Tarasow, T. M.; Lewis, C.; Hilvert, D., Investigation of Medium Effects in a Family of Decarboxylase Antibodies. *J. Am. Chem. Soc.* **116**, 7959-7963, (1994).

23. Cochran, A. G.; Schultz, P. G., Antibody-Catalyzed Porphyrin Metallation. *Science* **249**, 781-783, (1990).

24. Janda, K. D.; Schloeder, D.; Benkovic, S. J.; Lerner, R. A., Induction of an Antibody That Catalyzes the Hydrolysis of an Amide Bond. *Science* **241**, 1188-1191, (1988).

25. Iverson, B. L.; Lerner, R. A., Sequence-Specific Peptide Cleavage Catalyzed by an Antibody. *Science* **243**, 1184-1188, (1989).

26. Martin, M. T.; Nageles, T. S.; Sugasawara, R.; Aman, N. I.; Napper, A. D.; Darsley, M. J.; Sanchez, R. I.; Boothe, P.; Titmas, R. C., Antibody-Catalyzed Hydrolysis of an Unsubstituted Amide. *J. Am. Chem. Soc.* **116**, 6508-6512, (1994).

27. Suga, H.; Ersoy, O.; Williams, S. F.; Tsumuraya, T.; Margolies, M. N.; Sinskey, A. J.; Masamune, S., Catalytic Antibodies Generated via Heterologous Immunization. *J. Am. Chem. Soc.* **116**, 6025-6026, (1994).

28. Sarvetnick, N.; Gurushanthaiah, D.; Han, N.; Prudent, J.; Schultz, P.; Lerner, R., Increasing the Chemical Potential of the Germ-line Antibody Repertoire. *Proc. Natl. Acad. Sci. USA* **90**, 4008-4001, (1993).

29. Roberts, V. A.; Iverson, B. L.; Iverson, S. A.; Benkovic, S. J.; Lerner, R. A.; Getzoff, E.; Tainer, J. A., Antibody Remodeling: A General Solution to the Design of a

Metal-coordination Site in an Antibody Binding Pocket. *Proc. Natl. Acad. Sci. USA* **87**, 6654-6658, (1990).

30.   Wade, W. S.; Koh, J. S.; Han, N.; Hoekstra, D. M.; Lerner, R. A., Engineering Metal Coordination Sites into the Antibody Light Chain. *J. Am. Chem. Soc.* **115**, 4449-4456, (1993).

31.   Huse, W. D.; Sastry, L.; Iverson, S. A.; Kang, A. S.; Atlting-Mees, M.; Burton, D. R.; Benkovic, S. J.; Lerner, R. A., Generation of a Large Combinatorial Library of the Immunoglobin Repertoire in Phage Lambda. *Science* **246**, 1275-1281, (1989).

32.   Chen, J. Y.-C.; Danon, T.; Sastry, L.; Mubaraki, M.; Janda, K. D.; Lerner, R. A., Catalytic Antibodies from Combinatorial Libraries. *J. Am. Chem. Soc.* **115**, 357-358, (1993).

33.   Lesley, S. A.; Patten, P. A.; Schultz, P. G., A Genetic Approach to the Generation of Antibodies with Enhanced Catalytic Activities. *Proc. Natl. Acad. Sci. USA* **90**, 1160-1165, (1993).

34.   Tang, Y.; Hicks, J. B.; Hilvert, D., In Vivo Catalysis of a Metabolically Essential Reaction by an Antibody. *Proc. Natl. Acad. Sci. USA* **88**, 8784-8786, (1991).

35.   Tawfik, D. S.; Green, B. S.; Chap, R.; Sela, M.; Eshhar, Z., catELISA: A Facile General Route to Catalytic Antibodies. *Proc. Natl. Acad. Sci. USA* **90**, 373-377, (1993).

36.   MacBeath, G.; Hilvert, D., Monitoring Catalytic Activity by Immunoassay: Implications for Screening. *J. Am. Chem. Soc.* **116**, 6101-6106, (1994).

37.   Hilvert, D.; Hill, K. W.; Nared, K.; Auditor, M.-T. M., Antibody Catalysis of a Diels-Alder Reaction. *J. Am. Chem. Soc.* **111**, 9261-9262, (1989).

38.   Imoto, T.; Johnson, L. N.; North, A. C. T.; Phillips, D. C.; Rupley, J. A., Vertebrate lysozymes. In *The Enzymes* ; Boyer, P. D., Ed.; Academic Press: New York, 1970; pp 665, (1970).

39.   Kirby, A. J., Mechanism and Steroelectronic Effects in the Lysozyme Reaction. *CRC Critical Reviews in Biochemistry* **22**, 283-315, (1987).

40.   Phillips, D. C., The Three-dimensional Structure of an Enzyme Molecule. *Sci. Amer.* **215**, 78-90, (1966).

41.   Chipman, D. M.; Sharon, N., Mechanism of Lysozyme Action. *Science* **165**, 454-469, (1969).

42.   Chipman, D. M., A Kinetic Analysis of the Reaction of Lysozyme with Oligosaccharides from Bacterial Cell Walls. *Biochemistry* **10**, 1715-1722, (1971).

43.   Rupley, J. A.; Butler, L.; Gerring, M.; Pacoravo, R., Studies on the Enzymatic Activity of Lysozyme, III. The Binding of Saccharides. *Proc. Nat. Acad. Sci. U.S.A.* **57**, 1088-1095, (1967).

44.   Anet, F. A. L.; Brown, J. R., Nuclear Magnetic Resonance Line-Shape and Double-Resonance Studies of Ring Inversion in Cyclohexane-d_{11}. *J. Am. Chem. Soc.* **89**, 760-765, (1967).

45.   Strynadka, N. C. J.; James, M. N. G., Lysozyme Revisited: Crystallographic Evidence for Distortion of an N-Acetylmuramic Acid Residue Bound in Site D. *J. Mol. Biol.* **220**, 401-424, (1991).

46.   Patt, S. L.; Baldo, J. H.; Boekelheide, K.; Weisz, G.; Sykes, B. D., The Nuclear Magnetic Resonance Determination of the Conformation of Saccharides Bound in Subsite D of Lysozyme. *Can. J. Biochem.* **56**, 624-629, (1978).

47.   Pincus, M. R.; Scheraga, H. A., Prediction of the Three-Dimensional Structures of Complexes of Lysozyme with Cell Wall Substrates. *Biochemistry* **20**, 3960-3965, (1981).

48.   Post, C. B.; Karplus, M., Does Lysozyme Follow the Lysozyme Pathway? An Alternative Based on Dynamic, Structural, and Steroelectronic Considerations. *J. Am. Chem. Soc.* **108**, 1317-1319, (1986).

49.   Parsons, S. M.; Raftery, M. A., Ionization Behavior of the Catalytic Carboxyls of Lysozyme. *Biochem. Biophys. Res. Commun.* **41**, 45-49, (1970).

50.   Kuramitsu, S.; Ikeda, K.; Hamaguchi, K., Effect of Ionic Strength and Temperature on the Ionization of the Catalytic Groups, Asp 52 and Glu 35, in Hen Lysozyme. *J. Biochem.* **82**, 585-597, (1977).

51.   Malcom, B. A.; Rosenberg, S.; Corey, M. J.; Allen, J. S.; Baetselier, A. D.; Kirsh, J. F., Site-Directed Mutagenesis of the Catalytic Residues Asp-52 and Glu-35 of Chicked Egg White Lysozyme. *Proc. Natl. Acad. Sci. USA* **86**, 133-137, (1989).

52.   Withers, S. G.; Warren, A. J.; Street, I. P.; Rupitz, K.; Kempton, J. B.; Aebersold, R., Unequivocal Demonstration of the Involvement of a Glutamate Residue as a Nucleophile in the Mechanism of a "Retaining" Glycosidase. *J. Am. Chem. Soc.* **112**, 5887-5889, (1990).

53.   Legler, G., Glycoside Hydrolases: Mechanistic Information from Studies with Reversible and Irreversible Inhibitors. *Adv. Carbohydr. Chem. Biochem.* **48**, 319-384, (1990).

54.   Kajimoto, T.; Liu, K. K.-C.; Pederson, R. L.; Zhong, Z.; Ichikawa, Y.; Porco, J. J. A.; Wong, C.-H., Enzyme-Catalyzed Aldol Condensation for Asymmetric Synthesis of

Azasugars: Synthesis, Evaluation, and Modeling of Glycosidase Inhibitors. *J. Am. Chem. Soc.* **113**, 6187-6196, (1991).

55.   Look, G. C.; Fotsch, C. H.; Wong, C.-H., Enzyme-Catalyzed Organic Synthesis: Practical Routes to Aza Sugars and Their Analogs for Use as Glycoprocessing Inhibitors. *Acc. Chem. Res.* **26**, 182-190, (1993).

56.   Dale, M. P.; Ensley, H. E.; Kern, K.; Sastry, K. A. R.; Byers, L. D., Reversible Inhibitors of β-Glucosidase. *Biochemistry* **24**, 3530-3539, (1985).

57.   Tong, M. K.; Papandreou, G.; Ganem, B., Potent, Broad-Spectrum Inhibition of Glycosidases by an Amidine Derivative of a D-Glucose. *J. Am. Chem. Soc.* **112**, 6137-6139, (1990).

58.   Ganem, B.; Papandreou, G., Mimicking the Glucosidase Transition State: Shape/Charge Considerations. *J. Am. Chem. Soc.* **113**, 8984-8985, (1991).

59.   Legler, G., *Biochem. Biophys. Acta* **524**, 94-101, (1978).

60.   Knapp, S.; Purandare, A.; Rupitz, K.; Withers, S. G., A (1-4)-"Trehazoloid" Glucosidase Inhibitor with Aglycon Selectivity. *J. Am. Chem. Soc.* **116**, 7461-7462, (1994).

61.   Saul, R.; Molyneux, R. J.; Elbein, A. D., Castanospermine, a Tetrahydroxylated Alkaloid that Inhibits β-Glucosidase and β-Glucocerebrosidase. *Arch. Biochem. Biophys.* **221**, 593-597, (1983).

62.   Jespersen, T. M.; Dong, W.; Sierks, M. R.; Skrydstrup, T.; Lundt, I.; Bols, M., Isofagomine, a Potent, New Glycosidase Inhibitor. *Angew. Chem. Int. Ed. Engl.* **33**, 1778-1779, (1994).

63.   Fleet, G. W. J.; Nicholas, S. J.; Smith, P. W.; Evans, S. V.; Fellows, L. E., Potent Competitive Inhibition of α-Galactosidase and α-Glucosidase Activity by 1,4-Dideoxy-1,4-Iminopentitols: Synthesis of 1,4-Dideoxy-1,4-Imino-D-Lyxitol and of Both Enantiomers of 1,4-Dideoxy-1,4-Iminoarabinitol. *Tetrahedron Lett.* **26**, 3127-3130, (1985).

64.   Fife, T. H., General Acid Catalysis of Acetal, Ketal, and Ortho Ester Hydrolysis. *Acc. Chem. Res.* **5**, 264-272, (1972).

65.   Fife, T. H., Physical Organic Model Systems and the Problem of Enzymatic Catalysis. In *Advances in Physical Organic Chemistry* ; Gold, V., Ed.; Academic Press: New York, 1975; pp 81-112, (1975).

66.   Sinnot, M. L., Glycosyl Transfer. In *The Chemistry of Enzyme Action* ; Page, M. I., Ed.; Elsevier: New York, 1984; pp 389-431, (1984).

67. Atkinson, R. F.; Bruice, T. C., Ring Strain and General Acid Catalysis of Acetal Hydrolysis. Lysozyme Catalysis. *J. Am. Chem. Soc.* **96**, 819-824, (1974).

68. Deslongchamps, P., Steroelectronic Effects in Organic Chemistry. In ; Baldwin, J. E., Ed.; Pergamon Press: New York, 1983; pp Pages, (1983).

69. Deslongchamps, P., Intramolecular Strategies and Steroelectronic Effects. Glycosides Hydrolysis Revisited. *Pure & Appl. Chem.* **65**, 1161-1178, (1993).

70. Capon, B., Intramolecular Catalysis in Glycoside Hydrolysis. *Tetrahedron Lett.* 911-913, (1963).

71. Capon, B.; Page, M. I.; Sankey, G. H., The Kinetics and Mechanism of Hydrolysis of 2,3-(Phenylmethylenedioxy)benzoic Acid (*OO'*-Benzylidene-2,3-dihydroxybenzoic Acid). *J. Chem. Soc. Perkin II* 529-532, (1972).

72. Fife, T. A.; Anderson, E., Electrostatic Catalysis. IV. Intramolecular Carboxyl Group Electrostatic Facilitation of the A-1-Catalyzed Hydrolysis of Alkyl Phenyl Acetals of Formaldehyde. The Influence of Oxocarbonium Ion Stability. *J. Am. Chem. Soc.* **93**, 5725-5731, (1971).

73. Hermans, J. R.; Leach, S. J.; Scheraga, H. A., Hydrogen Bonding in Salicyclic Acid and its Implications for Proteins. *J. Am. Chem. Soc.* **85**, 1963, (1963).

74. Fife, T. H.; Jaffe, S. H.; Natarajan, R., Intramolecular General-Acid and Electrostatic Catalysis in Acetal Hydrolysis. Hydrolysis of 2-(Substituted phenoxy)-6-carboxythetrahydropyrans and 2-Alkoxy-6-carboxytetrahydropyrans. *J. Am. Chem. Soc.* **113**, 7646-7653, (1991).

75. Cherian, X. M.; Van Arman, S. A.; Cazrnik, A. W., Experimental Support for Asp-52's Importance in Lysozyme Using a Carbohydrate-Based Enzyme Model. Acetal Hydrolysis Catalyzed by a "Stereoelectronically Correct" Carboxylate Group. *J. Am. Chem. Soc.* 6566-6568, (1988).

76. Fife, T. H.; Przystas, T. J., Intramolecular General Acid Catalysis in the Hydrolysis of Acetals with Aliphatic Alcohol Leaving Groups. *J. Am. Chem. Soc.* **101**, 1202, (1979).

77. Lerner, R. A.; Benkovic, S. J.; Schultz, P. G., At the Crossroads of Chemistry and Immunology: Catalytic Antibodies. *Science* **252**, 659-667, (1991).

78. Thomas, N. R., Hapten Design for the Generation of Catalytic Antibodies. *Appl. Biochem. Biotech.* **47**, 345-372, (1994).

79. Reymond, J.-L.; Janda, K. D.; Lerner, R. A., Antibody Catalysis of Glycoside Bond Hydrolysis. *Angew. Chem. Int. Ed. Engl.* **30**, 1711-1713, (1991).

80.   Yum, J.; Hsieh, L. C.; Kochersperger, L.; Yonkovich, S.; Stephans, J. C.; Gallop, M. A.; Schultz, P. G., Progress Toward an Antibody Glycosidase. *Angew. Chem. Int. Ed. Engl.* **33**, 339-341, (1994).

81.   Suga, H.; Tanimoto, N.; Sinskey, A. J.; Masamune, S., Glycosidase Antibodies Induced to a Half-Chair Transition-State Analog. *J. Am. Chem. Soc.* **116**, 11197-11198, (1994).

82.   Backvall, J.-E., Palladium in Some Selective Oxidation Reactions. *Acc. Chem. Res.* **16**, 335-342, (1983).

83.   Backvall, J.-E.; Nystrom, J.-E.; Nordberg, R. E., Stereo- and Regioselective Palladium-Catalyzed, 1,4-Acetoxychlorination of 1,3-Dienes. 1-Acetoxy-4-chloro-2-alkenes as Versitile Synthons in Organic Transformations. *J. Am. Chem. Soc.* **107**, 3676-3686, (1985).

84.   Sommer, H. Z.; Lipp, H. I.; Jackson, L. L., Alkylation of Amines. A General Exhaustive Alkylation Method for the Synthesis of Quarternary Ammonium Compounds. *J. Org. Chem.* **36**, 824-828, (1971).

85.   Roth, W.; Pigman, W., D-Glucal and the Glycals. *Methods Carbohydrate Chemistry* **2**, 405-8, (1963).

86.   Humoller, F. L., L-Ribose. *Methods Carbohydrate Chemistry* **1**, 83-88, (1963).

87.   Ferrier, R. J.; Vethaviyaser, N., Allylic Isomerizations of Unsaturated Carbohydrate Derivatives. A New Approach to the Synthesis of Amino, Thio, and Branched-chain Sugars. *J. Chem. Soc. (C)* 1385-1387, (1970).

88.   Grynkiewicz, G.; Priebe, W.; Zamojski, A., Synthesis of Alkyl 4,6-Di-*O*-Acetyl-2,3-Dideoxy-α-D-*threo*-Hex-2-Enopyranosides from 3,4,6-Tri-*O*-Acetyl-1,5-Anhydro-2-Deoxy-D-*lyxo*-Hex-1-Enitol (3,4,6,-Tri-*O*-Acetyl-D-Galactal). *Carbohydr. Res.* **68**, 33-41, (1979).

89.   Bhate, P.; Horton, D.; Priebe, W., Allylic Rearrangement of 6-deoxyglycals Having Practical Utility. *Carbohydr. Res.* **144**, 331-337, (1985).

90.   Dunkerton, L. V.; Brady, K. T.; Mohamed, F., Palladium-Assisted Carbohydrate Reactions I. Sodium Cyanoborohydride Promoted Allylic Rearrangements of C-6 Substituted Pyranoside Glycals. *Tetrahedron Lett.* **23**, 599-602, (1982).

91.   Dunkerton, L. V.; Adair, N. K.; Euske, J. M.; Brady, K. T.; Robinson, P. D., Regioselective Synthesis of Substituted 1-Thiohex-2-enopyranosides. *J. Org. Chem.* **53**, 845-850, (1988).

92.   Priebe, W.; Zamojski, A., The Acid-Catalyzed Reaction of Thiols with Alkyl 2,3-Dideoxy-glyc-2-enopyranosides or Glycals. *Tetrahedron* **36**, 287-297, (1980).

93.   Williams, R. M.; Stewart, A. O., C-Glycosidation of Pyridyl Thioglycosides. *Tetrahedron Lett.* **24**, 2715-2718, (1983).

94.   Kometani, T.; Kondo, H.; Fujimori, Y., Boron Trifluoride-Catalyzed Rearrangement of 2-Aryloxytetrahydropyrans: A New Entry to C-Arylglycosidation. *Synthesis* 1005-1007, (1988).

95.   Casiraghi, G.; Cornia, M.; Rassu, G.; Zetta, L.; Fava, G. G.; Belicchi, M. F., Stereoselective Arylation of Pyranoid Glycals, Using Bromomagnesium Phenolates: An Entry to 2,3-Unsaturated C-α-Glycopyranosylarenes. *Carbohydr. Res.* **191**, 243-251, (1989).

96.   Mereyala, H. B.; Reddy, G. V., Stereoselective Synthesis of a-Linked Saccharides by Use of Per O-Benzylated 2-Pyridyl 1-Thio Hexopyranosides as Glycosyl Donors and Methyl Iodide as an Activator. *Tetrahedron* **47**, 6435-6448, (1991).

97.   Gurjar, M. K.; Dhar, T. G. M., Novel Synthesis of Hex-2-Enopyranosides. *J. Carbohydr. Chem.* **6**, 313-316, (1987).

98.   Ferrier, R. J.; Hay, R. W.; Vethaviyasar, N., A Potentially Versatile Synthesis of Glycosides. *Carbohydr. Res.* **27**, 55-61, (1973).

99.   Hanessian, S.; Bacquet, C.; Lehong, N., Chemistry of the Glycosidic Linkage. Exceptionally Fast and Efficient Formation of Glycosides by Remote Activation. *Carbohydr. Res.* **80**, C17-C22, (1980).